NORTH-WEST UNIVERSITY
YUNIBESITI YA BOKONE-BOPHIRIMA
NOORDWES-UNIVERSITEIT
POTCHEFSTROOMKAMPUS

The monoamine oxidase inhibition properties of caffeine analogues containing saturated C-8 substituents

Paul Grobler

B.Pharm

Dissertation submitted in partial fulfilment of the requirements for the degree Magister Scientiae in Pharmaceutical Chemistry at the North-West University, Potchefstroom Campus

Supervisor: Prof. J.J. Bergh

Co-supervisor: Prof. J.P. Petzer

Potchefstroom

2010

ACKNOWLEDGMENTS

This study was carried out at the Department of Pharmaceutical Chemistry, North-West University, Potchefstroom campus.

I give all my praise to the Lord my God who carried me throughout my life.
Thank you for all the talents and opportunities You have granted me.
Thank you for all the wonderful people in my life.
To you all the glory!!

I would like to express my gratitude to all the people who contributed to this dissertation. The following people and organizations, however, deserve special acknowledgment for their love, guidance and support:

- *My parents, Paul en Ronel, for their financial and moral support. Thank you for giving me the opportunity to study and find my own way in life. Dedicating this to you is an absolute privilege!*
- *My sister, Izelle. Thank you for all the love and support.*
- *Jacolien Marais for all the love and support. Thank you for always believing in me and helping me to believe in myself!*
- *My supervisor, Prof Jacques Petzer for all the support, encouragement and late hours. You are truly an inspiration for any young researcher.*
- *Prof Kobus Bergh for the helping hand when needed.*
- *Andre Joubert for the NMR experiments and Wits University for the MS measurements.*
- *All the people in the MAO functional group, for all the help and assistance during all the experiments and enzymology work.*
- *NWU and NRF for the bursaries.*

TABLE OF CONTENTS

Abstract

Title: The monoamine oxidase inhibition properties of caffeine analogues containing saturated C-8 substituents.

Key words: Parkinson's disease, dopaminergic nigrostriatal neurons, substantia nigra, monoamine oxidase, inhibitor, caffeine analogues, IC_{50} values.

Parkinson's disease (PD) is a progressive neurodegenerative disorder, characterized pathologically by a marked loss of dopaminergic nigrostriatal neurons and clinically by disabling movement disorders. PD can be treated by inhibiting monoamine oxidase (MAO), specifically MAO-B, since this is a major enzyme involved in the catabolism of dopamine in the substantia nigra of the brain. Inhibition of MAO-B may conserve the dopamine supply in the brain and may therefore provide symptomatic relief for PD patients.

Selegiline is an irreversible MAO-B inhibitor and is currently used for the treatment of PD. Irreversible inhibitors inactivate enzymes by forming stable covalent complexes. The process is not readily reversed either by removing the remainder of the free inhibitor or by increasing the substrate concentration. Even dilution or dialysis does not dissociate the enzyme inhibitor complex and restore enzyme activity. From a safety point of view it may therefore be more desirable to develop reversible inhibitors of MAO-B. In this study, caffeine was used as lead compound to design, synthesize and evaluate new reversible inhibitors of MAO-B. This study is based on the finding that C-8 substituted caffeine analogues are potent MAO inhibitors.

For example, (*E*)-8-(3-chlorostyryl)caffeine (CSC) is an exceptionally potent competitive inhibitor of MAO-B with an enzyme-inhibitor dissociation constant (K_i value) of 128 nM. In this study caffeine was similarly conjugated at C-8 to various side-chains. The effect that these chosen side-chains had on the MAO-B inhibition activity of C-8 substituted caffeine analogues will then be evaluated. The caffeine analogues were also evaluated as human MAO-A inhibitors. For the purpose of this study, saturated C-8 side chains were selected with the goal of discovering new C-8 side chains that enhance the MAO-A and –B inhibition potency of caffeine. As mentioned above, the styryl side chain is one example of a side chain that enhances the MAO-B inhibition potency of caffeine. Should a side chain with promising MAO inhibition activity be identified in

this study, the inhibition potency will be further optimized in a future study by the addition of a variety of substituents to the C-8 side chain ring. For example, halogen substitution of (*E*)-8-styrylcaffeine enhances the MAO-B inhibition potency by up to 10 fold. The saturated side chains selected for the present study included the phenylethyl (**1**), phenylpropyl (**2**), phenylbutyl (**3**) and phenylpentyl (**4**) functional groups. Also included are the cyclohexylethyl (**8**), 3-oxo-3-phenylpropyl (**5**), 4-oxo-4-phenylbutyl (**6**) moieties. A test compound containing an unsaturated linker between C-8 of caffeine and the side chain ring, the phenylpropenyl analogue **7**, was also included. This study is therefore an exploratory study to discover new C-8 moieties that are favorable for MAO- inhibition.

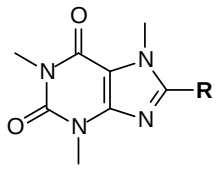

	R
1	$-(CH_2)_2-C_6H_5$
2	$-(CH_2)_3-C_6H_5$
3	$-(CH_2)_4-C_6H_5$
4	$-(CH_2)_5-C_6H_5$
5	$-(CH_2)_2-CO-C_6H_5$
6	$-(CH_2)_3-CO-C_6H_5$
7	$-(CH_2)-CH=CH-C_6H_5$
8	$-(CH_2)_2-C_6H_{11}$

All the target compounds were synthesized by reacting 1,3-dimethyl-5,6-diaminouracil with an appropriate carboxylic acid in the presence of a carbodiimide dehydrating agent. Following ring closure and methylation at C-7, the target inhibitors were obtained. Inhibition potencies were determined using recombinant human MAO-A and MAO-B as enzyme sources. The inhibitor potencies were expressed as IC_{50} values. The most potent MAO-B inhibitor was 8-(5-phenylpentyl)caffeine (**4**) with an IC_{50} value of 0.656 µM. In contrast, all the other test inhibitors were moderately potent MAO-B inhibitors. In fact the next best MAO-B inhibitor, 8-(4-phenylbutyl)caffeine (**3**) was approximately 5 fold less potent than **4** with an IC_{50} value of 3.25 µM. Since the 5-phenylpentyl moiety is the longest side chain evaluated in this study, this finding demonstrates that longer C-8 side chains are more favorable for MAO-B inhibition.

Interestingly, compound **5** containing a cyclohexylethyl side chain (IC_{50} = 6.59 µM) was approximately 4 fold more potent than the analogue containing the phenylethyl linker (**1**) (IC_{50} = 26.0 µM). This suggests that a cyclohexyl ring in the C-8 side chain of caffeine may be more optimal for MAO-B inhibition and should be considered in future studies. The caffeine analogues containing the oxophenylalkyl side chains (**5** and **6**) were weak MAO-B inhibitors with IC_{50} values of 187 µM and 46.9 µM, respectively. This suggests that the presence of a carbonyl group in the C-8 side chain is not favorable for the MAO-B inhibition potency of caffeine. The unsaturated phenylpropenyl analogue **7** was also found to be a relatively weak MAO-B inhibitor with an IC_{50} value of 33.1 µM.

In contrast to the results obtained with MAO-B, the test caffeine analogues were all weak MAO-A inhibitors. With the exception of compound **5**, all of the analogues evaluated were selective inhibitors of MAO-B. The most potent MAO-B inhibitor, 8-(5-phenylpentyl)caffeine (**4**) was the most selective inhibitor, 48 fold more potent towards MAO-B than MAO-A.

This study also shows that two selected analogues (**5** and **3**) bind reversibly to MAO-A and –B, respectively, and that the mode of MAO-A and -B inhibition is competitive for these representative compounds.

Opsomming

Titel: Die monoamienoksidase-inhiberingseienskappe van versadigde C-8 gekonstitueerde kafeïenanaloë.

Sleutelwoorde: Parkinson se siekte, dopaminergiese nigrostriatale neurone, substantia nigra, monoamienoksidase, inhibeerder, kafeïenanaloë, IC_{50}-waardes.

Parkinson se siekte is 'n progressiewe, neurodegeneratiewe siekte. Hierdie siekte word patologies gekenmerk deur 'n verlies aan dopaminergiese nigrostriatale neurone en klinies deur bewegingsteurnisse. Parkinson se siekte kan behandeling word deur die inhibisie van monoamienoksidase (MAO), veral MAO-B, aangesien hierdie ensiem betrokke is by die katabolisme van dopamien in die substantia nigra in die brein. Inhibisie van MAO-B kan tot verhoogde dopamienvlakke in die brein lei en sodoende simptomatiese verligting vir PD-pasiënte teweegbring.

Selegilien is 'n onomkeerbare MAO-B inhibeerder, wat tans gebruik word vir die behandeling van PD. Onomkeerbare inhibeerders inaktiveer ensieme deur die vorming van stabiele kovalente bindings. Omkering van die ensieminaktiveringsproses kan dus nie dadelik plaasvind nie. Nog verwydering van die vrye inhibeerder, nog verhoging in substraatkonsentrasie veroorsaak onmiddellike omkering van die ensieminaktiverigsproses. Verdunning en dialise bewerkstellig ook nie volledige dissosiasie van die ensieminhibeerderkompleks nie en herstel dus nie ensiemaktiwiteit nie. Vanuit 'n veiligheidsoorweging is dit beter om eerder omkeerbare MAO-B-inhibeerders te ontwikkel. In hierdie studie is kafeïen gebruik vir die ontwerp, sintese en evaluering van nuwe omkeerbare MAO-B-inhibeerders. Die bevinding dat C-8-gesubstitueerde kafeïenanaloë kragtige MAO-inhibeerders is, was die basis waarop die studie gegrond is.

'n Voorbeeld van 'n merkwaardige potente kompeterende MAO-B-inhibeerder is (*E*)-8-(3-chlorosteriel)kafeïen (CSC), met 'n ensiem-inhiberende dissosiasiekonstante (K_i-waarde) van 128nM. In hierdie studie is kafeïen, soos by CSC, ook op die C-8 posisie met verskeie sykettings gekonjugeer. Die kafeïenanaloë is ook as MAO-A-inhibeerders geëvalueer. Vir die doeleindes van hierdie studie, is versadigde C-8 sykettings geselekteer om sodoende nuwe C-8 sykettings daar te stel, wat die vermoë van kafeïen om MAO-A en -B te inhibeer, sal verbeter. Soos vermeld, is die sterielketting een voorbeeld van 'n syketting wat die MAO-B-inhibisie van

kafeïen verbeter. Indien 'n syketting met 'n belowende vermoë om MAO te inhibeer in hierdie studie geïdentifiseer word, sal die potensie verder geoptimaliseer word in 'n toekomstige studie, deur die aanbring van verskillende substituente aan die ring van die C-8 syketting. Byvoorbeeld, halogeensubstitusie van (*E*)-8-sterielkafeïen lei tot 'n 10-voudige verhoging van die MAO-B-inhiberingsvermoë. Die versadigde sykettings wat vir hierdie studie geselekteer is sluit die volgende groepe in: fenieletiel (**1**), fenielpropiel (**2**), fenielbutiel (**3**) en fenielpentiel (**4**). Sikloheksieletiel- (**8**), 3-okso-3-fenielpropiel- (**5**) en 4-okso-4-fenielbutielgroepe (**6**) is ook ingesluit. Die toetsverbinding met 'n onversadigde verbinding tussen die C-8 van die kafeïen en die sykettingring is die fenielpropenielanaloog **7**. Hierdie ondersoek is dus 'n ondersoekend studie na nuwe C-8-groepe wat belowend is vir MAO-inhibisie.

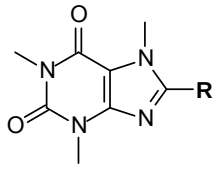

	R
1	$-(CH_2)_2-C_6H_5$
2	$-(CH_2)_3-C_6H_5$
3	$-(CH_2)_4-C_6H_5$
4	$-(CH_2)_5-C_6H_5$
5	$-(CH_2)_2-CO-C_6H_5$
6	$-(CH_2)_3-CO-C_6H_5$
7	$-(CH_2)-CH=CH-C_6H_5$
8	$-(CH_2)_2-C_6H_{11}$

Die teikenverbinding is gesintetiseer deur 1,3-dimetiel-5,6-diaminourasiel te laat reageer met die toepaslike karboksielsuur in die teenwoordigheid van 'n karbodiïmied dehidrerende verbinding. Die verlangde inhibeerders is verkry na ringsluiting en metilering op die C-7 posisie. Rekombinante menslike MAO-A en MAO-B is gebruik om die inhiberingspotensies te bepaal. Hierdie inhiberingspotensies is as IC_{50}-waardes uitgedruk. 8-(5fenielpentiel)kafeïen **(4)** was die mees potente MAO-B-inhibeerder met 'n IC_{50}-waarde van 0.656 µM. In kontras hiermee was al die ander toetsverbindings matige MAO-B-inhibeerders. Trouens, die tweede beste inhibeerder, 8-(4-feniebutiel)kafeïen (**3**), met 'n IC_{50}-waarde van 3.25 µM, was ongeveer 5 keer minder potent as **4.** Aangesien die 5-fenielpentielgroep die langste syketting is wat hier geëvalueer is, dui hierdie studie aan dat langer c-8 sykettings gunstiger is vir MAO-B-inhibisie.

Dit is meer potent was as verbinding **1** (IC_{50} = 26.0 µM) wat oor 'n fenieletielverbindingsgroep beskik. Dit is 'n aanduiding dat 'n sikloheksielring in die C-8-posisie van die kafeïensyketting meer potent mag wees vir MAO-B inhibisie en dat dit oorweeg moet word vir verdere studie. Die kafeïenanaloë met die oksofenielalkielsykettings (**5** en **6**) was swak inhibeerders met IC_{50} waardes van onderskeidelik 187 µM en 46.9 µM. Dit is 'n aanduiding dat 'n karbonielgroep in die C-8-syketting nie gunstig is vir die MAO-B-inhibisie van kafeïen nie. Die onversadigde fenielpropenielanaloog 8, was ook 'n relatief swak MAO-B-inhibeerder met 'n IC_{50}-waarde van 33.1 µM.

In teenstelling met die resultate wat met MAO-B behaal is, was al die kafeïenanaloë swak MAO-A-inhibeerders. Met die uitsondering van verbinding **5** was al die verbindings selektiewe MAO-B-inhibeerders. Die mees potente MAO-B-inhibeerder, 8-(5-fenielpenteil) kafeïen (**4**) was die mees selektiewe inhibeerder – 48 keer meer potent vir MAO-B as vir MAO-A.

Hierdie studie het ook getoon dat twee geselekteerde analoë (**5** en **3**), omkeerbaar aan MAO-A en-B bind en dat die aard van MAO-A- en -B-inhibisie kompetitief is vir hierdie twee verteenwoordigende verbindings.

ABBREVIATIONS

AD	- Alzheimer's disease
CNS	- Central nervous system
CSC	- (E)-8-(3-chlorostyryl)caffeine
DA	- Dopamine
DMSO	- Bimethylsulphoxide
EI-MS	- Electron ionization mass spectrometry
FAD	- Flavin-adenine dinucleotide
GSH	- Glurathione
MAO-A	- Monoamine oxidase A
MAO-B	- Monoamine oxidase B
$MMDP^+$	- 1-Methyl-4-(1-methylpyrrol-2-yl)-2,3-dihydropyridinium
MMP^+	- 1-Methyl-4-(1-metylpyrrol-2-yl)pyridinium
MMTP	- 1-Methyl-4-(1-methylpyrrol-2-yl)-1,2,3,6-tetrahydropyridine
Mp	- Melting point
$MPDP^+$	- 1-Methyl-4-phenyl-2,3-dihydropyridinium
MPP^+	- 1-Methyl-4-phenylpyridinium

MPTP	- 1-Methyl-4-phenyl-1,2,3,6-tetrahydropyridine
NMR	- Nuclear magnetic resonance spectroscopy
PD	- Parkinson’s disease
SEM	- Standard error of mean
SN	- Substantia nigra
TLC	- Thin layer chromatography

Chapter 1
Introduction

1.1. Monoamine oxidase

Monoamine oxidase (MAO) consists of two isoforms, MAO-A and MAO-B. These two isoforms have different substrate and inhibitor specificities. MAO-A is mainly involved in the oxidative catabolism of serotonin and noradrenalin and is irreversibly inhibited by clorgyline, while MAO-B mainly catalyses the oxidation of benzylamine and is irreversibly inhibited by (*R*)-deprenyl. Both isoforms utilize dopamine as substrate (Youdim *et al*., 2006).

MAO-B is considered a drug target for the treatment of Parkinson's disease (PD) because it is a major enzyme responsible for the catabolism of dopamine in the substantia nigra of the brain. Inhibition of MAO-B could therefore, conserve dopamine in the brain and provide symptomatic relief. In addition to symptomatic relief, MAO-B inhibitors are thought to have neuroprotective properties (Youdim & Bakhle, 2006). One such inhibitor, selegiline, is currently being used in the treatment of PD. However, selegiline has major side effects caused by an irreversible mode of inhibition and the formation of potentially toxic metabolic by-products (Rascol *et al.*, 2002). This justifies the need to develop new reversible inhibitors of MAO-B as a potential treatment strategy for PD. Inhibition of MAO-A gives rise to higher serotonin levels, resulting in these compounds being used as antidepressants (Youdim *et al*., 2006).

Recently it was discovered that (E)-8-styrylcaffeine and several of its derivatives are potent reversible inhibitors of MAO-B (figure 1.1) (Vlok *et al*., 2006). For example, (*E*)-8-(3-chlorostyryl)caffeine (CSC), a member of the (E)-8-styrylcaffeine class of MAO inhibitors, is an exceptionally potent competitive inhibitor of MAO-B with an enzyme-inhibitor dissociation constant (K_i value) of 128 nM (Vlok *et al*., 2006). (E)-8-styrylcaffeines consist of a caffeine ring with a styryl side chain at C-8 of the caffeine ring. Both of these moieties are critical for the MAO-B inhibition activity of this class of compounds. (E)-8-styrylcaffeine is thought to exhibit a dual binding mode with the caffeine ring located in the substrate cavity of the MAO-B enzyme while the styryl side chain extends into the entrance cavity (Vlok *et al*., 2006). In contrast, caffeine only weakly inhibits the enzyme which indicates that substitution at C-8 enhances affinity of caffeine analogues for the active site of MAO-B.

1.2. Objectives of this study

In this study, the aim is to synthesize novel, reversible MAO-B inhibitors using (E)-8-styrylcaffeine as lead compound. Caffeine will be conjugated at C-8 to a variety of other side-chains. The effects of these chosen side-chains on the MAO-B inhibition activity of the C-8 substituted caffeine analogues will then be evaluated using the human recombinant enzyme. These caffeine analogues will also be evaluated as human MAO-A inhibitors. The MAO-A and –B inhibition potencies (IC_{50} values) of the test compounds will then be compared to that of (E)-8-styrylcaffeine. This study will therefore attempt to discover novel C-8 side chains that endow caffeine with more potent MAO-B inhibition activity than observed with the (E)-styryl side chain.

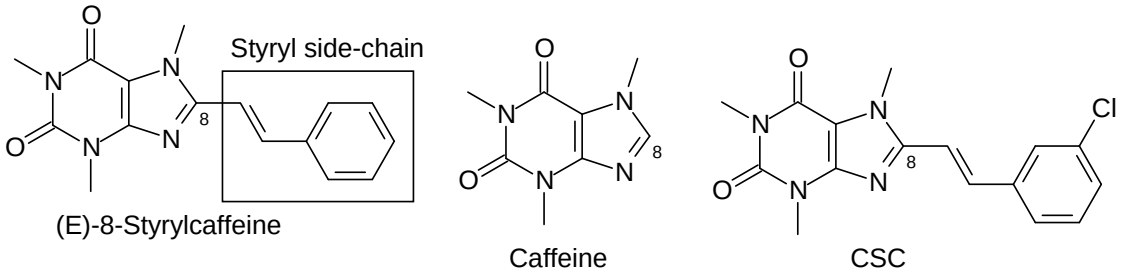

Figure 1.1. Structures of (E)-8-styrylcaffeine, caffeine and CSC

The present study is therefore an exploratory study to discover new C-8 moieties that are favorable for MAO inhibition. In this study, saturated side chains will be selected and substituted at C-8 of caffeine. The activities of this study can be summarized as follows:

1. A series of C-8 substituted caffeine analogues will be synthesized according to procedures described in the literature. The structures of the compounds that will be synthesized in this study are illustrated in figure 1.2.

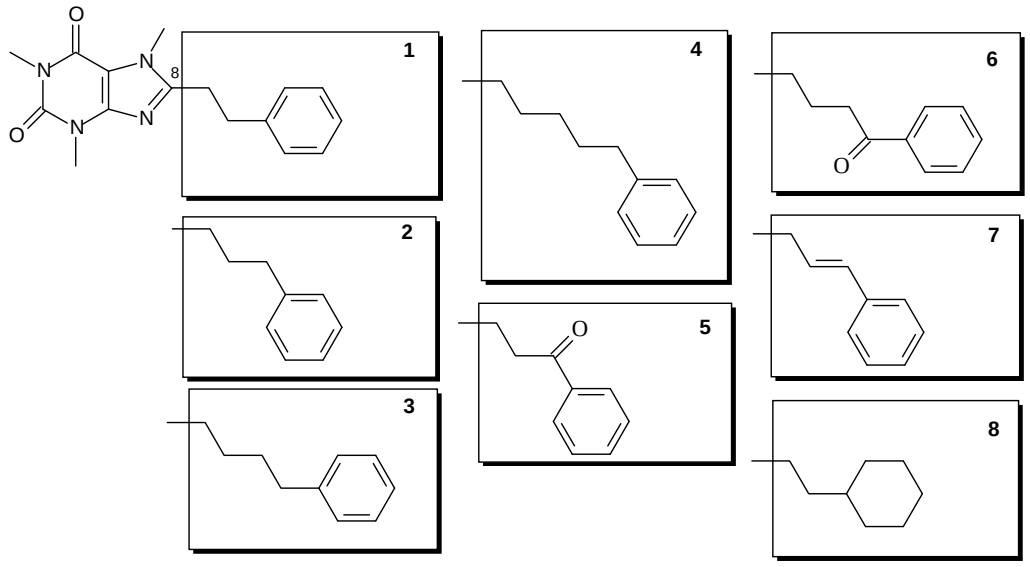

Figure 1.2. The structures of C-8 substituted caffeine analogues that will be examined in this study

- Linkers containing 2, 3, 4 and 5 carbon atoms will be used and will consist of the phenylethyl (**1**), phenylpropyl (**2**), phenylbutyl (**3**) and phenylpentyl (**4**) functional groups
- One compound with a cyclohexane ring, the corresponding cyclohexylethyl (**5**) will be included in the study
- Two compounds will have carbonyl functional groups in the side chain linker, the 3-oxo-3-phenylpropyl (**6**), 4-oxo-4-phenylbutyl (**7**) moieties
- One compound will have an unsaturated linker, the phenylpropenyl analogue **8**.

2. The C-8 substituted caffeine analogues will be evaluated as inhibitors of human MAO-A and MAO-B. For this purpose the recombinant human enzymes, which are commercially available, will be employed. The inhibition potencies will be expressed as the IC_{50} values (concentration of the inhibitor that produces 50% inhibition). A fluorometric assay will be used to measure the enzyme activities. The MAO activity measurements will be based on measuring the amount of 4-hydroxyquinoline that is produced when the substrate, kynuramine is oxidized by MAO. The quantity of 4-hydroxyquinoline in the reactions will subsequently be determined by measuring the fluorescence of the supernatant at an

excitation wavelength of 310 nm and an emission wavelength of 400 nm (Strydom *et al.,* 2010).

3. The time-dependency of inhibition of both MAO-A and –B by selected test inhibitors will be evaluated. This will be done in order to determine if the inhibitors interact reversibly or irreversibly with the MAO isozymes.

4. If the inhibition is found to be reversible, a set of Lineweaver-Burke plots will be generated for selected test inhibitors in order to determine if the mode of MAO-A and –B inhibition is competitive.
5. The MAO-A and –B inhibition potencies (IC_{50} values) of the test compounds will be compared to the IC_{50} values for the inhibition of MAO-A and –B by the lead compound, (E)-8-styrylcaffeine.

Chapter 2
Literature study

2.1 Parkinson's disease

2.1.1 General background

Parkinson's disease (PD) affects mostly older patients and has a mean onset of 55 years. Degeneration and death of dopaminergic neurons in the substantia nigra pars compacta region of the brain (SNpc) primarily cause depleted dopamine levels in the striatum, which result in PD (Przedborski, 2005).

Because dopamine depletion and neurodegeneration increase over time, the course of the disease is progressive. The motoric function of the body is controlled by dopamine and as the concentration of dopamine decreases in the brain, movement disorders such as tremor at rest, rigidity, slowness or involuntary movements, postural instability and freezing can occur (Przedborski, 2005). Although clinically and pathologically similar, familial and sporadic PD are very different in many significant aspects. Both, however, exhibit a dramatic depletion of dopamine in the brain.

Intraneuronal inclusions, called Lewy bodies, are a significant feature of the neurological profile of a patient suffering from PD. Lewy bodies, found in all affected brain areas, are spherical eosinophilic cytoplasmic aggregates that consist of a variety of proteins, such as neurofilaments, parkin, α- synuclein and ubiquitin (Przedborski, 2005).

Uncertainty still remains about the role of environmental and genetic factors, and their contribution to the development of PD (Dauer & Przedborski, 2003).

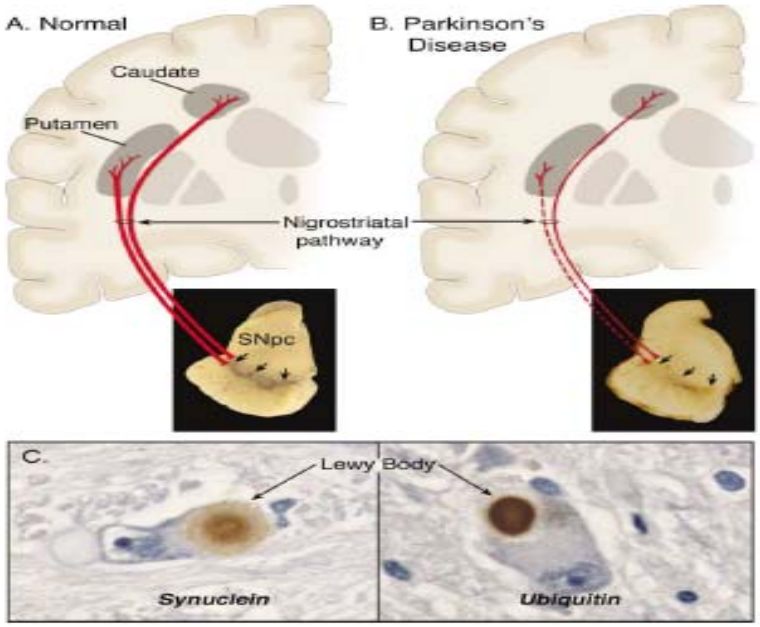

Figure 2.1.1 Neuropathology of Parkinson's disease (a) showing a normal nigrostriatal pathway, (b) a diseased nigrostriatal pathway with depigmentation of the SNpc as the the nigrostriatal pathway degenerates and (c) immunohistochemical labelling of intraneuronal inclusions, termed Lewy bodies, in a SNpc dopaminergic neuron (Daeur & Przedborski, 2003).

Monoamine oxidase, iron and neurodegenerative disease

The levels of iron in animals and humans are known to have an influence on the activity of monoamine oxidase (Symes *et al*., 1969; Youdim *et al*., 1975). More links between iron and CNS dysfunction have been uncovered over the years, for example, the sites of neuronal death in the brain, of a patient suffering from PD, are also sites at which iron accumulates (Zecca *et al*., 2004: Mandel *et al*., 2005).

It appears that oxidative stress may be the link between MAO, neuronal damage and iron. Hydrogen peroxide is a normal by-product of monoamine oxidation by MAO. In the Fenton reaction, iron (Fe^{2+}) reacts with hydrogen peroxide to produce the highly reactive hydroxyl free radical (Figure 2.1.3). The hydroxyl radical reacts with and damages lipids, proteins and DNA and decreases cellular anti-oxidants. Another factor which may contribute to oxidative stress is reduced brain levels of glutathione (GSH) found in PD

patients.Glutathione peroxidase uses GSH to reduce and inactivate hydrogen peroxide in the brain. Low levels of brain GSH may therefore result in increased levels of hydrogen peroxide which is then available for the Fenton reaction (Riederer *et al*., 1989).

As age increases, brain iron and brain MAO-B also increases. Since these are both components of the Fenton reaction, the potential for hydroxyl radical generation is increased. Several previous studies have shown increased activity of MAO-B in the brain and blood platelets of patients suffering from neurodegenerative diseases such as PD and Alzheimer's disease (AD). The use of MAO inhibitors in these patients will have more than one beneficial effect. Inhibitors will increase the levels of monoamines, so that the membrane receptors can be activated, and will also decrease the production of hydrogen peroxide and the potential for producing the hydroxyl radical and the consequent oxidative stress.

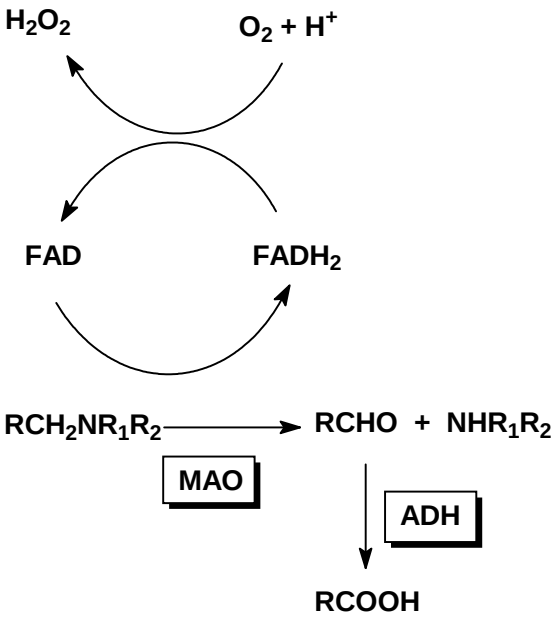

Figure 2.1.2 Reaction pathway of monoamine metabolism by oxidative deamination by mitochondrial MAO (Youdim & Bakhle, 2006).

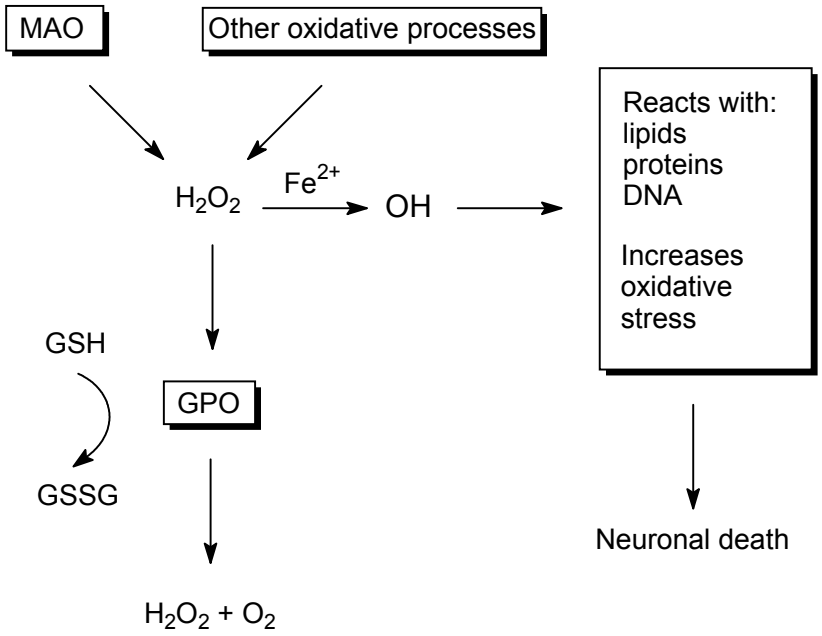

Figure 2.1.3 The mechanism of neurotoxicity induced by iron and hydrogen peroxide, via the Fenton reaction (Youdim & Bakhle, 2006).

2.1.2 Treatment

The main goal in the treatment of patients suffering from PD is to restore the function of striatal dopamine. Almost all of the drugs that are used to manage the motor symptoms and complications in PD are based on this specific strategy. To restore the function of dopamine in the striatum, the dopamine precursor, levodopa, is most often used (Lees, 2005).

In recent years, the focus has shifted to an approach which involves neuroprotection, instead of symptomatic treatment. While levodopa relieves the symptoms of PD, it does not protect against neurodegeneration. Effective therapy in PD should prevent the progression of the disease and eradicate the motor and cognitive handicap. So far, none of the existing drugs have met all of these requirements.

2.1.2.1 Levodopa

Orally administered levodopa (L-3,4-dihydroxyphenylalanine) (Figure 2.1.4) has been one of the first successful methods to treat the symptoms of Parkinson's disease (Lees, 2005). Levodopa is currently still the most important drug for the treatment for PD (Factor, 2008). The drug, which is absorbed rapidly from the small bowel by the transport system for aromatic amino acids, has a very high patient coherence due to its oral administration. Since dietary amino acids compete with the compound for absorption, patients should have the correct diet to prevent sub-optimal absorption of the drug.

Levodopa cannot cross the bloodbrain-barrier via passive diffusion and uses the transport system for amino acids to enter the brain. As in the gastrointestinal tract, amino acids also compete with levodopa for entry into the brain.

In the brain, decarboxylation converts levodopa to dopamine, primarily within the presynaptic terminals of dopaminergic neurons in the striatum. The therapeutic effectiveness of levodopa in PD depends on the dopamine it produces. After dopamine is released, it is either transported back into dopaminergic terminals by the presynaptic uptake mechanism or metabolized by the actions of catechol-O-methyltransferase (COMT) or MAO. In practice, carbidopa (Figure 2.1.5), a peripherally acting inhibitor of aromatic L-amino acid decarboxylase, is almost always administered in combination with levodopa. Carbidopa does not penetrate well into the CNS and therefore does not inhibit the decarboxylation of levodopa in the brain. Less than 1% of the levodopa will penetrate the CNS if it is administered alone. Levodopa is to a large degree decarboxylated by enzymes in the intestinal mucosa and other peripheral sites. The aim is to inhibit peripheral decarboxylase and, as a result, more of the administered levodopa would then cross the blood-brain barrier and penetrate the CNS. This can also reduce the incidence of gastrointestinal side-effects. Levodopa therapy can be used to treat the signs and symptoms of PD (Lees, 2005).

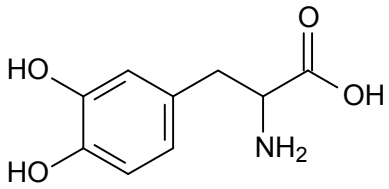

Figure 2.1.4 The chemical structure of L-Dopa

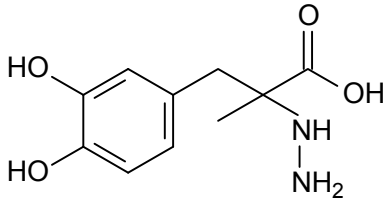

Figure 2.1.5 The chemical structure of carbidopa, a peripheral decarboxylase inhibitor

Levodopa treatment is effective for about 3-4 years. After this period, complications with this therapy can occur. Gastric effects, like nausea, vomiting and anorexia are some of the adverse effects. Cardiovascular effects include cardiac arrhythmias. Dyskinesia is probably the most marked effect with long term levodopa therapy. These include chorea, ballismus, dystonia, tics, tremors, myoclonus and athetosis (Lees, 2005).

2.1.2.2 Dopamine receptor agonists

Dopamine receptor agonists are direct agonists of striatal dopamine receptors. This approach offers several potential advantages. These drugs do not require enzymatic conversion, thus they do not depend on the functional capacities of the nigrostriatal neurons. Dopamine agonists have a longer lasting therapeutic effect than levodopa and therefore are useful in the management of dose-related fluctuations in motor state. By lowering endogenous release of dopamine and also the need for exogenous levodopa, dopamine receptor agonists may be able to change the course of PD (Deleu *et al., 2002*).

Dopamine agonists act on the dopamine D_2-receptors, thus striatal dopaminergic output increases (Deleu *et al*., 2002). Bromocriptine (PARLODEL) (Fig 2.1.6), pergolide (PERMAX) (Fig 2.1.7), ropinirole (REQUIP) (Fig 2.1.8) and pramipexole (MIRPEX) (Fig 2.1.9) are orally administered dopamine receptor agonists that are available for the treatment of PD. Bromocriptine and pergolide are older agents, and are both ergot derivates, which have similar spectra of therapeutic effectiveness and adverse effects. Ropinirole and pramipexole are newer, more selective compounds (specifically regarding D_2 and D_3 receptor proteins). All four of these drugs can relieve the clinical symptoms of PD (Lees, 2005).

The benefits and risks of early agonist therapy must be carefully balanced in older patients as elderly patients have a greater rate of unendurable adverse effects, such as hallucinations, orthostatic hypotention, somnolence and oedema (Lees, 2005).

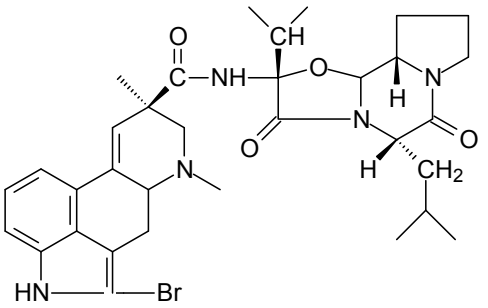

Figure 2.1.6 The chemical structure of bromocriptine

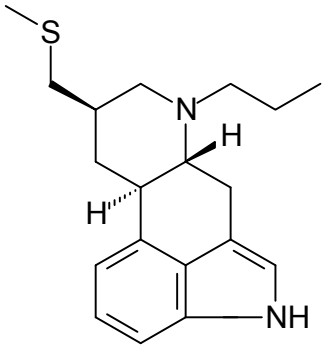

Figure 2.1.7 The chemical structure of pergolide

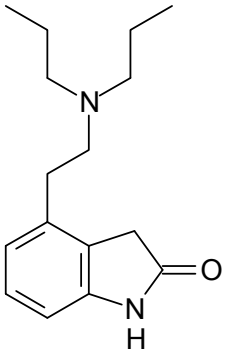

Figure 2.1.8 The chemical structure of ropinirole

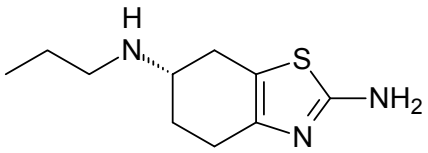

Figure 2.1.9 The chemical structure of pramipexole

2.1.2.3 Catechol-O-methyltransferase (COMT) inhibitors

COMT inhibitors are also used in the treatment of PD. COMT is an enzyme responsible for the catabolism of dopamine and also levodopa. 99% of orally administered levodopa is catabolized and will not reach the brain. Inhibitors of COMT are used to prevent the conversion of levodopa to 3-O-methyl DOPA, thus increasing both the plasma half-life of levodopa and the percentage of the dose that reaches the CNS.

Tolcapone (TASMAR) and entacapone (COMTAN) are two COMT inhibitors that are currently being used in the United States. Tolcapone and entacapone have been shown to reduce the clinical symptoms of 'wearing off' in patients suffering from PD who are treated with levodopa (Parkinson Study Group, 1996). Tolcapone has a longer duration of action than entacapone, which has to be administered simultaneously with each dose of levodopa and/or carbidopa. Adverse effects of both these agents include nausea, orthostatic hypotention, confusion, vivid dreams and hallucinations. Hepatotoxicity is an important adverse effect associated with tolcapone. A fixed-dose combination of entacapone with levodopa and/or carbidopa is also available and is very effective for treating the symptoms of PD.

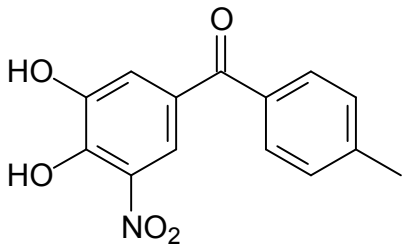

Figure 2.1.10 The chemical structure of tolcapone

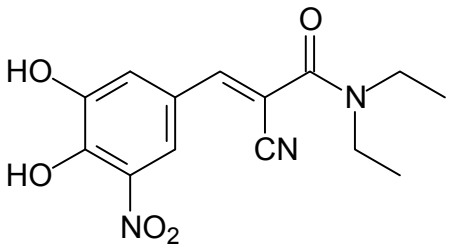

Figure 2.1.11 The chemical structure of entacapone

2.1.2.4 Selective MAO-B inhibitors

Monoamines are oxidized by two isoenzymes of MAO, MAO-A and MAO-B. MAO-A and MAO-B are both present in the periphery and inactivate monoamines of intestinal origin. MAO-B is the most important form in the striatum and oxidizes most of the dopamine in

the brain. At doses of 10 mg/day or less, selegiline (ELDEPRYL) (Figure 2.1.12) selectively inhibits MAO-B, which leads to irreversible inhibition of MAO-B (Olanow, 1993).

Selegiline can be taken safely with levodopa, because of the fact that it does not inhibit peripheral metabolism of catecholamines. MAO inhibitors such as phenelzine, tranylcypromine and isocarboxazid, in contrast, are nonspecific inhibitors of MAO and may lead to serious adverse effects when the peripheral oxidation of catecholamines by MAO-A is also inhibited. High doses of selegiline should be avoided and dosages should not exceed 10 mg per day due to the fact that higher doses can produce inhibition of MAO-A. Selegiline decreases the catabolism of dopamine in the striatum and although its benefit is modest, it has been used as a symptomatic treatment for PD for numerous years.

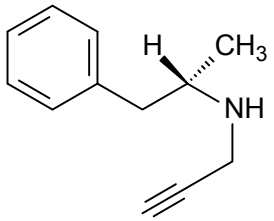

Figure 2.1.12 The chemical structure of selegiline

According to Lees (2005) and Riederer *et al* (2004a), selegiline is not effective as a monotherapy drug in the treatment of PD. Selegiline is metabolized to toxic metabolites (L-N-desmethylselegiline, L-metamphetamine and L-amphetamine) (Figure 2.1.13) that are responsible for the observed psychotoxic effects and higher incidence of cardiovascular events and could also cause adverse symptoms, including anxiety and insomnia. Rasagiline, also a MAO-B inhibitor, does not give rise to these undesirable metabolites. The efficacy of rasagiline has been shown in both early and advanced PD (Riederer *et al*., 2004a). Rasagiline is currently used, in conjunction with levodopa, to treat levodopa induced motor fluctuations.

A MAO inhibitor specific for the MAO-B isoform should be used for treating PD. When the MAO inhibitor also inhibits MAO-A, as with tranylcypromine, the 'cheese reaction' may develop. Tyramine is an indirect acting symptomimetic agent, found in fermented foods and is metabolized by MAO-A. Combining MAO-A inhibitors with tyramine

containing foods can induce a hypertensive crisis due to the higher concentration of tyramine and an enhanced symptomatic response, which can be fatal in some cases.

Rasagiline and selegiline, both specific MAO-B inhibitors, do not cause the 'cheese reaction' (Lees, 2005: Youdim & Bakhle, 2006; Przedborski, 2005; Riederer *et al*., 2004b).

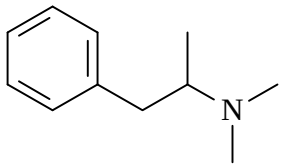

Figure 2.1.13 The chemical structure of metamphetamine, a metabolite of selegiline

2.1.2.5 Muscarinic receptor antagonists

Muscarinic acetylcholine receptor antagonists were used extensively for treating PD, before levodopa was discovered. Trihexyphenidyl (ARTANE) (Figure 2.1.14), benztropine mesylate (COGENTIN) and diphenhydramine hydrochloride (BENADRYL) (Figure 2.1.15) are a few of the drugs with anticholinergic properties that are currently still being used to treat PD. They all are useful in the treatment of early PD or as an adjunct to dopamimetic therapy. Adverse effects of these drugs include sedation and mental confusion, constipation, urinary retention and blurred vision as a result of cycloplegia. Patients suffering from narrow-angle glaucoma should be very cautious of muscarinic receptor antagonists.

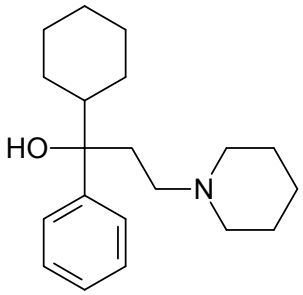

Figure 2.1.14 The chemical structure of trihexyphenidyl

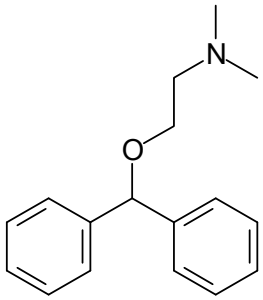

Figure 2.1.15 The chemical structure of diphenhydramine

2.1.2.6 Amantadine

Amantadine (SYMMETREL) (Figure 2.1.16) is an antiviral drug. It is used for the treatment as well as the prophylaxis of influenza A, but also has anti-parkinsonian activity. It is thought to enhance dopamine release in the striatum, and also has the significant ability to block NMDA glutamate receptors. Amantadine's effects in PD are modest (Hallett & Standaert, 2004).

Amantadine is used as initial therapy of mild PD, but is also used in patients, treated with levodopa, suffering from dose-related fluctuations and dyskinesias. It is administered in a dose of 100 mg twice a day and adverse effects are mild and reversible.

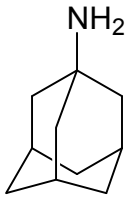

Figure 2.1.16 The chemical structure of amantadine

2.1.3 Drugs for neuroprotection

Many drugs have shown promise as neuroprotectants in animal PD models, but these results have not yet translated into therapies that are clearly neuroprotective in human PD. The barriers to establishing a neuroprotective therapy, stem from the complexity of the disease process as well as the limits of the clinical tools available to monitor the

progression of the disease. These are both extremely important factors in seeking a neuroprotective effect (Yacoubain & Standaert, 2009).

2.1.3.1 Levodopa as a neuroprotective agent – the ELLDOPA trial

There has been concern that treatment of PD patients with L-dopa could potentially promote neurodegeneration in PD, because of the free radicals produced by dopamine catabolism. Contrary to this concern, a variety of preclinical data has shown a neuroprotective effect (LeWitt & Taylor, 2008). At this time, it is uncertain whether L-dopa is neuroprotective, but the risk of its potential toxicity has been somewhat reduced by the ELLDOPA trial (Yacoubain & Standaert, 2009).

2.1.3.2 Dopamine receptor agonists

Dopamine receptor agonists have been hypothesized as being potentially neuroprotective. The agonists act upon the D_2 autoreceptors found on SN terminals. Here the agonists suppress dopamine release, which leads to reduced oxidative stress (LeWitt & Taylor, 2008). Dopamine receptor agonists can also reduce dopaminergic cell death.

2.1.3.3 Antioxidant therapies

Several antioxidant agents have been studied in clinical trials, including selegiline, vitamin E, rasagiline, coenzyme Q10 and creatine. Selegiline, a MAO-B inhibitor, reduces dopamine oxidation and significantly delayed the time of onset of L-dopa treatment (LeWitt & Taylor, 2008). There were no differences between patients treated with vitamin E and placebo-treated patients. Vitamin E had no added beneficial effects on patients being treated with selegiline. Rasagiline, a newer and more potent MAO-B inhibitor than selegiline, has metabolites with potential antioxidant properties (Yacoubain & Standaert, 2009). Coenzyme Q10 is a cofactor in the electron transport chain in the mitochondria and studies in mouse PD models have shown reduced dopaminergic neurodegeneration (Yacoubain & Standaert, 2009). Creatine promotes mitochondrial ATP production and has shown to be neuroprotective in animal PD models (LeWitt & Taylor, 2008).

2.1.3.4 Anti-apoptotic agents

Anti-apoptotic agents have been examined in clinical trials. The glycolytic enzyme glyceraldehydes-3-phosphate dehydrogenase (GAPDH), which can initiate apoptosis, is inhibited by the propargylamine TCH346 (LeWitt & Taylor, 2008). The propargylamine TCH346 is therefore an anti-apoptotic factor. TCH346 has effected reduced dopaminergic cell loss in both 6-OHDA and 1-methyl-4-phenyl-1,2,3,6-tetrahydropyridine (MPTP) animal models (Yacoubain & Standaert, 2009).

2.1.3.5 Trophic factors

Several neurotrophic factors have been evaluated in human clinical trials. So far, the delivery is primarily by direct infusion of the protein into the brain (Ho *et al*., 2000). A small trial has shown effectiveness. Recent gene therapy efforts have used a neurotrophic factor related to glial-derived neurotrophic factor (GDNF), neurturin, that also promotes dopaminergic neuronal survival in cultures (Ho *et al*., 2000).

2.1.3.6 Adenosine receptor antagonists

Epidemiological studies have shown that caffeine may reduce the incidence of PD in men. Clinical trials of the A_{2A} antagonist, istradefylline, have indicated potential symptomatic effects in advanced PD. Caffeine and istradefylline are both neuroprotective in MPTP animal models. Caffeine has also been identified as a priority agent to be tested for neuroprotection in clinical trials (Yacoubain & Standaert, 2009).

2.1.3.7 Anti-inflammatory agents

The role of inflammation in PD has recently become more recognized. NSAIDs have shown to lower the risk of PD by 45% (Yacoubain & Standaert, 2009). Minocycline, a second generation tetracycline and inflammatory agent, blocks microglial activation and may also have anti-apoptotic activity in culture. Minocycline also protects against dopaminergic cell loss in both the MPTP and 6-OHDA animal models (Yacoubain & Standaert, 2009).

2.1.4 Mechanisms of neurodegeneration

Current therapies for PD significantly improve the quality of life for patients suffering from this neurodegenerative disease (Yacoubain & Standaert, 2009). The goal, however, is to prevent the progression of the disease. Mechanisms of neurodegeneration include oxidative stress, mitochondrial dysfunction, protein aggregation and misfolding, inflammation, excitotoxicity, and apoptosis (Yacoubain & Standaert, 2009).

2.1.4.1 Oxidative stress and mitochondrial dysfunction

An overabundance of reactive free radicals, secondary to either an overproduction of reactive species or a failure of cell buffering mechanisms that normally limit their accumulation, results in oxidative stress. Oxidative stress is promoted by dopamine metabolism through the production of quinines, peroxides and other reactive oxygen species (ROS). Another source for the production of ROS is mitochondrial dysfunction. MPP^+ and rotenone, both inhibitors of complex I, in the mitochondrial oxidative chain, cause a parkinsonian syndrome in animal models (Yacoubain & Standaert, 2009).

2.1.4.2 Protein aggregation and misfolding

Protein aggregation and misfolding are important mechanisms in many neurodegenerative disorders, including PD, AD, and Huntington's disease. The primary aggregating protein in PD is alpha-synuclein (α-syn). α-Synuclein is the main component of lewy bodies and lewy neurites found in sporadic PD. Gene duplication of the α-syn locus also causes PD. Overproduction or impaired clearance of α-syn results in aggregation and may be a central mechanism for PD (Yacoubain & Standaert, 2009).

2.1.4.3 Neuroinflammation

It has been increasingly recognised than neuroinflammation is a primary mechanism involved in PD pathogenesis. Activation of microglia has been demonstrated in the SN and striatum from post mortem PD brains. Treatment with anti-inflammatory agents has been investigated to establish their neuroprotective potential. NSIADs reduce dopaminergic cell death in animal PD models (Yacoubain & Standaert, 2009).

2.1.4.4 Excitotoxicity

Glutamate is the primary excitatory transmitter in the mammalian central nervous system. Excessive NMDA receptor activation by glutamate has the potential to increase intracellular calcium levels that then activate cell death pathways. Calcium influx can also promote peroxynitrite production through the activation of nitric oxide synthase. NMDA receptor antagonists protect against dopaminergic cell loss in MPTP models (Yacoubain & Standaert, 2009).

2.1.4.5 Apoptosis

Programmed cell death, or apoptosis, is a mechanism that has been identified to participate in neural development and to be responsible for some forms of neural injury. Activation of cell death pathways most likely represents end-stage processes in PD neurodegeneration. Inhibitors of cell death pathways have been proposed as potential neuroprotective agents regardless of the initial cause for neurodegeneration in PD (Yacoubain & Standaert, 2009).

2.1.4.6 Loss of trophic factors

The loss of trophic factors has been demonstrated as a potential contributor to cell death observed in PD. As a result, treatment with growth factors has been proposed as a potential neuroprotective therapy in PD. Glial-derived neurotrophic factors (GDNF) and a related growth factor, neurturin, are both protective against neurodegeneration in animal PD models (Yacoubain & Standaert, 2009).

2.2. Monoamine oxidase

2.2.1 General background of MAO-B

Monoamine oxidase (MAO) activity is very important for normal brain function and development, and plays a major role in various aspects of personality and addictive behaviour (Youdim *et al*., 2006).

MAO is a flavin-adenine dinucleotid (FAD) containing enzyme, located on the outer membrane of the mitochondria of certain cells. MAO consists of two isoforms (MAO-A and MAO-B) and they are both present in most mammalian tissues, but the proportion of the two isoenzymes vary from tissue to tissue (Binda *et al*., 2002a). They share 70% sequence identity as deduced from their cDNA clones and for each, the FAD co-factor is covalently attached to a conserved cysteinyl residue via a thioether linkage (Edmondson *et al*., 2004). The two isoforms have different substrate and inhibitor specificities, whilst MAO-B is mainly responsible for dopamine oxidation.

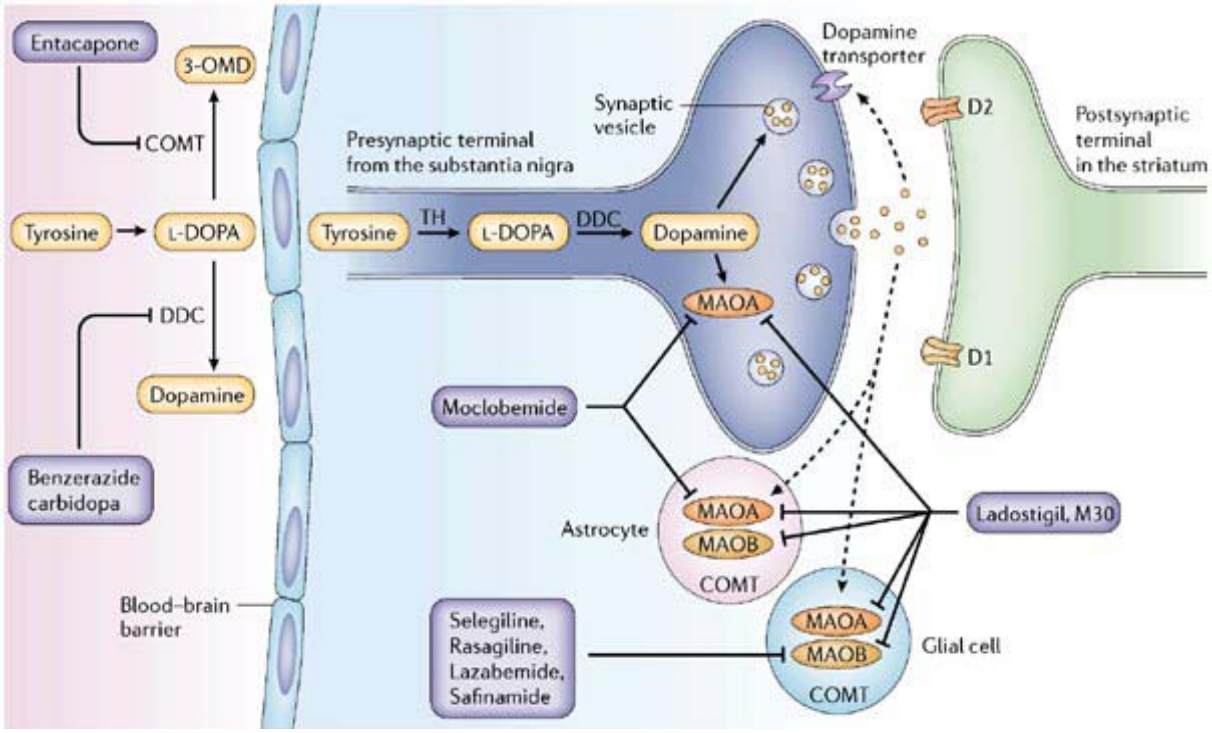

Figure 2.2.1 Dopamine synthesis and its metabolism by MAO-A and MAO-B (Youdim *et al*., 2006)

MAO-B catalyzes the oxidation of a variety of amines to their corresponding aldehydes. These include monoamines which are oxidized to ammonia and hydrogen peroxide. These products, in high concentrations, can be damaging and harmful to tissues and may contribute to neurodegeneration as seen in PD (Riederer *et al*., 2004b).

MAO-B can be obtained from various sources. A particularly important method is the recombinant expression of MAO-B by the *Pichia pastoris* yeast (Newton-Vinson *et al*., 2000). MAO-A can be extracted from human placenta and MAO-B from blood platelets and bovine liver (Salach *et al*., 1987; Vlok *et al*., 2006). MAO-B is a membrane bound enzyme and its activity may rely on this. Reduction in activity is observed when enzymatically extracting MAO-B from the mitochondrial membrane (Newton-Vinson *et al*., 2000).

Inhibiting MAO-A and MAO-B may have a range of therapeutic benefits. MAO-A inhibitors are already being used as anti-depressant drugs. MAO-B inhibitors, for example selegiline, are used to treat patients suffering from PD (Youdim *et al*., 2006).

Dopamine is metabolized by MAO-A, as well as by MAO-B. The striatum contains MAO-A (Green *et al*., 1977). If one isoform of MAO is fully inhibited, the other isoform will metabolize dopamine adequately (Youdim *et al*., 1972; Riederer & Youdim, 1986), suggesting that the levels of dopamine in the human striatum will not change drastically, with selective inhibition of MAO-A or MAO-B (Riederer & Youdim, 1986).

2.2.2 Biological function of MAO-B

Monoamine oxidase B is an important enzyme in the treatment of PD. In PD patients there are usually an increase in MAO-B levels and a decrease in dopamine levels in the brain. MAO-B deaminates arylalkyamines such as benzylamine and phenylethylamine and is irreversibly inhibited by selegiline. MAO-B is mainly responsible for dopamine oxidation. The role of MAO-B in serotonergic neurons is to eliminate foreign amines and to minimize their access to synaptic vesicles (Youdim *et al*., 2006).

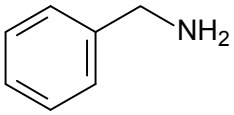

Benzylamine

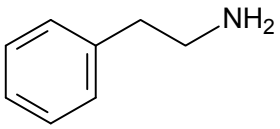

Phenylethylamine

Figure 2.2.2 The chemical structures of benzylamine and phenylethylamine

2.2.3 Biological function of MAO-A

Monoamine oxidase A is an important enzyme in the treatment of depression. MAO-A preferentially deaminates serotonin and norepinephrine, and is irreversibly inhibited by tranylcypromine.

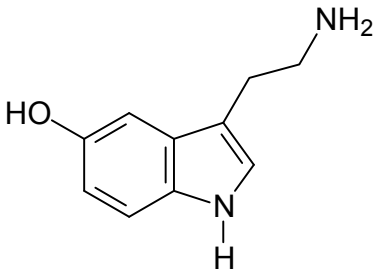

Serotonin

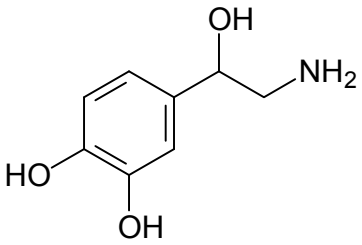

Norepinephrine

Figure 2.2.3 Chemical structures of serotonin and norepinephrin

2.2.3.1 The cheese reaction

Tranylcypromine was one of the first clinically used MAO-inhibitors. A potentially serious side effect of tranylcypromine is that it induces the 'cheese reaction' (Youdim & Bakhle, 2006). Tyramine and other indirectly acting sympathomimetic amines, present in some food and fermented drinks, induce the 'cheese reaction'. In the presence of a non-selective irreversible MAO inhibitor, MAO-A in the gastrointestinal tract is inactivated and tyramine is no longer metabolized by MAO-A and enters the circulation. A significant amount of noradrenaline is released from peripheral adrenergic neurons and leads to a severe hypertensive response, which can be fatal in some cases (Finberg *et al*., 1981; Finberg *et al.,* 1982; Youdim *et al*., 2006).

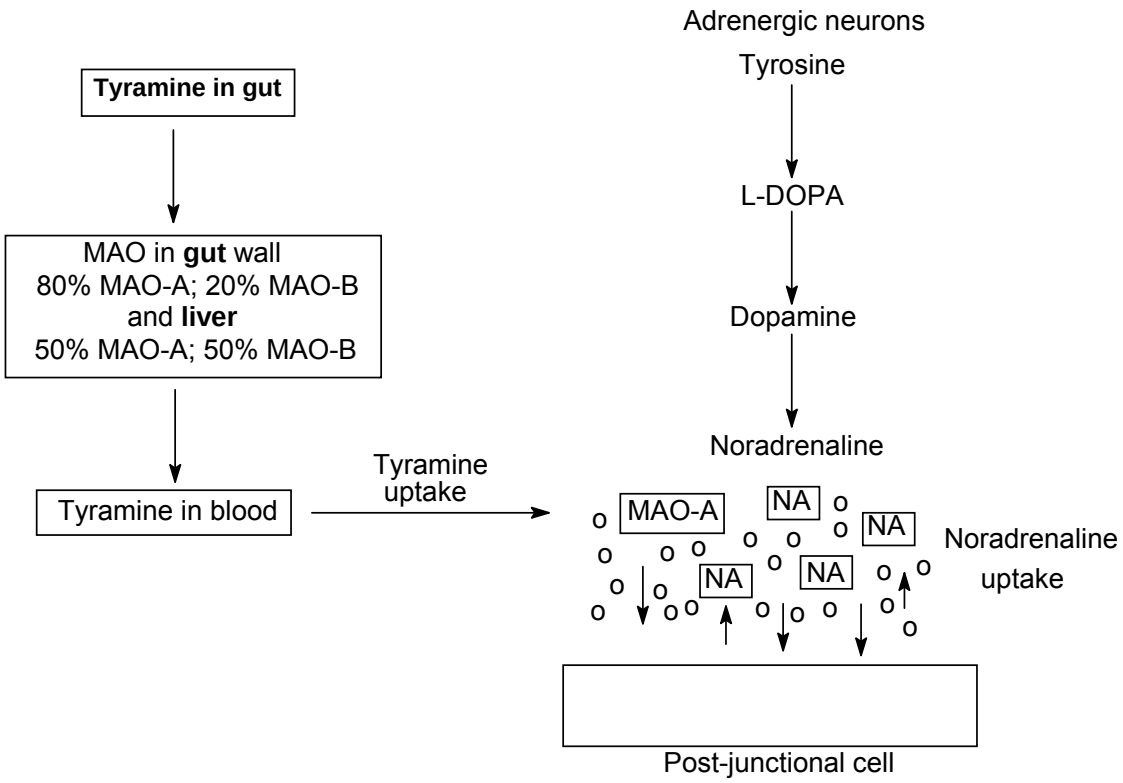

Figure 2.2.4 The 'cheese reaction' (Youdim & Bakhle, 2006)

Table 1 MAO inhibitors used and under development in the treatment of depression and PD (Youdim & Bakhle, 2006).

Antidpressant	Inhibitor selectivity	Mode of action
Iproniazid	A + B	Irreversible
Phenelzine	A + B	Irreversible
Isocarboxazid	A + B	Irreversible
Tranylcypromine	A + B	Irreversible
Nialamide	A + B	Irreversible

Clorgyline	A	Irreversible
Moclobemide	A	Reversible
Brofaromine	A	Reversible
Under development		
Ladostigil	A + B	Irreversible
M30	A + B	Irreversible
Befloxatone	A	Reversible
Anti-PD		
Selegiline	B	Irreversible
Rasagiline	B	Irreversible
Lazabemide	B	Reversible
Under development		
M30	A + B	Irreversible
Ladostigil	A + B	Irreversible

2.2.4 The role of MAO-B in Parkinson's disease

The primary role of MAO-A and MAO-B include the regulation of biogenic and xenobiotic amines in the brain and the peripheral tissue by catalyzing their oxidative deamination. Dopamine is metabolized in the brain primarily by MAO-B. This reaction yields toxic by-products including dopaldehyde, hydrogen peroxide and ammonia. Patients suffering from PD exhibit low glutathione peroxide and aldehyde dehydrogenase activities, which metabolizes H_2O_2 and aldehydes, respectively. High concentration of aldehydes are neurotoxic and harmful, while H_2O_2 contributes to ROS formation and damages neuronal cells (Riederer *et al*., 2004b).

Inhibition of MAO-B reduces the production of these toxic by-products and may therefore be used to prevent further neurodegeneration. MAO-B inhibitors conserve depleted dopamine and therefore may be used to treat the symptoms of PD (Youdim & Bakhle, 2006).

MAO-B inhibitors are used in combination with levodopa, since this combination significantly elevates dopamine levels in the striatum, resulting in relief from the symptoms of PD (Lees, 2005).

It is therefore evident that inhibition of MAO-B could relieve the symptoms of PD, firstly by causing increased dopamine levels and secondly by preventing the production of aldehydes and H_2O_2, MAO-B inhibition could arrest neurodegeneration (Fernandez *et al*., 2007).

2.2.5 Catalytic cycle of MAO-B

MAO-A and MAO-B are flavin containing enzymes, thus they both rely on a FAD co-factor for catalysis. MAO-B catalyses the oxidation of some amines and during this process the FAD co-factor is reduced and an imine is yielded (Figure 2.2.7). The yielded primary imine is hydrolyzed to produce an aldehyde and ammonia, and in the case of secondary or tertiary amines, another amine will be produced. The reduced FAD reacts with oxygen to produce H_2O_2. Oxygen is therefore the last electron acceptor to produce the potentially harmful by-product, H_2O_2 (Edmondson *et al*., 2004).

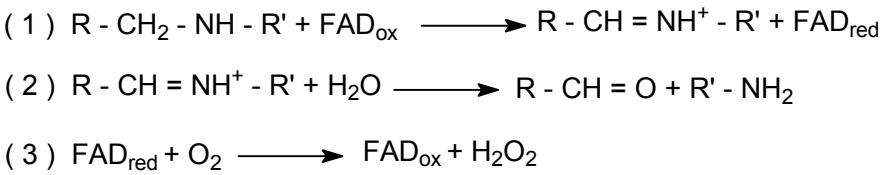

Figure 2.2.5 The oxidation reaction catalyzed by MAO-B

There are two proposed mechanisms for MAO catalysis (Silverman, 1995).

1.) The single electron transfer (SET) mechanism

2.) The polar nucleophilic mechanism

2.2.5.1 The SET mechanism

The generally accepted mechanism for the MAO catalyzed α-carbon oxidation of amines, according to Silverman (Silverman, 1995), proceeds via an initial single electron transfer step (Figure 2.2.6), from the nitrogen lone pair of the substrate to the oxidized flavin FAD, to generate an aminyl radical cation and the flavin semiquinone FAD. α-Carbon deprotonation then yields the α-amino radical. This α-amino radical transfers the second electron to the semiquinone to give the reduced flavin $FADH^-$ and the iminium ion.

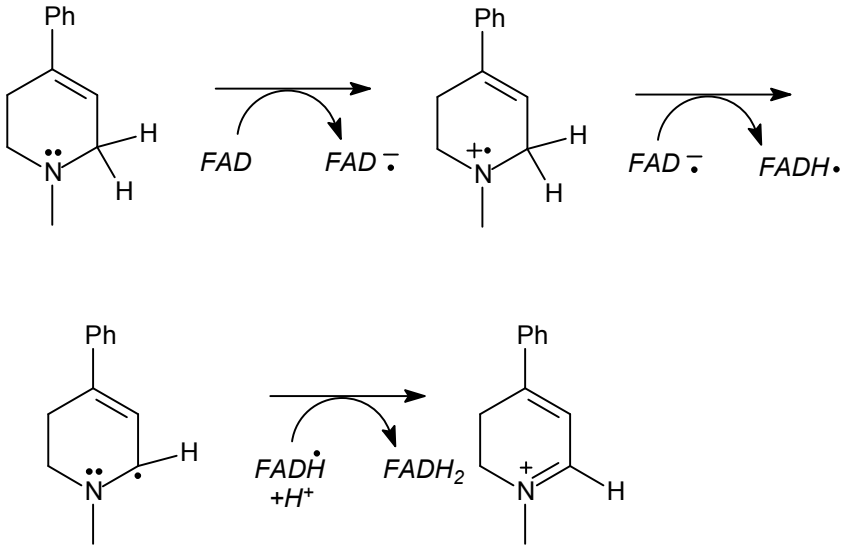

Figure 2.2.6 The proposed SET oxidation pathways for MAO catalysis as illustrated with MPTP as substrate (Silverman, 1995).

2.2.5.2 The polar-nucleophilic mechanism

An early proposal, based on flavin model reactions, suggested a polar nucleophilic mechanism, which involved attack of the deprotonated amine substrate at the flavin C-4a position, to form a substrate–flavin adduct (Figure 2.2.7). This is followed by proton abstraction from the *α*-carbon of the amine-flavin adduct that occurs by an active site base on the enzyme. Formation of the protonated imine product results from its elimination from the reduced flavin. The reactivity at the flavin C-4a atom is considered additional evidence for this catalytic mechanism. In lieu of active site base, the highly basic N5 atom of the flavin, which is generated following nucleophilic attack of the substrate, may also act as base for the deprotonation of the substrate α-carbon (Miller & Edmondson, 1999).

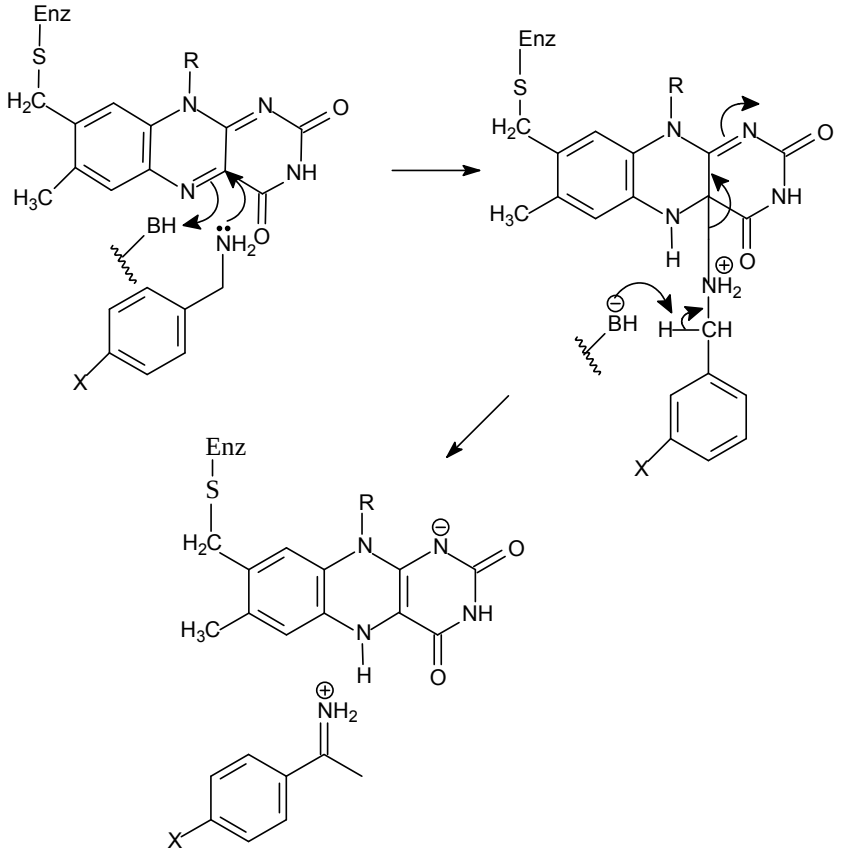

Figure 2.2.7 The proposed polar nucleophilic mechanism for MAO catalysed oxidation of benzylamine (Miller & Edmondson, 1999).

Selegiline, a mechanism-based inhibitor of MAO-B is also a substrate for MAO-B. MAO-B substrates are thought to react with the FAD co-factor at the 5 or 4a position. The FAD is then reduced while the substrates are oxidized. In the first step the substrate's amine binds to the specific position (5 or 4a) on the FAD co-factor. This position depends on the properties of the substrate. In the second step an interaction occurs between the substrate and the FAD co-factor, resulting in the cleavage of the α-CH bond of the substrate with the simultaneous reduction of the FAD co-factor (Li *et al*., 2006). The irreversible inhibitor of MAO-B, rasagiline, binds to position 5 of FAD (Figure 2.2.8) (Binda *et al*., 2004).

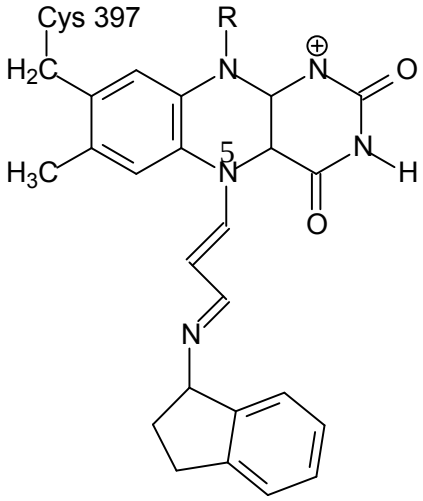

Figure 2.2.8 Rasagiline binds at position 5 of the FAD co-factor

MPTP is a pro-neurotoxin, inducing Parkinsonlike symptoms. MAO-B catalyses the two electron oxidation of MPTP to produce $MPDP^+$, an intermediate product. $MPDP^+$ is further oxidized by another two electron oxidation, via an unknown mechanism, to form the active toxin, MPP^+. MPP^+ leads to a syndrome that is pathologically and symptomatically similar to PD. The mechanism by which MPTP is oxidized to MPP^+ is shown in Figure 2.2.9.

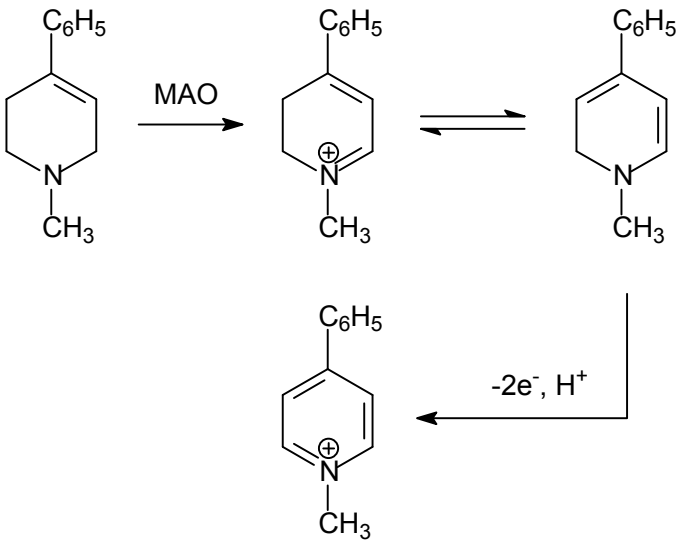

Figure 2.2.9 The mechanism by which MPTP is oxidized to MPP^+

2.2.6 Three-dimensional structure of MAO-B

MAO-B is a mitochondrial outer membrane flavoenzyme, which binds to the membrane through a C-terminal, transmembrane helix and a polar loop located at different positions in the sequence. An aromatic cage, formed by Tyr 398 and Tyr 435, is the recognition site for the substrate amino group. As stated previously, MAO-B functions in the oxidative deamination of neurotransmitters and exogenous arylalkylamines (Binda *et al*., 2002a).

The human MAO-B structure was recently characterized to 3 Å resolution and the crystal structure showed the enzyme to be dimeric (Figure 2.2.11) but not covalently linked, MAO-B consists of 520 amino acids that folds into a compact structure (Binda *et al*., 2002a).

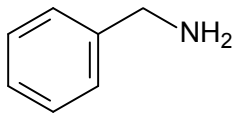

Benzylamine

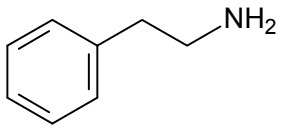

Phenylethylamine

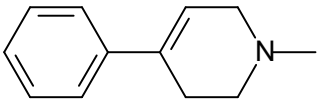

MPTP

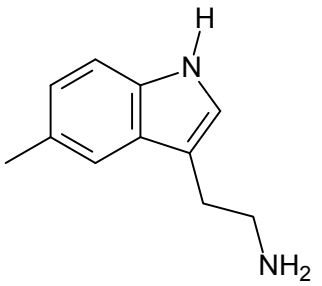

Serotonin

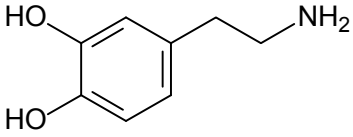

Dopamine

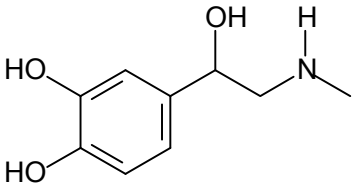

Epinephrine

Figure 2.2.10 The structures of selected MAO substrates

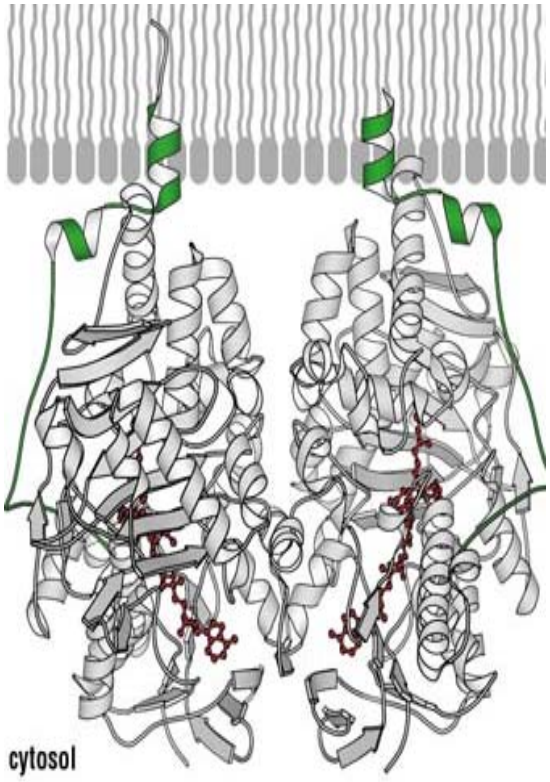

Figure 2.2.11 Ribbon diagram of the MAO-B dimer (Binda *et al*., 2004)

MAO-B is tightly attached to the outer mitochondrial membrane. The C-terminal amino acids, 461-520, form the protein region responsible for membrane attachment. Analysis and investigation of the MAO-B amino acid sequence predicts that a transmembrane helix, 27 amino acids long, will be formed by residues 489-515. The presence of exposed hydrophobic side chains, including (Phe 481, Leu 482, Leu 486 and Pro 487), suggests that membrane attachment does not only involve the C-terminal helix, but also additional hydrophobic patches of the protein surface. A flat cavity with a volume of 420 Å^3 forms the substrate binding site (Figure 2.2.12). This cavity is lined by aromatic and aliphatic amino acids. This provides the strong hydrophobic environment predicted by substrate specificity and QSAR studies (Binda *et al*., 2002b, 2004).

The distance of substrate migration from the flavin ring to the surface of the entrance cavity is a total of ~20Å. Loop 99-112 may be used by the entrance cavity as a 'gating switch'. The flat shape of the cavity restricts the orientation of the aromatic ring and therefore the amino groups binds between the phenolic side chains of Tyr 398 and Tyr

435. Tyr 398 and Tyr 435 and the flavin, form an aromatic caged environment. This environment is responsible for the amino group to be recognised (Binda *et al*., 2002b).

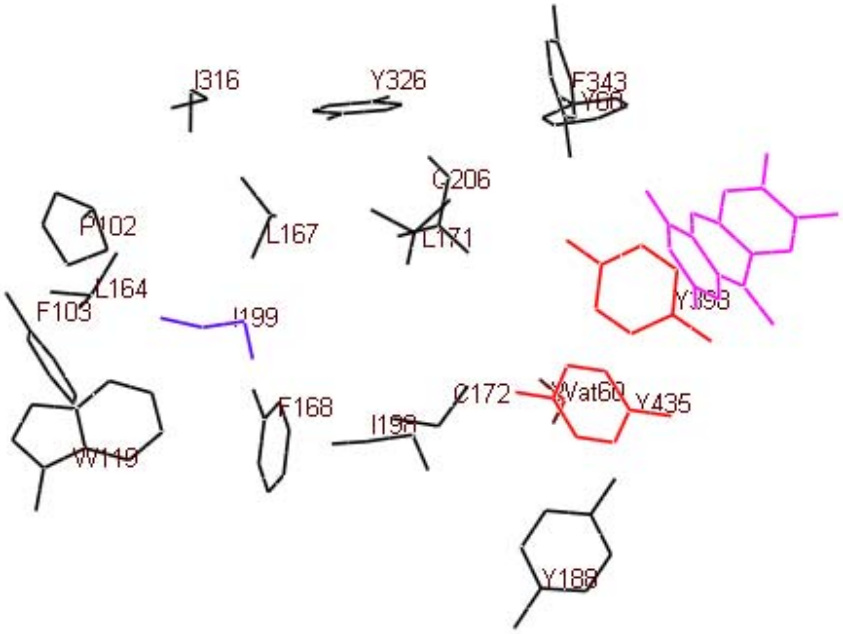

Figure 2.2.12 A model of the active site of human recombinant MAO-B. The residues Try 398, and Try 435, forming the aromatic cage are in red, Ile 199, the "gate" of the cavity is in blue and the FAD cofactor is in purple (Strydom *et al*., 2010)

2.2.7 Irreversible inhibitors of MAO-B

Irreversible inhibitors are compounds that form stable covalent complexes. This blocks the access of the substrate to the target amino acid residues of the active site (Rodwell & Kennely, 2000). The process is not readily reversed; neither by removing the remainder of the free inhibitor nor by increasing the substrate concentration (Rodwell & Kennely, 2000).

Selegiline (Figure 2.2.13), when administered at low concentrations, is a drug that selectively inhibits MAO-B irreversibly and has been shown to inhibit the oxidative deamination of dopamine *in vivo* (Youdim & Green, 1975; Youdim & Bakhle, 2006). Selegiline also has a neuroprotective effect. However, this drug is subject to the first pass effect and is metabolized by the liver before it can exert an optimal therapeutic effect. Furthermore, the drug is metabolized to metamphetamine that causes sympathomimetic side effects. These problems were overcome by developing another irreversible inhibitor without the side effects of selegiline, namely rasagiline. Rasagiline (Figure 2.2.13), is not metabolized to amphetamine derivates (Riederer *et al*., 2004b).

Selegiline Rasagiline

Figure 2.2.13 The chemical structure of selegiline and rasagiline

These MAO inhibitors were discussed in **2.1.2.4.**

Another example of an irreversible inhibitor of MAO-B is pargyline (Figure 2.2.14). Pargyline binds with the FAD cofactor of MAO-B to form a covalent bond, as seen in Figure 2.2.15.

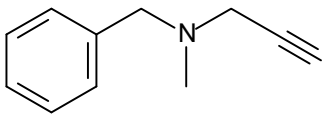

Figure 2.2.14 The structure of the irreversible MAO-B inhibitor, pargyline.

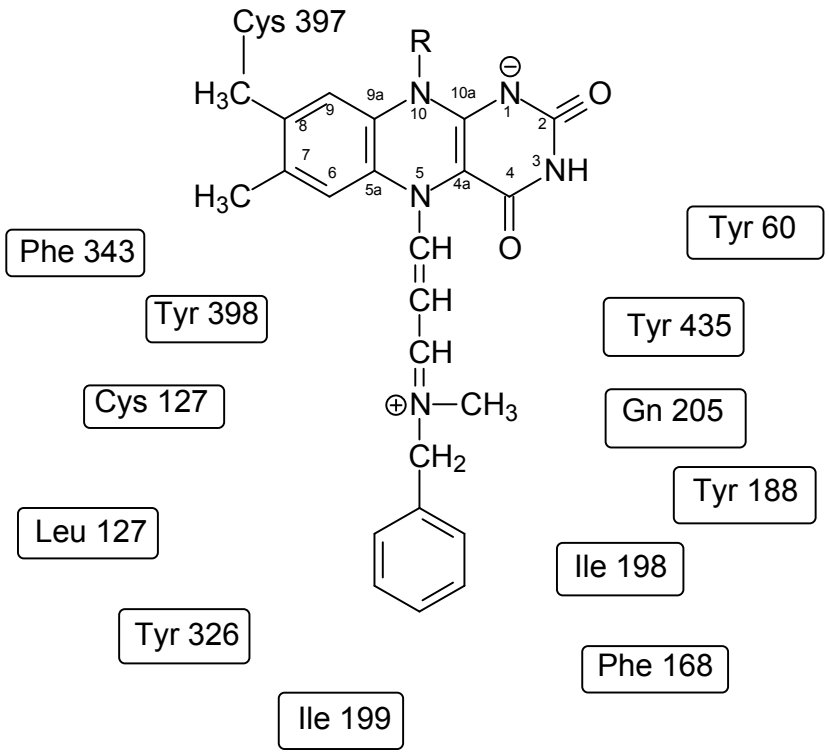

Fig. 2.2.15 Schematic representation of pargyline forming a covalent bond with the FAD cofactor of MAO-B (Binda *et al*., 2002).

2.2.8 Reversible inhibitors of MAO-B

Reversible inhibitors are compounds that interact with enzymes mainly via hydrogen bonding and hydrophobic interactions. Reversible inhibitors are therapeutically more desirable than irreversible inhibitors, since enzyme activity can be regained relatively quickly following withdrawal of the inhibitor.

2.2.8.1 Isatin, a small molecule inhibitor, which is reported to inhibit human MAO-B with a K_i value of 3 μM (Hubalek *et al*., 2005). X-ray crystal structures with human recombinant MAO-B in complex with isatin, have indicated that isatin binds within the substrate cavity and is stabilized via hydrogen bonding. The 2–oxo groups and the pyrrole NH are hydrogen bonded to ordered water molecules present in the active site, whereas the 3-oxo group is not involved in any hydrogen bonding (Binda *et al.,* 2003).

For this binding mode the side chain of Ile-199 is rotated into its normal position, separating the entrance from the substrate cavity.

2.2.8.2 (E)-8-(3-Chlorostyryl)caffeine (CSC), an A_{2A} adenosine receptor antagonist (Chen *et al*., 2001) has recently been found also to be an exceptionally potent MAO-B inhibitor with a K_i value of 0.128 μM for the inhibition of baboon liver MAO-B (Vlok *et al*., 2006). Although the exact binding mode of CSC to the active site of MAO-B is unknown, its relatively large planar structure suggests that this inhibitor traverses both the entrance and substrate cavities of the enzyme. This dual mode of binding may explain the potent action of CSC as a MAO-B inhibitor.

2.2.8.3 1,4-Diphenyl-2-butene, a contaminant of polystyrene bridges, has been used in the MAO-B crystallization process and was found to be a moderately potent competitive inhibitor of human MAO-B with a K_i value of 0.7 μM (Hubalek *et al*., 2005). Based on X-ray crystal structures, 1,4-diphenyl-2-butene is also shown to bind to both the substrate and entrance cavities of MAO-B.

2.2.8.4 Trans,trans-farnesol, a component of tobacco (Hubalek *et al*., 2005), has been found to be a moderately potent competitive inhibitor of human MAO-B with a K_i value of 2.3 μM. X-ray crystal structures with human recombinant MAO-B in complex with *trans,trans*-farnesol have indicated that *trans,trans*-farnesol exhibits a dual binding mode that involves traversing both the entrance and substrate cavities of the enzyme (Hubalek *et al*., 2005). The polar OH moiety is reported to be in close contact with the flavin, located in the substrate cavity, where it is stabilized via hydrogen bonding (Hubalek *et al*., 2005), while the aliphatic chain extends into the entrance cavity. The gate separating the two cavities, is the side chain of Ile-199, which is shown to exhibit a different rotamer conformation, that allows for the fusion of the two cavities in order to accommodate *trans,trans*-farnesol (Binda *et al*., 2003). The potency of MAO-B inhibition by *trans,trans*-farnesol may possibly be explained by dual mode of interaction.

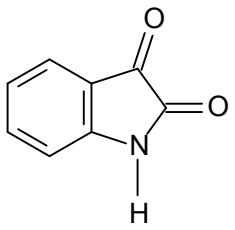

Isatin

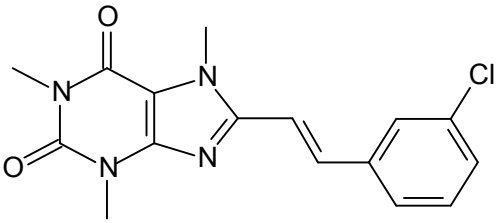

(E)-8-(3-chlorostyryl)caffeine (CSC)

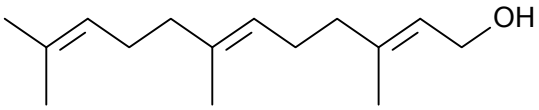

trans,trans Farnesol

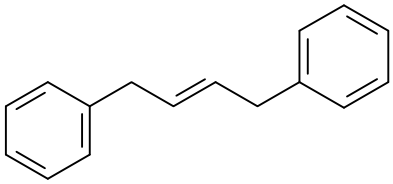

1,4-Diphenylbutene

Figure 2.2.16 The chemical structures of isatin, (E)-8-(3-chlorostyryl)caffeine, trans,trans-farnesol and 1,4-diphenyl-2-butene.

2.2.9 How MAO-A and MAO-B catalytic activities are measured *in vitro*

MAO-A and MAO-B activities are measured by adding a substrate to MAO-A or MAO-B. The concentration of the product formed is then measured after a specific time period.

- Ammonia-selective electrode: Some amines form ammonia during oxidation by MAO-B (Holt *et al*., 1997). The ammonia formed during the oxidation of the specific amine is measured continuously (Nicotra & Parvez, 1999).
- Luminometric: O'Brien *et al* (1993) developed this highly specific and accurate method. H_2O_2, a by-product of MAO-B oxidation catalyses a reaction, in which luminol is transformed into a substance that produces light. Luminol must oxidize the chosen substrate more readily than H_2O_2 (O'Brien *et al*., 1993). The MAO-B activity correlates with the extent of the light produced.

- Fluorometric: Some MAO-B substrates form fluorescent products when oxidized. A fluorescence spectrophotometer can measure the generation of these products. When kynuramine is oxidized, it forms a fluorescent compound, 4-hydroxyquinoline (Zhou *et al*., 1996) (Nicotra & Parvez, 1999).
- Polarographic: Oxygen consumption by MAO-A and MAO-B can be measured polarographically. This method is accurate and reproducible, but lacks specificity and sensitivity. The amount of oxygen consumed is an indicator of the extent to which oxidation takes place.
- Radiometric: Unlike the polarographic method, this widely used discontinuous method has a high level of sensitivity and specificity. It relies in the formation of radio labeled aldehydes (Holt *et al*., 1997). It is a popular method due to the availability of radio labeled physiological substrates (Nicotra & Parvez, 1999).
- MMTP is frequently used as substrate. It is non-selective, thus has affinity for MAO-A and MAO-B. MMTP is oxidized to $MMDP^+$ and the $MMDP^+$ concentration is measured spectrophotometrically. The specified wavelength for measurement is 420 nm, as neither MMTP (the substrate) nor the enzyme source absorb light at this wavelength. $MMDP^+$ does not undergo further oxidation and is highly stable for *in vitro* measurements (Holt *et al*., 1997).

2.3 Enzyme kinetics

Enzymes are proteins that function as catalysts for biological reactions and the products of these reactions are organic compounds which show very little tendency for reactions outside the cell (Rodwell, & Kennely, 2000). Enzymes are extremely efficient and display great catalytic power by accelerating the rates of reactions. They achieve this by providing a new reaction pathway with a lower energy of activation than the rate-determining step of the uncatalyzed reaction. Enzymes often need coenzymes which are smaller organic molecules or metallic cations possessing special chemical reactivities or structural properties (Rodwell & Kennely, 2000).

2.3.1 Michaelis-Menten kinetics

Enzymes have localized catalytic sites and the substrate (S) binds at the active site to form an enzyme-substrate complex (ES). Subsequent steps transform the bound substrate into product (P) and regenerate the free enzyme E, capable to interact with another molecule of S (Silverman, 1995).

$$E+S \underset{k_{-1}}{\overset{k_1}{\rightleftharpoons}} ES \underset{k_{-2}}{\overset{k_2}{\rightleftharpoons}} E+P$$

Figure 2.3.1 Enzyme-catalyzed reaction.

Unlike a first order reaction where the rate of reaction is directly proportional to the substrate concentration, the rate of reaction for an enzyme catalyzed reaction initially increases with increase in substrate concentration and then achieves a steady state where the rate is no longer dependent on increased substrate concentration and the overall speed of the reaction depends on the concentration of ES. Based on the steady-state kinetics analysis assumption, shortly after the enzyme and substrate are mixed, ES becomes approximately constant and remains so for a period of time, that is the steady state. The rate (V) of the reaction in the steady state usually has a hyperbolic dependence on the substrate concentration and is proportional to [S] at low concentrations, but approaches a maximum (V_{max}) when the enzyme is fully occupied with substrate (Figure 2.3.2).

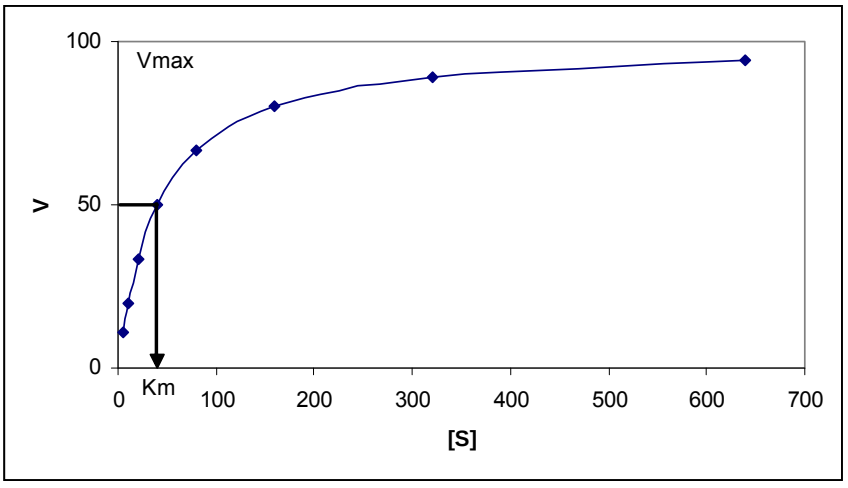

Figure 2.3.2 A graph of the rate, V, versus substrate concentration, [S], illustrating the Michaelis-Menten behaviour of enzymes.

This behaviour is described by the Michaelis-Menten equation:

$$V = \frac{V_{\max} \times [S]}{K_m + [S]}$$

$$V = \frac{K_{cat} \times [E]\ [S]}{K_m + [S]}$$

The maximum velocity (V_{max}), is obtained when all the enzyme is in the form of the enzyme-substrate complex. The Michaelis constant (K_m), is the substrate concentration at which the velocity is half maximal. If ES is in equilibrium with the free enzyme E and substrate S, K_m is equal to the dissociation constant for the complex (K_s). More generally, K_m depends on at least three rate constants and is larger than K_s. The turnover number (k_{cat}), represents the maximal catalytic activity of the enzyme and is the maximum number of molecules of substrate converted to product per active site per unit time and it is V_{max} divided by the total enzyme concentration [E]. For the Michaelis–Menten reaction, under conditions of initial velocity measurements, then $k_2 = k_{cat}$.

The specificity constant (k_{cat}/K_m), provides a measure of how rapidly an enzyme can work at low substrate concentration [S]. It is useful for comparing the relative abilities of different compounds to serve as substrates for the same enzyme. The larger this number, the better the substrate.

2.3.2 Measurement of kinetic parameters

Kinetic parameters are determined by measuring the initial reaction velocity as a function of the substrate concentration. The usual procedure for measuring the rate of an enzymatic reaction is to mix enzyme with substrate and observe the formation of product or disappearance of substrate as soon as possible after mixing, when the substrate concentration is still close to its initial value and the product concentration is small. From the hyperbolic shape of V versus S plots, V_{max} can only be determined by extrapolation of the asymptotic approach of V to limiting value of S as it increases indefinitely and this determination is usually approximate. Instead, the Michaelis–Menten equation can be transformed into a straight line equation which is similar to the equation for a straight line graph with a plot of 1/V versus 1/[S]:

$$1/V = (K_m / V_{\max})(1/[S]) + 1/V_{\max}$$

giving the intercept as $1/ V_{max}$ and the slope as K_m/V_{max}.

Such a plot is known as the Lineweaver–Burke double reciprocal plot and K_m and V_{max} can readily be obtained from a plot of $1/V$ versus $1/[S]$ (Figure 2.3.3).

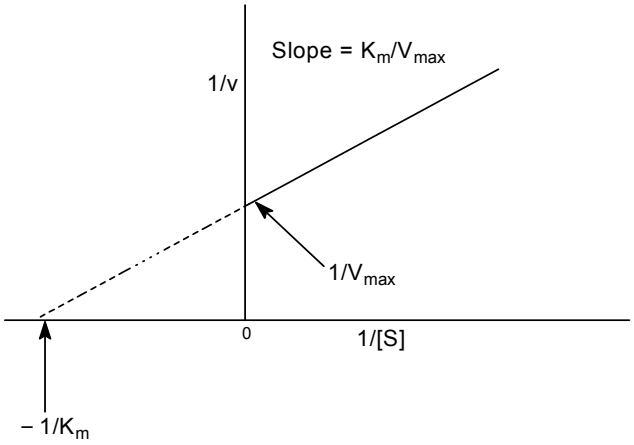

Figure 2.3.3 The Lineweaver-Burke double-reciprocal plot.

2.3.3 Competitive inhibition

Enzymes can be inhibited by agents that interfere with the binding of substrate or with conversion of the ES complex into products. There are two major classes of inhibitors: reversible and irreversible inhibitors (Silverman, 1995). Reversible inhibitor interacts with the enzyme through non covalent association or dissociation reactions. Reversible inhibitors include competitive, noncompetitive and uncompetitive inhibitors. A competitive inhibitor competes for the same binding site on the enzyme (the active site) as the substrate. Consequently, a sufficiently high concentration of substrate can eliminate the effect of a competitive inhibitor.

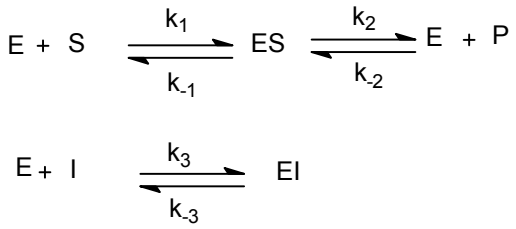

Figure 2.3.4 Formation of enzyme complexes where I binds reversibly to the enzyme at the same site as the substrate.

Irreversible inhibitors (inactivators) are compounds that produce irreversible inhibition of the enzyme by forming stable covalent complexes that block the access of the inhibitor to the target amino acid residues. These complexes can be characterized and they often provide information on the active site of the enzyme. They generally modify the amino acid residues in the enzymes that play essential roles in catalysis. The process is not readily reversed either by removing the remainder of the free inhibitor or by increasing the substrate concentration. Dilution or dialysis of the solution does not dissociate the enzyme inhibitor complex and restore enzyme activity (Rodwell, & Kennely, 2000).

In this study we will however, focus on competitive inhibition, as the compounds under investigation are expected to act in a reversible competitive manner. Competitive inhibition may be represented graphically by the Lineweaver-Burke plot (Figure 2.3.5). A competitive inhibitor increases the slope of the straight line while the y-axis intercept remains unaffected. The intercept on the x-axis increasingly becomes less negative. Therefore a competitive inhibitor raises the apparent substrate K_m value while V_{max} remains unchanged. The Michaelis-Menten equation describing competitive inhibition is:

$$V_i = \frac{V_{\max} \times \frac{[S]}{K_m}}{1 + \frac{[S]}{K_m} + \frac{[I]}{K_i}}$$

The inverse of this equation describes the double reciprocal plot in the presence of a competitive inhibitor:

$$\frac{1}{V_i} = \frac{K_m}{V_{\max}}\left(1 + \frac{[I]}{K_i}\right) \times \frac{1}{[S]} + \frac{1}{V_{\max}}$$

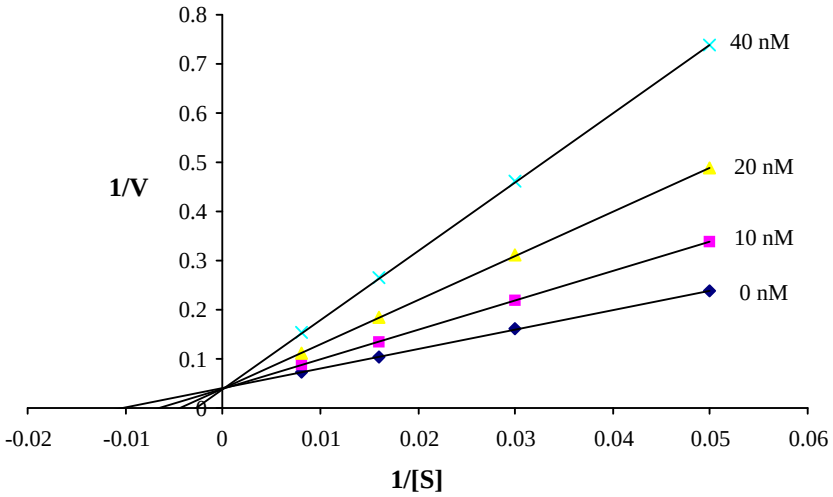

Figure 2.3.5 The double reciprocal plot or Lineweaver-Burke plots in the presence of various concentrations of a competitive inhibitor.

The K_i value of a competitive inhibitor is the enzyme-inhibitor dissociation constant. For a series of competitive inhibitors, those with the lowest K_i values will cause the greatest degree of inhibition at a fixed concentration of inhibitor [I]. The K_i value for an inhibitor can be determined from the secondary plot in which the slope of each reciprocal plot is graphed versus the corresponding inhibitor concentration (Figure 2.3.6). The x-axis value is equal to $-K_i$. In the presence of a concentration of inhibitor [I] that is approximately equal to K_i, the substrate concentration has to double to maintain the same initial velocity as in the absence of the inhibitor.

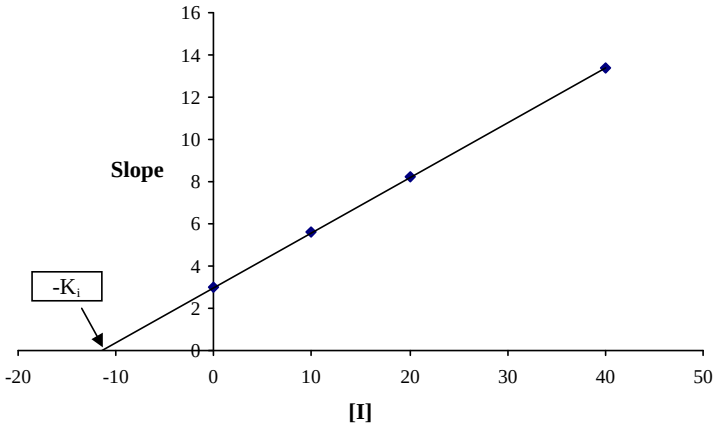

Figure 2.3.6 Graph of the slopes from the double reciprocal plot versus inhibitor concentration.

2.3.4 The FAD cofactor

Flavin coenzymes act as co-catalysts with enzymes in a large number of redox reactions, many of which involve O_2. Flavin-adenine dinucleotide (FAD) and flavin mononucleotide (FMN) are the coenzymatically active forms of vitamin B2 (riboflavin) (Figure 2.3.7).

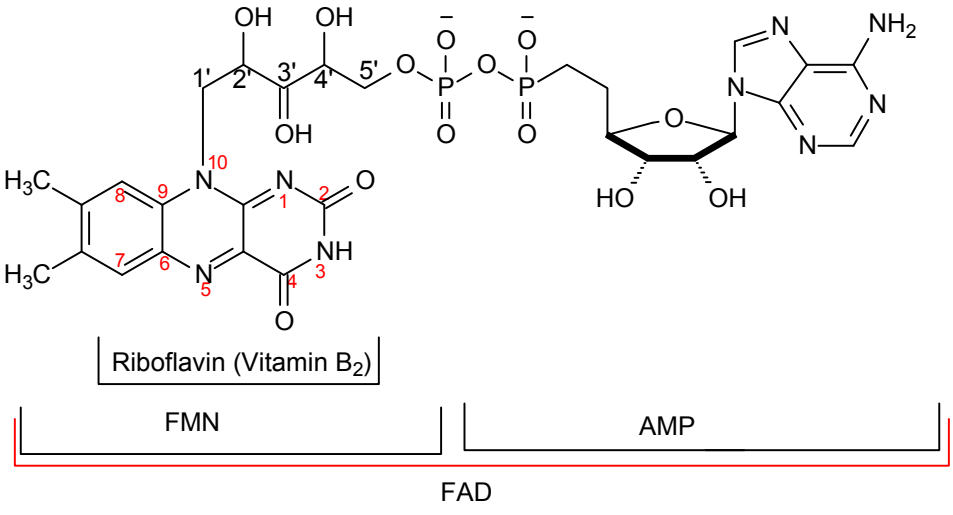

Figure 2.3.7 Structures of the vitamin riboflavin and the derived flavin coenzymes.

The catalytically functional portion of the coenzymes is the isoalloxazine ring, specifically the N-5 and C-4a positions, which are thought to be the immediate sites of catalytic action. The flavin coenzymes exist in four spectrally distinguishable oxidation states that account in part for their catalytic functions (Fig. 2.3.8). They are the yellow oxidized form, the red or blue one-electron reduced form, and the colourless two-electron reduced form.

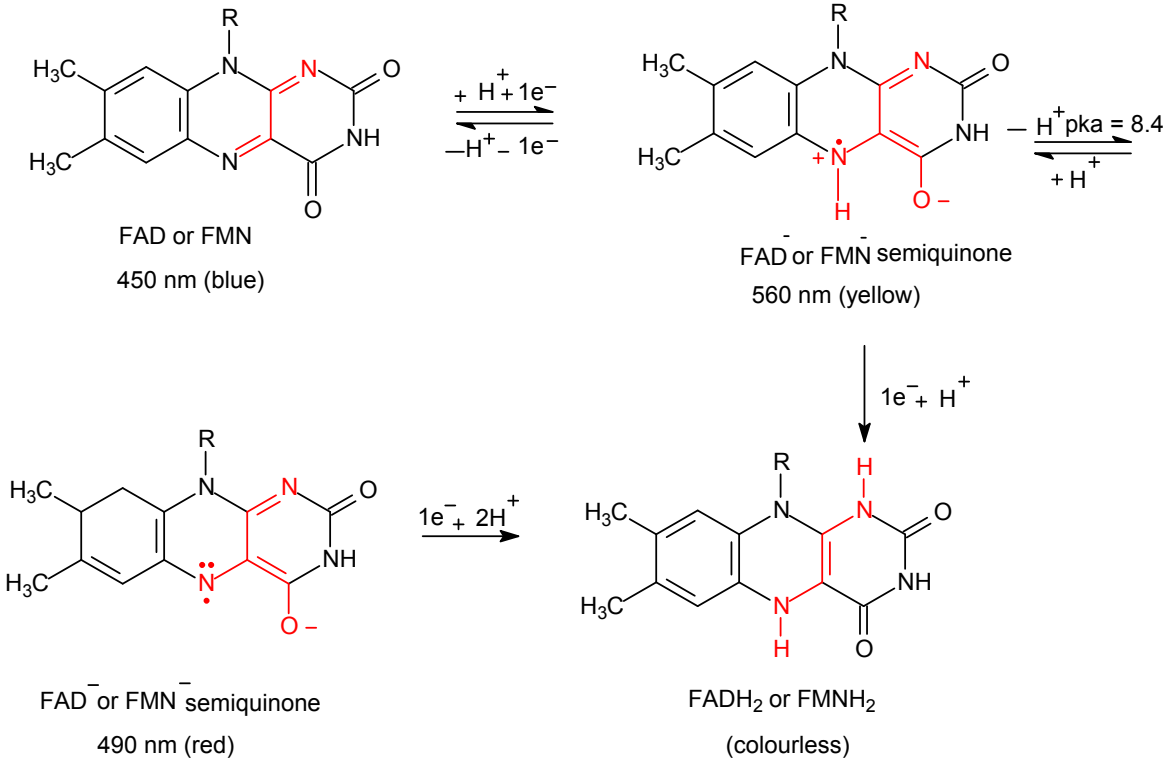

Figure 2.3.8 The oxidation states of flavin coenzymes.

2.4 Animal models of Parkinson's disease

2.4.1 The neurotoxin MPTP

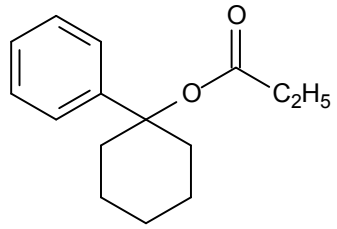

Figure 2.4.1 MPPP

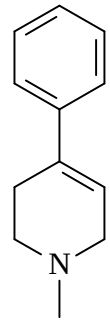

Figure 2.4.2 MPTP

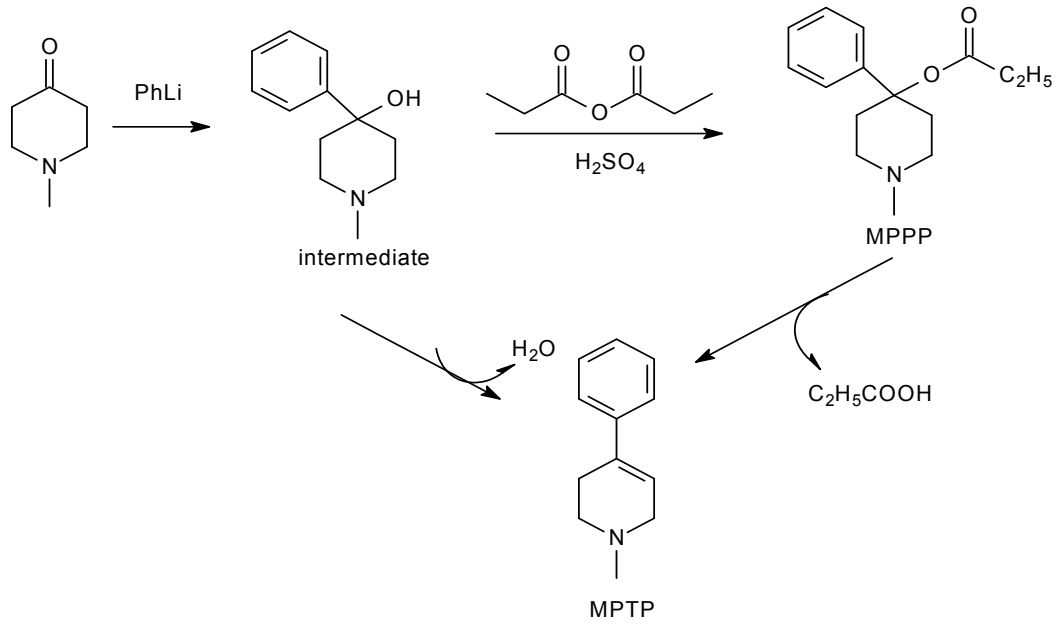

Figure 2.4.3 The preparation of MPTP from MPPP

The neurotoxin, MPTP (1-methyl-4-phenyl-1,2,3,6-tetrahydropyridine), is activated only after being metabolized by MAO-B to $MMDP^+$. $MMDP^+$ is then oxidized via an unknown mechanism to the active toxin MPP^+ in astrocytes. MPP^+ accumulates in the nigrostriatal neurons, via the dopamine transport system (DAT) of these neurons, where it inhibits mitochondrial ATP production (Smeyne & Jackson-Lewis, 2004). This action

triggers a series of events, involving the production of toxic reactive oxygen species and decreased synthesis of cellular ATP, leading to the eventual death (Ramsay *et al*., 1986). Although this appeared to be the major step in the blockade of mitochondrial function, studies have shown that MPP^+ also directly inhibited complexes III and IV of the electron transport chain (Mizuno *et al*., 1988). Based upon the finding that MPP^+ depletes cellular energy due to interference with complex I–III, and as such was related to the etiology of human Parkinson's disease, the MPTP model has become the reference for most studies of toxin based models. Despite the fact that inhibition of complex I by MPP^+ reduces energy production within dopaminergic neurons and causes loss of cellular energy with several deleterious consequences, it has been shown that this is not the immediate cause of the neuronal death. The exact mechanism leading to cell death is still not clear and it is thought to take place through a complicated pathway (Langston, 1990). One possibility is the production of increased free radicals due to complex I inhibition or via MPP^+-induced dopamine leakage from synaptic vesicles to the cytosol (Smeyne & Jackson-Lewis, 2004). The result is the selective destruction of the nigrostriatal neurons and dopamine depletion in the striatum which leads to a syndrome that is pathologically and symptomatically identical to PD (Singer *et al*., 1988). Alternatively, MPP^+ can be absorbed by vesicles or may be bound to neuromelanin, which inactivates MPP^+. These are mechanisms of protection against MPTP-induced neurotoxicity (Blum *et al*., 2001). Today animals are treated with MPTP to create models of PD. MPTP's neurotoxic effects are prevented by MAO-B inhibitors which block MPTP's activation to the active toxin MPP^+ (Smeyne & Jackson-Lewis, 2004).

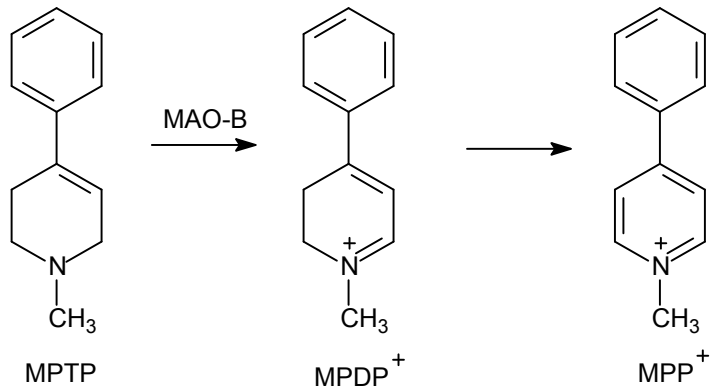

Figure 2.4.4 The MAO catalyzed oxidation of MPTP to the dihydropyridinium species, $MPDP^+$ and the pyridinium MPP^+.

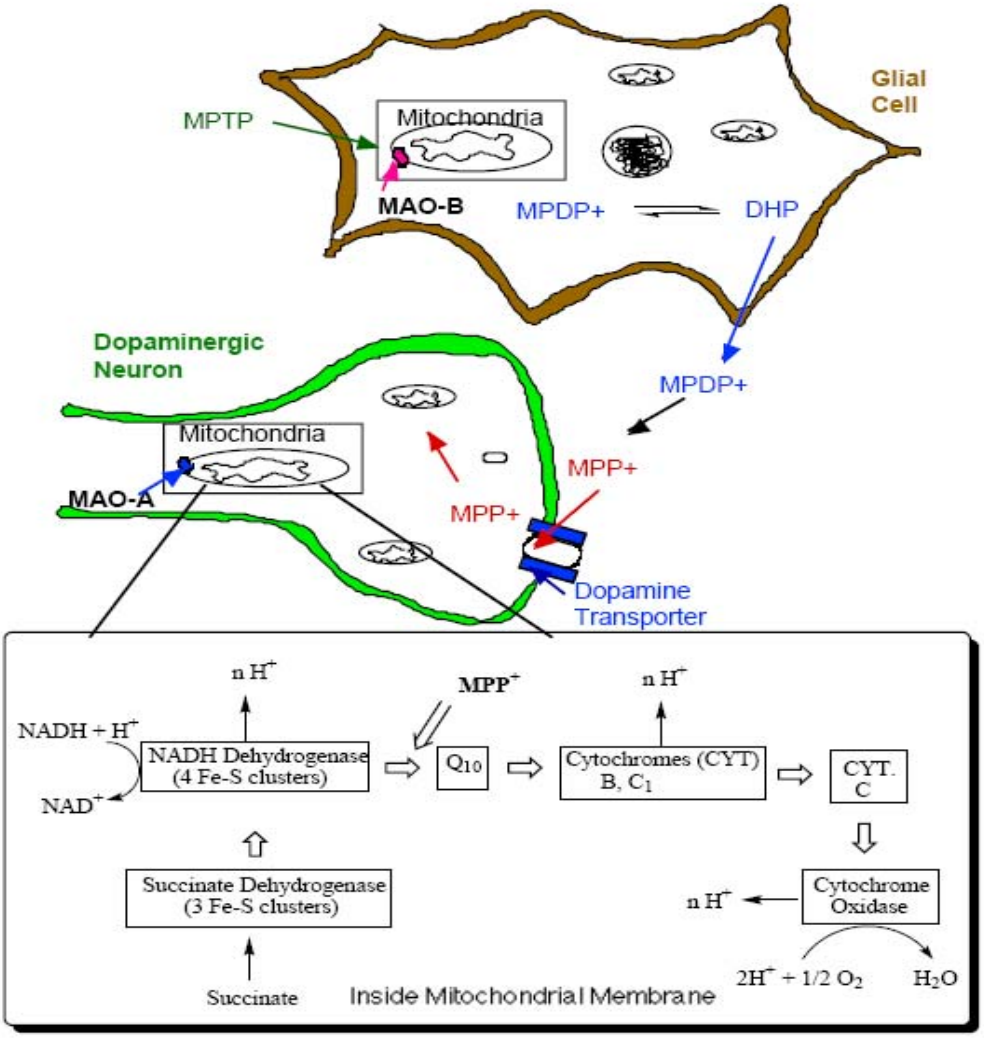

Figure 2.4.5 Schematic representation of the mechanism of MPTP-induced neurotoxicity (Javitch *et al*., 1985).

2.4.2 Hydroxydopamine (6-OHDA)

6-OHDA-induced toxicity is relatively selective for monoaminergic neurons, resulting from preferential uptake by DA and noradrenergic transporters (Luthman *et al*., 1989). Inside neurons, 6-OHDA accumulates in the cytosol, generating ROS and inactivating biological macromolecules by generating quinones that attack nucleophilic groups. 6-OHDA cannot cross the blood-brain barrier, therefore it must be administered by local stereotaxic injection into the substantia nigra, median forebrain bundle or striatum to target the nigrostriatal dopaminergic pathway (Javoy et al., 1976). So far, however, none of the modes of 6-OHDA intoxication have led to the formation of Lewy-body like inclusions. For striatal stereotaxic lesions, 6-OHDA is injected unilaterally, with the contralateral side serving as control (Ungerstedt, 1971). These injections produce an asymmetric circling behaviour in animals (Hefti *et al*., 1980). However, it is not clear whether the mechanism by which 6-OHDA kills dopaminergic neurons shares key molecular features with PD.

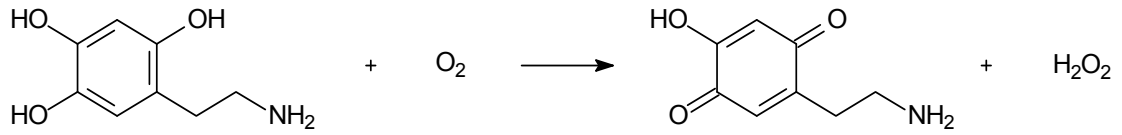

Figure 2.4.6 Oxidation of 6-OHDA (Bovè *et al*., 2005).

2.4.3 Paraquat

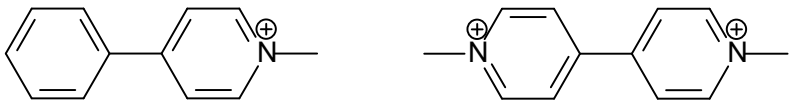

MPP^+ Paraquat

Figure 2.4.7 Structural similarity between paraquat and MPP^+ (Dauer & Przedborski, 2003).

The herbicide, paraquat (N,N'-dimethyl-4-4'-bipiridinium), also induces a toxic model of PD. Paraquat shows structural similarity to MPP^+ (Figure 2.4.7). Paraquat does not

easily penetrate the blood-brain barrier. The toxicity of paraquat appears to be mediated by the formation of superoxide radicals (Day *et al*., 1999). Systemic administration of paraquat to mice leads to SNpc dopaminergic neuron degeneration accompanied by α-synuclein containing inclusions, as well as increases in α-synuclein immunostaining in the frontal cortex (Maning-Bog *et al*., 2002).

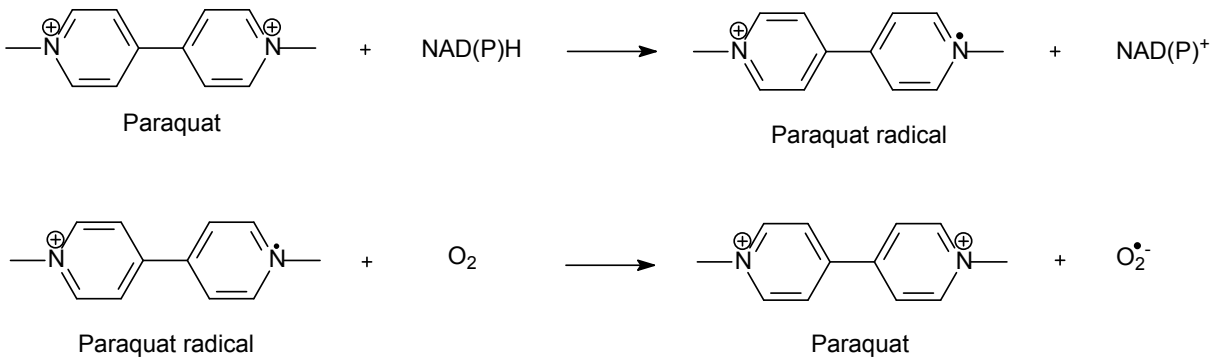

Figure 2.4.8 Reduction-oxidation cycling reaction of paraquat (Bovè *et al*., 2005).

The ability of paraquat to induce dopaminergic neuronal loss and α-synuclein-positive inclusions in a reliable fashion may prove valuable for studies of the role of α-synuclein in neurodegeneration (Dauer & Przedborski, 2003).

2.4.4 Rotenone

Rotenone is widely used as an insecticide and fish poison. Rotenone is highly lipophilic and readily gains access to all organs (Taipade *et al*., 2000). Rotenone binds at the same site as MPP^+, and inhibits mitochondrial complex I. Low-dose intravenous rotenone produces selective degeneration of nigrostriatal dopaminergic neurons accompanied by α-synuclein positve Lewy-bodies like inclusions in rats (Betarbet *et al*., 2000). Lewy-body-associated dopaminergic neurodegeneration in this model should enable investigators to perform a novel series of experiments exploring the relationship between aggregate formation and neuronal death.

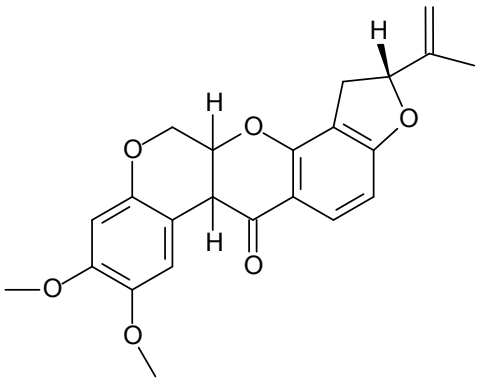

Figure 2.4.9 Chemical structure of rotenone (Bovè *et al*., 2005).

2.5 Summary

Parkinson's disease, a neurodegenerative disorder, is characterized mainly by the loss of dopamine nigrostriatal neurons which results in a disabling movement disorder. There are various therapeutic strategies available for the treatment of Parkinson's disease. Most of these provide relief from the symptoms of the disease while the underlying cause of neurodegeneration is left untreated. Dopamine replacement therapy with the dopamine precursor levodopa, is currently used as first line therapy. Levodopa is frequently combined with the MAO-B inhibitor (R)-deprenyl. Inhibition of MAO-B in the brain may conserve the already depleted supply of dopamine and also stoichiometrically decreases the dopaldehyde and H_2O_2 production associated with dopamine oxidation in the brain. MAO-B inhibitors may therefore provide a neuroprotective effect in addition to symptomatic relief for Parkinson's disease patients.

Chapter 3

Preparation of synthetic targets

3.1. Introduction

In this chapter the synthesis and characterization of the C-8 substituted caffeine analogues will be described. The structures of the target compounds are illustrated in Figure 3.1 (**1-8**). Each target compound was synthesized from an appropriate commercially available carboxylic acid Figure 3.2 (**9-18**).

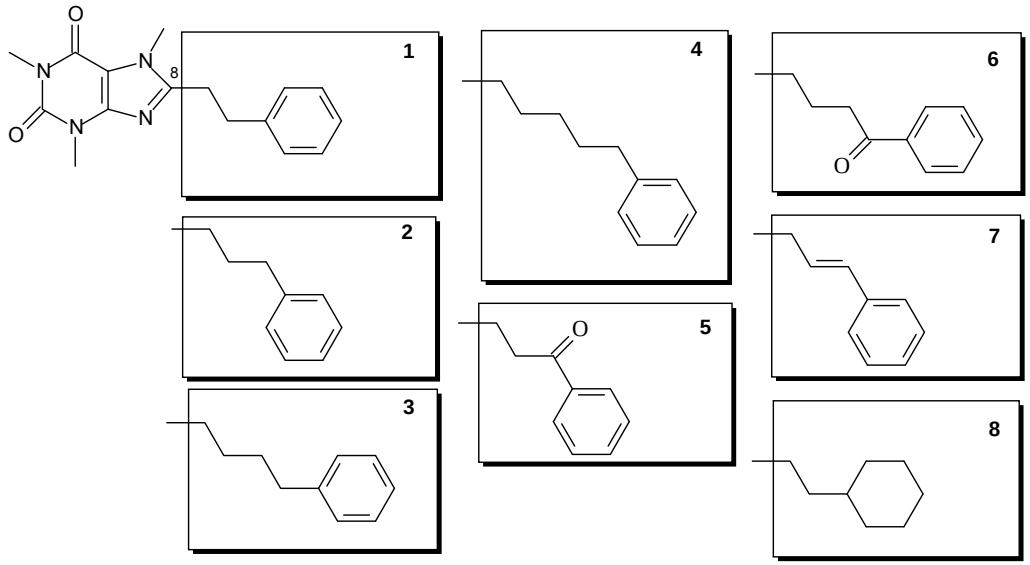

Figure 3.1. The structures of C-8 substituted caffeine analogues that were synthesized in this study.

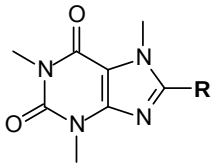

	R
1	$-(CH_2)_2-C_6H_5$
2	$-(CH_2)_3-C_6H_5$
3	$-(CH_2)_4-C_6H_5$
4	$-(CH_2)_5-C_6H_5$

5	-$(CH_2)_2$-CO- C_6H_5
6	-$(CH_2)_3$-CO- C_6H_5
7	-(CH_2)-CH=CH-C_6H_5
8	-$(CH_2)_2$-C_6H_{11}

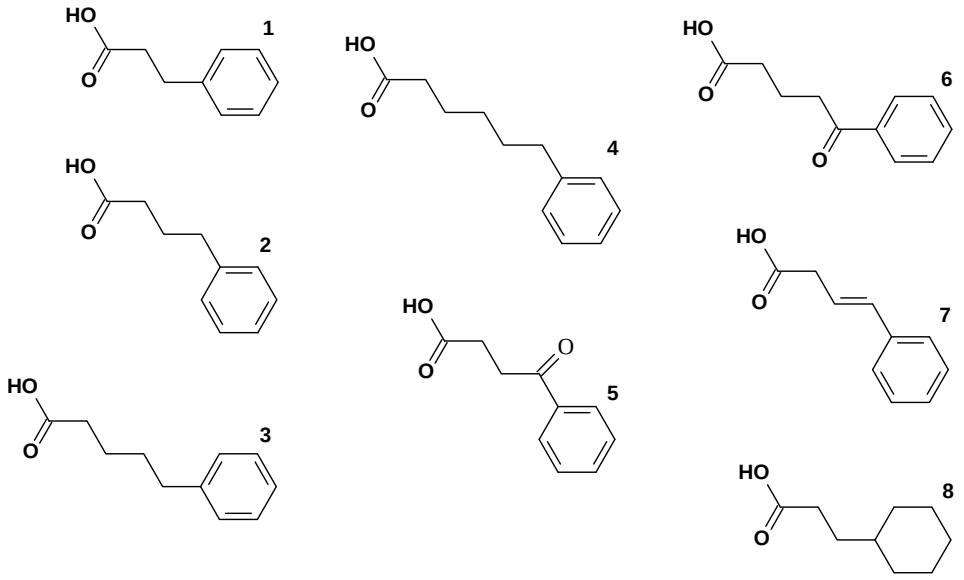

Figure 3.2. The structures of the carboxylic acids used for the synthesis of **1-8**. These reagents were all commercially available.

3.2. Literature method for the synthesis of C-8 substituted caffeine analogues.

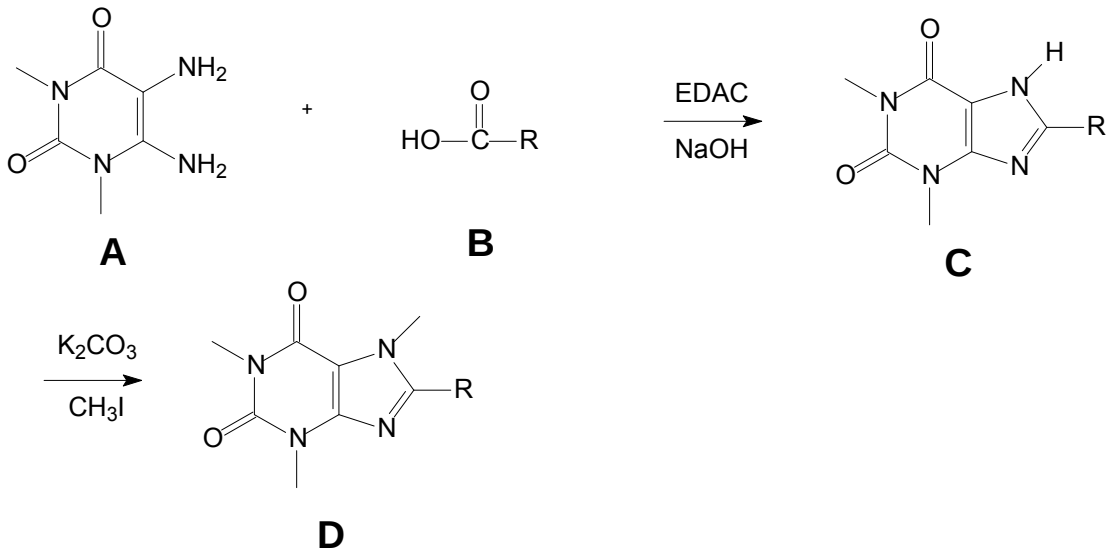

Scheme 3.1. The synthesis of C-8 substituted caffeine analogues from the 1,3-dimethyl-5,6-diaminouracil.

A convenient synthetic route for the preparation of C-8 substituted caffeine analogues has been described by Suzuki *et al*. (1992) This route is illustrated in Scheme 3.1. The C-8 substituted caffeine analogues were prepared in high yield according to the procedure previously reported for the preparation of (*E*)-8-styrylcaffeinyl analogues. The key starting materials for the procedure, 1,3-dimethyl-5,6-diaminouracil (**A**) was allowed to react with the appropriate carboxylic acid (**B**) in the presence of the carbodiimide activating reagent *N*-(3-dimethylaminopropyl)-*N*′-ethylcarbodiimide hydrochloride (EDAC). The commercially available carboxylic acids were used for the preparation of the target compounds. The resulting amidyl intermediates subsequently underwent ring closure when heated under reflux in aqueous sodium hydroxide to yield the corresponding 1,3-dialkyl-8-sustituted-7*H*-xanthinyl analogues (**C**). Without further purification, the crude xanthinyl intermediates were selectively 7N-alkylated with an excess of iodomethane and potassium carbonate to yield the target compounds (**D**). Following crystallization from a suitable solvent, analytically pure samples of the target compounds were obtained. A mechanism for these reactions is proposed in Scheme 3.2.

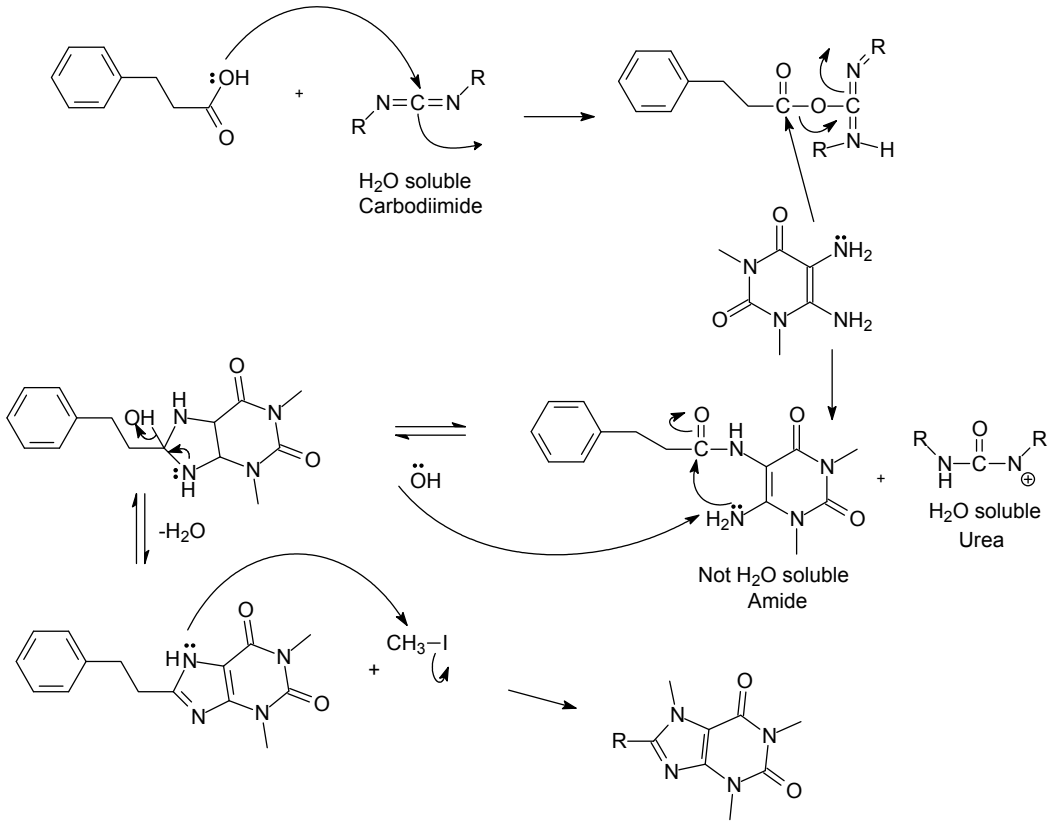

Scheme 3.2. The mechanism for the synthesis of C-8 substituted caffeine analogues

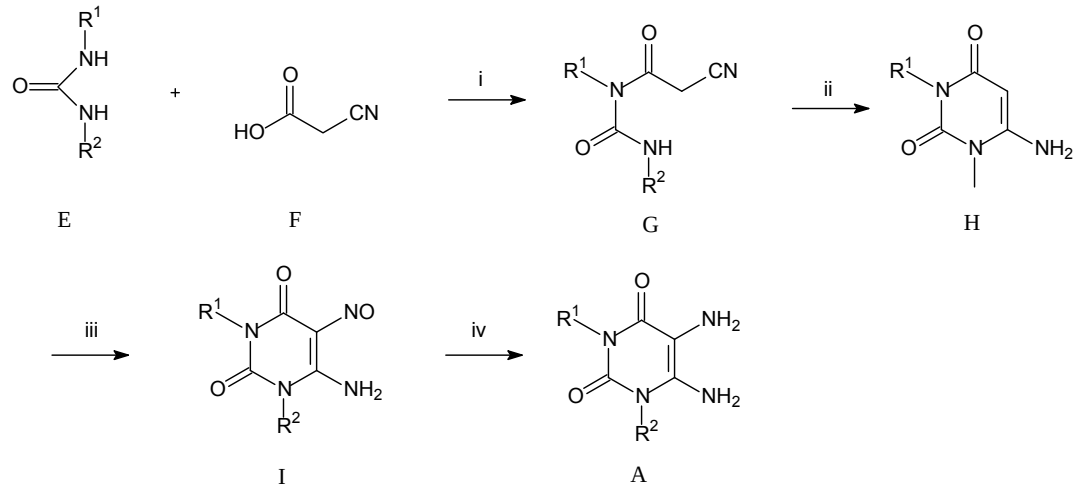

(i) acetic anhydride
(ii) NaOH
(iii) $NaNO_2$, CH_3CO_2H
(iv) $Na_2S_2O_4$

Scheme 3.3. Synthetic pathway to substituted 1,3-diethyl-5,6-diaminouracil (**A**)

As shown in scheme 3.3 the key starting material used for the caffeine synthesis, 1,3-dimethyl-5,6-diaminouracil, was in turn synthesized from N,N-dimethylurea.

3.3. Chemicals and instrumentation

Unless otherwise noted, all starting materials were obtained from Sigma-Aldrich and were used without purification. Proton (^{1}H) and carbon (^{13}C) NMR spectra were recorded on a Bruker Avance III 600 spectrometer at frequencies of 600 MHz and 150 MHz, respectively. All NMR measurements were conducted in $CDCl_3$ and the chemical shifts are reported in parts per million (δ) downfield from the signal of tetramethylsilane added to the deuterated solvent. Spin multiplicities are given as s (singlet), brs (broad singlet), d (doublet), dd (doublet of doublets), t (triplet) or m (multiplet). Direct insertion electron impact ionization (EIMS) and high resolution mass spectra (HRMS) were obtained on a DFS high resolution magnetic sector mass spectrometer (Thermo Electron Corporation) in electrospray ionization (ESI) mode. Melting points (mp) were determined on a Stuart SMP10 melting point apparatus and are uncorrected. Thin layer chromatography (TLC) was carried out using silica gel 60 (Merck) with UV_{254} fluorescent indicator. To determine the purity of the synthesized compounds, HPLC analyses were conducted with an Agilent 1100 HPLC system equipped with a quaternary pump and an Agilent 1100 series diode array detector (see Supplementary Material). HPLC grade acetonitrile (Merck) and Milli-Q water (Millipore) was used for the chromatography.

3.4. The synthesis of 1,3-dimethyl-5-nitroso-6-aminouracil

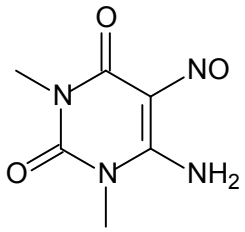

Figure 3.3. Chemical structure of 1,3-dimethyl-5-nitro-6-aminouracil (**I**)

The N,N'-Dimethylurea (**E**) (50 mmol) and cyanoacetic acid (**F**) (50 mmol) was placed in a roundbottom flask and acetic anhydride (6.25 ml) was added. With a $CaCl_2$ trap attached, the reaction was heated (60 °C) for 3 hours to yield a colourless to light yellow solution. The

reaction was cooled on an ice bath, and the 10% sodium hydroxide (60 ml) was added to yield a white suspension (compound **H**). The pH tested 11 and the reaction was stirred for a further 30 minutes at room temperature. A solution of sodium nitrate (60 mmol) was added followed by 8 ml of glacial acetic acid. The reaction turned pink. At this stage the pH tested 5. A further 7 ml glacial acetic acid was added over a period of an hour. Stirring was continued for a additional hour and the purple product (**I**) was collected via filtration and washed with 20 ml diethylether.

3.5. The synthesis of 1,3-dimethyl-5,6-diaminouracil

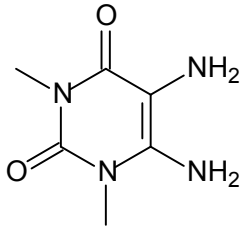

Figure 3.4. Chemical structure of 1,3-dimethyl-5,6-diaminouracil (**A**)

1,3-Dimethyl-5-nitroso-6-aminouracil (**I**) was powderized and 20 ml ammonia water (32%) was added to yield an orange suspension. The suspension was heated to 40 °C and freshly prepared sodium hydrosulfite (11 g in 50 ml water) was added over a period of 15 minutes. The suspension became a red solution and then green. Approximately 47 ml sodium hydrosulfite was added. The reaction was cooled on ice for 4 hours. The light yellow crystals (compound **A**) which formed were collected via filtration and were washed with 20 ml water. The crystals were left to dry in the hood overnight.

3.6. The synthesis of the 1,3-dimethyl-8-substituted-xanthinyl intermediates (C)

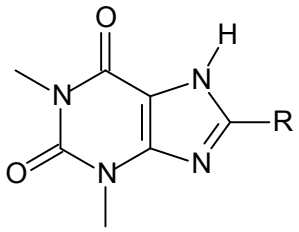

Figure 3.5. Chemical structure of an 1,3-dimethyl-8-substituted-xanthinyl intermediate (**C**)

The C-8 substituted caffeine analogues were prepared according to the procedure described in the literature. 1,3-Dimethyl-5,6-diaminouracil (**A**) (10 mmol) and *N*-(3-dimethylaminopropyl)-*N′*-ethylcarbodiimide hydrochloride (EDAC; 13.4 mmol) were dissolved in 103 mL dioxane/H_2O (1:1) and the appropriate carboxylic acid (**B**) [structures **9**-**18**, 10 mmol] was added. A suspension was obtained and the pH was adjusted to 5-6 with 2 M aqueous hydrochloric acid. The reaction mixture was stirred for an additional 2 h at room temperature and then neutralized with 1 M aqueous sodium hydroxide. After cooling to 0 °C, the precipitate that formed was collected by filtration. A solution of this crude amide in 100 ml aqueous sodium hydroxide (1 M)/dioxane (1:1) was heated (100-110 °C) under reflux for 2 h, cooled to 0 °C and then acidified to a pH of 4 with 4 M aqueous hydrochloric acid. The resulting precipitate, the corresponding 1,3-dimethyl-8-substituted-xanthinyl analogue (**C**) was collected by filtration, washed with 50 ml water and dried in the oven at 50 °C.

3.7. The synthesis of the target C-8 substituted caffeine analogues

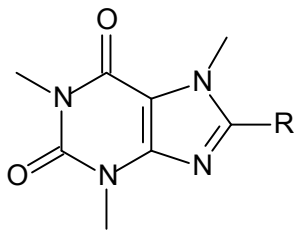

Figure 3.6 The general chemical structure of the target C-8 substituted caffeine analogues (**D**)

The 1,3-dimethyl-8-substituted-xanthinyl intermediate (**C**) (3.5 mmol) was dissolved in a minimum amount of DMF (10 ml) at 90 °C. Potassium carbonate (8.75 mmol) was added. Iodomethane (7 mmol) was subsequently added and the reaction became lighter in colour. The reaction was heated (90 °C) under reflux for 60 minutes. After TLC indicated completion of the reaction, the insoluble materials were removed by filtration. Water (350 ml) was added to the filtrate to precipitate the product and the resulting mixture was cooled on ice for 3 hours. The precipitate was collected via filtration and dried overnight at room temperature.

The product was dissolved in 50 ml boiling methanol. The clear solution was allowed to recrystallize at room temperature for a minimum of 12 hours. The crystals were collected and

washed with 20 ml ethylacetate and analytically pure samples of the target compounds were obtained.

3.8 Physical characterization

The structures and purity of the compounds were verified by ^{1}H-NMR and ^{13}C-NMR, as well as by nominal and high resolution mass spectrometry. For those compounds previously reported, the physical data and melting points were determined and compared to literature values.

The purities of the target caffeine derivatives were demonetrated by HPLC analysis (see annexture). For the purpose of the HPLC analysis, strong eluting condition (up to 85% acetonitrile) were employed and the eluent was monitored at 210 nm, a wavelength where most organic compounds absorb UV light. It is therefore likely that impurities, if present, will elute and be detected under these conditions.

3.9 Results

8-(2-Phenylethyl)caffeine (1)

The title compound was prepared from 3-phenylpropanoic acid in a yield of 88%: mp 154–157 °C (methanol). ^{1}H NMR (Bruker Avance III 600, $CDCl_3$) δ 2.98 (t, 2H, J = 7.2 Hz), 3.05 (t, 2H, J = 7.2 Hz), 3.34 (s, 3H), 3.55 (s, 3H), 3.57 (s, 3H), 7.08 (d, 2H, J = 7.2 Hz), 7.18 (t, 1H, J = 7.2 Hz), 7.24 (m, 2H); ^{13}H NMR (Bruker Avance III 600, $CDCl_3$) δ 27.8, 28.9, 29.7, 31.3, 34.0, 107.1, 126.6, 128.3, 128.7, 139.9, 147.9, 151.6, 153.3, 155.2; ESI-HRMS *m*/*z*: calcd for $C_{16}H_{19}O_2N_4$, 299.1508, found 299.1502; Purity (HPLC): 99.7%.

8-(3-Phenylpropyl)caffeine (2)

The title compound was prepared from 4-phenylbutanoic acid in a yield of 66%: mp 115–117 °C (methanol). ^{1}H NMR (Bruker Avance III 600, $CDCl_3$) δ 2.09 (qn, 2H, J = 7.5 Hz), 2.71 (q, 4H, J = 7.5 Hz), 3.37 (s, 3H), 3.55 (s, 3H), 3.80 (s, 3H), 7.17 (m, 3H), 7.28 (t, 2H, J = 7.5 Hz); ^{13}H NMR (Bruker Avance III 600, $CDCl_3$) δ 26.0, 27.8, 28.7, 29.7, 31.6, 35.1, 107.3, 126.2, 128.4, 128.5, 140.9, 148.0, 151.7, 153.9, 155.3; ESI-HRMS *m*/*z*: calcd for $C_{17}H_{21}O_2N_4$, 313.1665, found 313.1659; Purity (HPLC): 99.4%.

8-(4-Phenylbutyl)caffeine (3)

The title compound was prepared from 5-phenylpentanoic acid in a yield of 68%: mp 131–133 °C (methanol). ^{1}H NMR (Bruker Avance III 600, $CDCl_3$) δ 1.69–1.79 (m, 4H), 1.79 (t, 2H, J = 7.2 Hz), 1.77 (t, 2H, J = 7.2 Hz), 3.37 (s, 3H), 3.54 (s, 3H), 3.85 (s, 3H), 7.15 (m, 3H), 7.25 (m, 2H); ^{13}H NMR (Bruker Avance III 600, $CDCl_3$) δ 26.7, 27.1, 27.8, 29.7, 30.9, 31.7, 35.5, 107.3, 125.9, 128.3, 128.4, 141.8, 148.0, 151.7, 154.1, 155.3; ESI-HRMS *m*/*z*: calcd for $C_{18}H_{23}O_2N_4$, 327.1821, found 327.1812; Purity (HPLC): 99.2%.

8-(5-Phenylpentyl)caffeine (4)

The title compound was prepared from 6-phenylhexanoic acid in a yield of 44%: mp 114–116 °C (methanol). ^{1}H NMR (Bruker Avance III 600, $CDCl_3$) δ 1.41 (qn, 2H, J = 7.5 Hz), 1.66 (qn, 2H, J = 7.9 Hz), 1.75 (qn, 2H, J = 7.5 Hz), 2.61 (t, 2H, J = 7.5 Hz), 2.69 (t, 2H, J = 7.9 Hz), 3.38 (s, 3H), 3.54 (s, 3H), 3.87 (s, 3H), 7.15 (m, 3H), 7.25 (m, 2H); ^{13}H NMR (Bruker Avance III 600, $CDCl_3$) δ 26.8, 27.5, 27.8, 28.3, 29.7, 31.0, 31.7, 35.7, 107.3, 125.8, 128.3, 128.4, 142.3, 148.0, 151.7, 154.3, 155.3; ESI-HRMS *m*/*z*: calcd for $C_{19}H_{25}O_2N_4$, 341.1978, found 341.1974; Purity (HPLC): 99.0%.

8-(3-Oxo-3-phenylpropyl)caffeine (5)

The title compound was prepared from 4-oxo-4-phenylbutanoic acid in a yield of 59%: mp 191–194 °C (methanol). ^{1}H NMR (Bruker Avance III 600, $CDCl_3$) δ 3.11 (t, 2H, J = 7.4 Hz), 3.36 (s, 3H), 3.46 (s, 3H), 3.58 (t, 2H, J = 7.4 Hz), 4.01 (s, 3H), 7.46 (t, 2H, J = 7.5 Hz), 7.57 (t, 1H, J = 7.5 Hz), 7.98 (d, 2H, J = 7.5 Hz); ^{13}H NMR (Bruker Avance III 600, $CDCl_3$) δ 20.7, 27.8, 29.6, 31.7, 35.6, 107.4, 128.1, 128.7, 133.4, 136.4, 147.9, 151.7, 153.2, 155.3, 198.1; ESI-HRMS *m*/*z*: calcd for $C_{17}H_{19}O_3N_4$, 327.1457, found 327.1469; Purity (HPLC): 92.2%.

8-(4-Oxo-4-phenylbutyl)caffeine (6)

The title compound was prepared from 5-oxo-5-phenylpentanoic acid in a yield of 62%: mp 145–146 °C (methanol). ^{1}H NMR (Bruker Avance III 600, $CDCl_3$) δ 2.20 (qn, 2H, J = 7.15 Hz), 2.83 (t, 2H, J = 7.5 Hz), 3.11 (t, 2H, J = 6.4 Hz), 3.37 (s, 3H), 3.48 (s, 3H), 3.93 (s, 3H), 7.44 (t, 2H, J = 7.5 Hz), 7.55 (t, 1H, J = 7.2 Hz), 7.92 (d, 2H, J = 7.2 Hz); ^{13}H NMR (Bruker Avance III 600, $CDCl_3$) δ 21.6, 26.0, 27.9, 29.6, 31.8, 37.0, 107.5, 127.9, 128.7, 133.3, 136.7, 147.9, 151.7, 153.5, 155.3, 199.2; ESI-HRMS *m*/*z*: calcd for $C_{18}H_{21}O_3N_4$, 341.1614, found 341.1606; Purity (HPLC): 98.9%.

8-[(2E)-3-Phenylprop-2-en-1-yl]caffeine (7)

The title compound was prepared from styrylacetic acid in a yield of 76%: mp 169–171 °C (methanol). ^{1}H NMR (Bruker Avance III 600, $CDCl_3$) *δ* 3.38 (s, 3H), 3.57 (s, 3H), 3.93 (s, 3H), 3.69 (d, 2H, J = 6.4 Hz), 6.28 (m, 1H), 6.44 (d, 1H, J = 15.8 Hz), 7.22 (m, 1H), 7.29 (t, 2H, J = 7.5 Hz), 7.32 (d, 2H, J = 7.5 Hz); ^{13}H NMR (Bruker Avance III 600, $CDCl_3$) *δ* 27.9, 29.8, 30.9, 31.9, 107.7, 122.5, 126.3, 127.9, 128.6, 133.3, 136.3, 148.0, 151.7, 155.3; ESI-HRMS *m*/*z*: calcd for $C_{17}H_{19}O_2N_4$, 311.1508, found 311.1493; Purity (HPLC): 99.2%.

8-(2-Cyclohexylethyl)caffeine (8)

The title compound was prepared from 3-cyclohexylpropanoic acid in a yield of 78%: mp 133–134 °C (methanol). ^{1}H NMR (Bruker Avance III 600, $CDCl_3$) *δ* 0.95 (m, 2H), 1.20 (m, 4H), 1.57–1.75 (m, 7H), 2.70 (t, 2H, J = 7.9 Hz), 3.37 (s, 3H), 3.54 (s, 3H), 3.88 (s, 3H); ^{13}H NMR (Bruker Avance III 600, $CDCl_3$) *δ* 24.4, 26.2, 26.5, 27.8, 29.7, 31.6, 33.0, 34.9, 37.5, 107.3, 148.0, 151.7, 154.8, 155.3; ESI-HRMS *m*/*z*: calcd for $C_{16}H_{25}O_2N_4$, 305.1978, found 305.1977; Purity (HPLC): 99.8%.

In the table below the structures of the target caffeine derivatives are given and correlated with the ^{1}H NMR data. All of the appropriate signals were observed for each compound **1**-**8**. These include the 3 singlets for the caffeine methyl groups, the signals for the linker located between the caffeine ring and aromatic and aliphatic protons of the C8 substituent`s ring. The appropriate integration values and chemical shifts were also observed for all signals. In addition, the ^{13}C NMR data (not tabulated) also corresponded to each of the target structures in terms of the number of ^{13}C signals and their expected chemical shifts.

	Structure	^{1}H NMR signal assignment
1	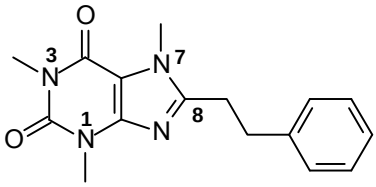	**a**. Methyl groups at N-1, N-3 and N-7 – singlets at 3.34 (3H), 3.55 (3H) and 3.57 (3H) ppm. **b**. CH_2-CH_2 – triplets at 2.98 (2H) and 3.05 (2H) ppm. **c**. Aromatic protons – signals at 7.08 (2H), 7.18 (1H) and 7.24 (2H) ppm.
2	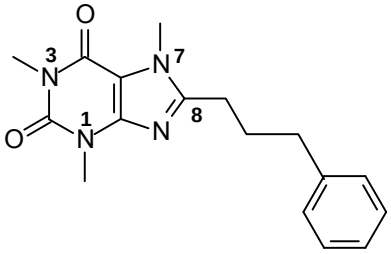	**a**. Methyl groups at N-1, N-3 and N-7 – singlets at 3.37 (3H), 3.55 (3H) and 3.80 (3H) ppm. **b**. CH_2-CH_2-CH_2 – quartet and quintet at 2.09 (2H) and 2.71 (4H) ppm. **c**. Aromatic protons – signals at 7.17 (3H), 7.28 (2H) ppm.
3	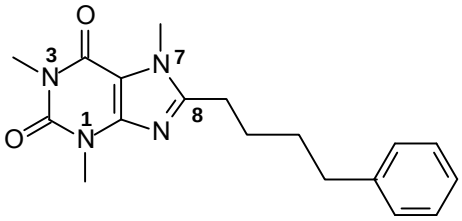	**a**. Methyl groups at N-1, N-3 and N-7 – singlets at 3.37 (3H), 3.54 (3H) and 3.85 (3H) ppm. **b**. $(CH_2)_4$ side chain – signals at 1.69 (4H) 1.79 (2H) and 1.77 (2H) ppm **c**. Aromatic protons – signals at 7.15 (3H), 7.25 (2H) ppm.
4	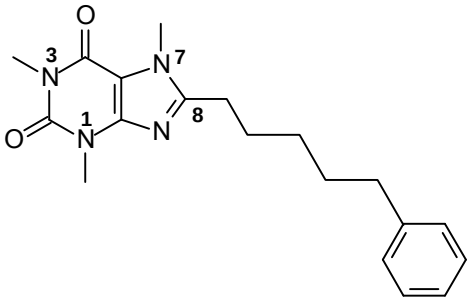	**a**. Methyl groups at N-1, N-3 and N-7 – singlets at 3.38 (3H), 3.54 (3H) and 3.87 (3H) ppm. **b**. $(CH_2)_5$ side chain – signals at 1.41 (2H), 1.66 (2H), 1.75 (2H), 2.61 (2H) and 2.69 (2H) ppm. **c**. Aromatic protons – signals at 7.15 (3H) and 7.35 (2H) ppm.

5	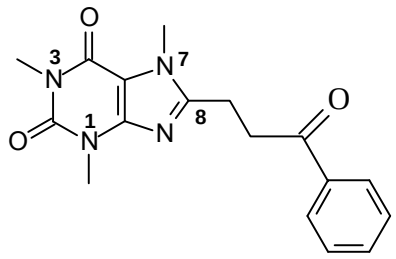	**a**. Methyl groups at N-1, N-3 and N-7 – singlets at 3.36 (3H), 3.46 (3H) and 4.01 (3H) ppm. **b**. $(CH_2)_2$ side chain – signals at 3.11 (2H) 3.58 (2H) ppm. **c**. Aromatic protons – signals at 7.46 (2H), 7.57 (1H) and 7.98 (2H) ppm.
6	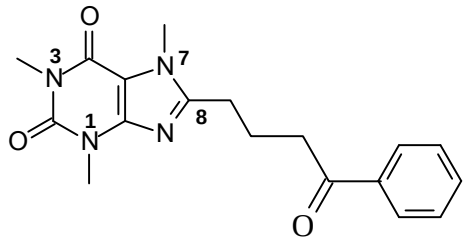	**a**. Methyl groups at N-1, N-3 and N-7 – singlets at 3.37 (3H), 3.48 (3H) and 3.93 (3H) ppm. **b**. $(CH_2)_3$ side chain – signals at 2.20 (2H) 2.83 (2H), 3.11 (2H), ppm. **c**. Aromatic protons – signals at 7.44 (2H), 7.55 (1H) and 7.92 (2H) ppm.
7	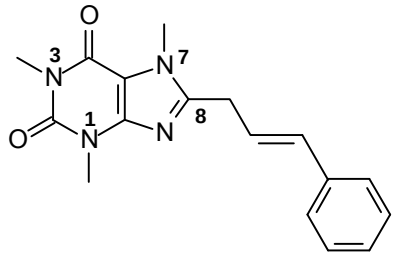	**a**. Methyl groups at N-1, N-3 and N-7 – singlets at 3.38 (3H), 3.57 (3H) and 3.93 (3H) ppm. **b**. CH_2-CH=CH side chain – doublets at 3.69 (2H) and 6.44 (1H) and signal at 6.28 (1H) ppm. **c**. Aromatic protons – signals at 7.22 (1H), 7.29 (2H) and 7.32 (2H) ppm.
8	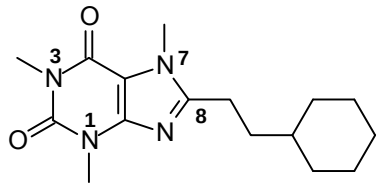	**a**. Methyl groups at N-1, N-3 and N-7 – singlets at 3.37 (3H), 3.54 (3H) and 3.88 (3H) ppm. **b**. CH_2 – triplet at 2.70 (2H) ppm. **c**. Cyclohexyl and CH_2 protons – signals at 0.95 (m, 2H), 1.20 (m, 4H), 1.57–1.75 (m, 7H) ppm

As shown in table 3.2 the high resolution masses that were obtained for each of the target caffeine analogues very closely corresponded to the calculated values. This is further confirmation of the structures of these compounds.

Table 3.2. Correlation of the calculated exact masses with the experimentally obtained masses of the caffeine analogues

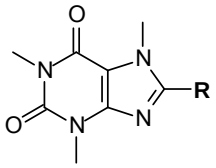

			Mass Spectrometry		
Compound	**R^1**	**Formula**	**Calcd.**	**Found**	**Ppm**
1	$-(CH_2)_2-C_6H_5$	$C_{16}H_{19}O_2N_4$	299.1508	299.1502	2
2	$-(CH_2)_3-C_6H_5$	$C_{17}H_{21}O_2N_4$	313.1665	313.1659	1.9
3	$-(CH_2)_4-C_6H_5$	$C_{18}H_{23}O_2N_4$	327.1821	327.1812	2.8
4	$-(CH_2)_5-C_6H_5$	$C_{19}H_{25}O_2N_4$	341.1978	341.1974	1.17
5	$-(CH_2)_2-CO-C_6H_5$	$C_{17}H_{19}O_3N_4$	327.1457	327.1469	3.67
6	$-(CH_2)_3-CO-C_6H_5$	$C_{18}H_{21}O_3N_4$	341.1614	341.1606	2.3
7	$-(CH_2)-CH=CH-C_6H_5$	$C_{17}H_{19}O_2N_4$	311.1508	311.1493	4.8
8	$-(CH_2)_2-C_6H_{11}$	$C_{16}H_{25}O_2N_4$	305.1978	305.1977	3.3

ppm = [(found – calcd.)/calcd]. x 1000000. In general a ppm difference smaller than 5 is considered to be good agreement.

3.10 Summary

A series of C-8 substituted caffeine analogues were synthesized by reacting 1,3-dimethyl-5,6-diaminouracil with the appropriate carboxylic acid in the presence of a carbodiimide dehydrating agent. Following ring closure and methylation at C-7, the target inhibitors were obtained. The structures of the compounds were confirmed by MS, ^{1}H-NMR and ^{13}C-NMR. The purities of the compounds were confirmed by HPLC. HPLC analysis revealed a single peak for each compound analysed (see annexture).

Chapter 4

Enzymology

This chapter will discuss the procedures for the determination of the MAO-A and MAO-B inhibition potencies of target C-8 substituted caffeine analogues. The results of these studies will be presented and discussed.

4.1. General enzymology

The C-8 substituted caffeine analogues (**1-8**) examined here were evaluated as inhibitors of recombinant human MAO-B and MAO-A. The IC_{50} values (concentration of the inhibitor that produces 50% inhibition) for the inhibition of MAO by each test compound were determined. Since the test inhibitors exhibited a competitive mode of inhibition (see below), the IC_{50} values were converted to the corresponding K_i values (enzyme–inhibitor dissociation constants) using the Cheng–Prusoff equation (Cheng & Prusoff, 1973). These K_i values enabled the calculation of MAO-A/B selectivity ratios.

To evaluate compounds **1-8** as potential inhibitors of recombinant human MAO-A and MAO-B, the enzyme activity measurements were based on the extent to which kynuramine is oxidized to 4-hydroxyquinoline by the MAO isoforms (Novaroli *et al*., 2005). The formation of 4-hydroxyquinoline was measured fluorometrically at excitation and emission wavelengths of 310 and 400 nm, respectively. None of the test inhibitors fluoresced at this excitation/emission wavelength or quenched the fluorescence of 4-hydroxyquinoline at the concentrations used for the inhibition studies. This fluorometric protocol is considerably more sensitive than the corresponding spectrophotometric technique and is thus more suitable for the measurement of recombinant human MAO-A and MAO-B activities which are relatively low compared to other enzymatic preparations.

4.2. Chemicals and instrumentation

For fluorescence spectrophotometry, a Varian Cary Eclipse fluorescence spectrophotometer was employed. Microsomes from insect cells containing recombinant human MAO-A and –B (5 mg/mL) and kynuramine.2HBr were obtained from Sigma-Aldrich.

4.3. The experimental method for determining IC_{50} values.

Microsomes from insect cells containing recombinant human MAO-A and MAO-B (5 mg/mL) were obtained from Sigma–Aldrich, pre-aliquoted and stored at −70 °C. All enzymatic reactions were carried out in potassium phosphate buffer (100 mM, pH 7.4, made isotonic with KCl) containing MAO-A (0.075 mg/mL) or MAO-B (0.075 mg/mL), various concentrations of the test inhibitor (0–400 μM) and kynuramine. The final concentrations of kynuramine in the reactions were 45 μM and 30 μM where MAO-A and -B, respectively, served as substrates. The final volume of the reactions was 500 μL. Stock solutions of the test inhibitors were prepared in DMSO and added to the reactions to yield a final concentration of 4% (v/v) DMSO. The reactions were incubated for 20 min at 37 °C and terminated with the addition of 400 μL NaOH (2 M). Distilled water (1000 μL) was added to each reaction before it was centrifuged for 10 min at 16,000 g. The concentrations of the MAO generated 4-hydroxyquinoline in the reactions were determined by measuring the fluorescence of the supernatant at an excitation wavelength of 310 nm and an emission wavelength of 400 nm (Novaroli *et al*., 2005). Quantitative estimations of 4-hydroxyquinoline were made by means of a linear calibration curve ranging from 0.0469 to 1.5 μM. Each calibration standard was prepared to a final volume of 500 μL in potassium phosphate buffer (100 mM, pH 7.4) and contained 4% DMSO. To each standard was added 400 μL NaOH (2 M) and 1000 μL distilled water. IC_{50} values were determined by plotting the initial rate of oxidation versus the logarithm of the inhibitor concentration to obtain a sigmoidal dose–response curve. These kinetic data were fitted to the one site competition model incorporated into the Prism software package and the IC_{50} values were determined in duplicate and are expressed as mean ± standard deviation (SD). The K_i values were calculated from the experimental IC_{50} values according to the equation by Cheng and Prusoff: $K_i = IC_{50}/(1 + [S]/K_m)$. For human MAO-B, [S] = 30 μM and K_m (kynuramine) = 22.7 μM while [S] = 45 μM and K_m (kynuramine) = 16.1 μM for human MAO-A (Cheng & Prusoff, 1973).

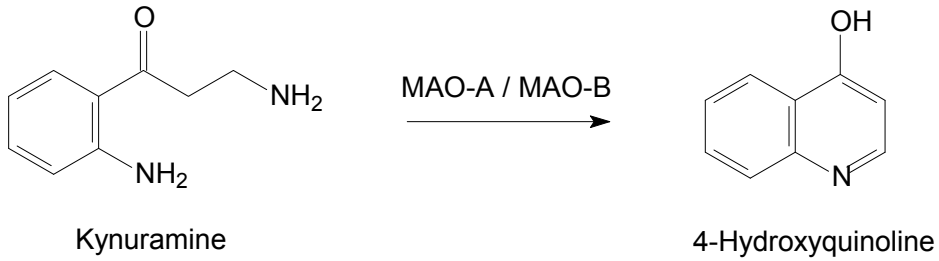

Figure 4.1. Oxidation of kynuramine to form 4-hydroxyquinoline

4.4. The experimental method for determining the reversibility of inhibition

Time-dependant inhibition studies were carried out in order to determine whether selected inhibitors, **5** and **3**, act as a reversible inhibitors or as time-dependant inactivators of human MAO-A and human MAO-B, respectively. The respective MAO preparations were preincubated for periods of 0, 15, 30, 60 min at 37 °C with **5** at a concentration of 20.8 µM for human MAO-A and with **3** at a concentration of 6.5 µM for human MAO-B. For this purpose the concentrations of the enzyme preparations were 0.03 mg/mL for human MAO-A and human MAO-B. The incubations were carried out in potassium phosphate buffer (100 mM, pH 7.4, made isotonic with KCl) for studies with the recombinant human enzymes. A final concentration of 45 µM kynuramine for human MAO-A and 30 µM kynuramine for human MAO-B were then incubated with the preincubated enzyme preparations at 37 °C for 15 min. The final volumes of these incubations were 500 µL and the final concentrations of **5** and **3** were 10.4 µM and 3.25 µM for human MAO-A and human MAO-B, respectively. These concentrations of the inhibitors are approximately equal to the IC_{50} values for the inhibition of the respective enzyme preparations by **5** and **3**. The final concentrations of the enzyme preparations were 0.015 mg/mL for human MAO-A and human MAO-B. The reactions with the recombinant human enzymes were terminated with 400 µL NaOH (2 M). A volume of 1000 µL distilled water was added to the incubations containing the recombinant human MAO preparations. The rate of formation of 4-hydroxyquinoline was measured as described above (section 4.3). All measurements were carried out in triplicate and are expressed as mean ± standard deviation (SD).

4.5. The construction of Lineweaver-Burk plots to determine the mode of inhibition

For selected inhibitors, Lineweaver–Burk plots were constructed in order to determine the modes of inhibition. For this purpose the initial rates of oxidation at four different substrate concentrations in the absence and presence of three different concentrations of the inhibitors were used to construct Lineweaver–Burke plots. Where recombinant human MAO-A was used as enzyme source, compound **5** at concentrations of 0–10.4 μM was selected as inhibitor and kynuramine (15–90 μM) served as substrate. Where recombinant human MAO-B was used as enzyme source, compound **3** at concentrations of 0–3.2 μM was selected as inhibitor and kynuramine (15–90 μM) also served as substrate. All enzymatic reactions and measurements were carried out as described above. Linear regression analysis was performed using the SigmaPlot software package (Systat Software Inc.).

4.6. Results and discussion

4.6.1. The IC_{50} values for the inhibition of MAO-A and –B by 1-8.

Table 4.1 The IC_{50} values and calculated K_i values for the inhibition of recombinant human MAO-A and MAO-B by compounds **1**–**8**[a]

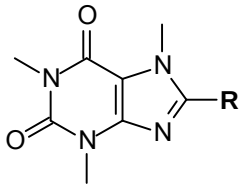

		IC_{50} (μM)		K_i (μM)[b]		
	R	MAO-A	MAO-B	MAO-A	MAO-B	SI[c]
1	$-(CH_2)_2-C_6H_5$	172 ± 26.5	26.0 ± 5.57	45.3	11.2	4
2	$-(CH_2)_3-C_6H_5$	117 ± 0.071	43.3 ± 6.20	30.8	18.7	2
3	$-(CH_2)_4-C_6H_5$	125 ± 22.1	3.25 ± 0.176	32.9	1.40	24
4	$-(CH_2)_5-C_6H_5$	51.6 ± 2.37	0.656 ± 0.0048	13.6	0.283	48
5	$-(CH_2)_2-CO-C_6H_5$	10.4 ± 0.767	187 ± 7.21	2.74	80.5	0.03
6	$-(CH_2)_3-CO-C_6H_5$	216 ± 5.73	46.9 ± 7.65	56.9	20.2	2.8
7	$-(CH_2)-CH=CH-C_6H_5$	68.4 ± 1.94	33.1 ± 4.50	18.0	14.3	4
8	$-(CH_2)_2-C_6H_{11}$	73.3 ± 10.0	6.59 ± 1.54	19.3	2.84	7

[a] All values are expressed as the mean ± SD of duplicate determinations.

[b] The K_i values were calculated from the experimentally measured IC_{50} values according to the equation by Cheng and Prusoff: $K_i = IC_{50}/(1 + [S]/K_m)$ with [S] = 45 μM and K_m (kynuramine) = 16.1 μM for human MAO-A and [S] = 30 μM and K_m (kynuramine) = 22.7 μM for human MAO-B (Cheng & Prusoff, 1973; Strydom *et al*., 2010).

[c] The selectivity index is the selectivity for the MAO-B isoform and is given as the ratio of K_i(MAO-A)/K_i(MAO-B).

As shown in Table 4.1 the caffeine analogues (**1**-**8**) evaluated in this study were inhibitors of both human MAO-A and -B. The following general observations may be made from the IC_{50} values given in table 4.1:

- All of the caffeine analogues evaluated were weak MAO-A inhibitors. The only possible exception is compound **5** which is a moderately potent MAO-A inhibitor with an IC_{50} value of 10.4 μM.

- In general the caffeine analogues were also found to be moderate to weak MAO-B inhibitors. Compounds **1, 2, 5, 6** and **7** may be considered weak MAO-B inhibitors with IC_{50} values in the higher μM range. Compound **8** and **3** are considered to be moderate MAO-B inhibitors IC_{50} value of 6.59 μM and 3.25 μM, respectively. Compound **4** was found to be the most potent MAO-B inhibitor identified in this study with an IC_{50} value of 0.656 μM. As shown in the table below, this compound (**4**) was found to be 5-285 fold more potent than the other compounds evaluated in this study.

  Table 4.2. A comparison of the IC_{50} values for the inhibition of MAO-B of the less potent MAO caffeine analogues with that of compound **4**.

Compound	IC_{50} value (μM)	Ratio **X**/**4**[a]
4	0.656 ± 0.0048	1
1	26.0 ± 5.57	39.63
2	43.3 ± 6.20	66.01
3	3.25 ± 0.176	5
5	187 ± 7.21	285.1
6	46.9 ± 7.65	71.5
7	33.1 ± 4.50	50.5
8	6.59 ± 1.54	10.05

[a]The ratio of IC_{50}(**1-3,5-8**)/IC_{50}(**4**)

- Except for compound **5** all of the target compounds are selective for MAO-B.

- As shown in the table below, the MAO-B inhibition potencies increased as the length of the carbon linker of each compound increased. Compound **3** with a 4-carbon linker is two-fold more potent than compound **2** with a 3-carbon linker. The most potent MAO-B inhibitor, compound **4**, has a 5-carbon linker which is the most optimal for MAO-B inhibition among the compounds studied.

  Table 4.3. A comparison of the IC_{50} values for the inhibition of MAO-B of **2** and **3** with that of compound **4**.

Compound	IC_{50} value (μM)	Ratio **X**/**4**[a]
4	0.656 ± 0.0048	1
2	43.3 ± 6.20	66.01
3	3.25 ± 0.176	4.96

[a]The ratio of IC_{50}(**2, 3**)/IC_{50}(**4**)

- The carbonyl functional groups present in the side chains of **5** and **6** did not have a significant effect on MAO-A and MAO-B inhibitor potencies. In fact, those homologues containing carbonyl groups were weaker MAO-B inhibitors than the compounds not containing a carbonyl group in the C-8 side chain linker. In the table below the MAO-B inhibition potencies of the compound containing carbonyl functional groups are compared to compounds without carbonyl groups in the side chain linker. Compounds containing the same amount of carbons in the linker are compared to each other below.

  Table 4.4. A comparison of the IC_{50} values for the inhibition of MAO-B by **5** and **6** with that of **2** and **3**, respectively.

Compound	IC_{50} value (μM)	Ratio **X**/**2**[a]
2	43.3 ± 6.20	1
5	187 ± 7.21	4.32

Compound	IC_{50} value (μM)	Ratio **X**/**3**[a]
3	3.25 ± 0.176	1
6	46.9 ± 7.65	14.44

[a]The ratio of IC_{50}(**2**, **3**)/IC_{50}(**3, 6**)

- Compound **7** which contained an unsaturated HC=CH in the linker was found to be a moderately potent MAO-A and MAO-B inhibitor.

- As shown in the table below, interestingly, **8** which was substituted with a cyclohexyl ring was more potent (IC_{50} = 6.59 μM) than **1** (IC_{50} = 26.0 μM) which indicates that the cyclohexyl ring is perhaps more optimal for MAO-B inhibition than the phenyl ring in the series studied.

Table 4.5. A comparison of the IC_{50} value for the inhibition of MAO-B by **8** with that of **1**.

Compound	IC_{50} value (μM)	Ratio **8**/**1**[a]
1	26.0 ± 5.57	1
8	6.59 ± 1.54	0.25

[a]The ratio of IC_{50}(**8**)/IC_{50}(**1**)

The main goal of this study was to discover a novel moiety that may be attached to the C-8 position of caffeine in order to enhance it`s MAO-B inhibition potency. The lead compound for this study was (E)-8-styrylcaffeine with an IC_{50} value of 2.86 μM for the inhibition of MAO-B (Vlok *et al*., 2006). In the table below, the IC_{50} values for the inhibition of MAO-B by the caffeine analogues examined in this study are compared to that of (E)-8-styrylcaffeine. As shown, compound **4** is the only compound with significantly more potent MAO-B inhibition than (E)-8-styrylcaffeine.This suggests that the C-8 phenylpentyl side chain is more optimal for enhancing the MAO-B inhibition potency of caffeine than the styryl side chain. This study therefore proposes that the phenylpentyl side chain be further optimized via substitution (especially with halogens) on the phenyl ring. Halogen substitution enhances the MAO-B inhibition potency of (E)-8-styrylcaffeine by several orders of a magnitude (Vlok *et al*., 2006). For example, (*E*)-8-(3-

Chlorostyryl)caffeine (CSC), a member of the (E)-8-styrylcaffeine class of MAO inhibitors, is an exceptionally potent competitive inhibitor of MAO-B with an enzyme-inhibitor dissociation constant (K_i value) of 128 nM (Vlok *et al*., 2006).

Table 4.6. A comparison of the IC_{50} values for the inhibition of MAO-B by (E)-8-styrylcaffeine with the caffeine analogues examined in this study. .

Compound	IC_{50} value (μM)	Ratio **X/1-8**[a]
(E)-8-styrylcaffeine	2.86	1
1	26.0 ± 5.57	9.1
2	43.3 ± 6.20	15.1
3	3.25 ± 0.176	1.1
4	0.656 ± 0.0048	0.2
5	187 ± 7.21	65.4
6	46.9 ± 7.65	16.4
7	33.1 ± 4.50	11.6
8	6.59 ± 1.54	2.3

[a]The ratio of IC_{50}(**1-8**)/IC_{50}((E)-8-styrylcaffeine)

4.6.2. Sigmoidal dose-response curve

IC_{50} values represent the concentration of a drug that is required for 50% inhibition *in vitro*. These are sigmoidal graphs of the measured MAO catalytic rate versus the log inhibitor concentration and are provided here as example of how the IC_{50} values documented in Table 4.1 were calculated.

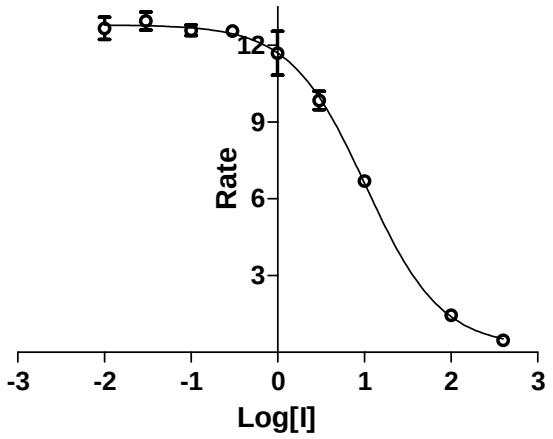

Panel A (MAO-A)

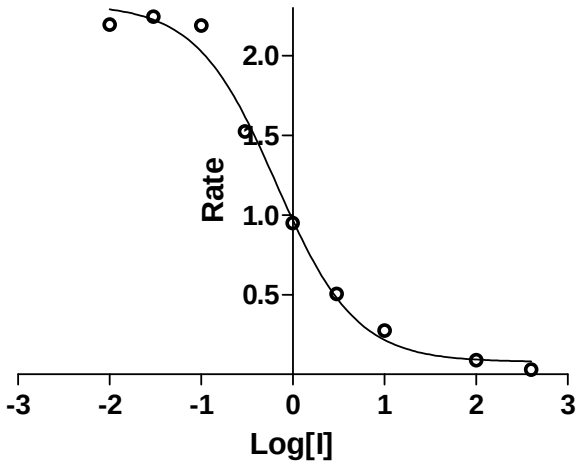

Panel B (MAO-B)

Figure 4.2 The sigmoidal dose-response curve of the initial rates of oxidation of kynuramine by recombinant human recombinant human MAO-A (Panel A) and MAO-B (Panel B) vs. the

logarithm of concentration of inhibitor **5** and **7** (expressed in μM), respectively. The determinations were carried out in duplicate and the values are expressed as the mean ± SD. The concentrations of kynuramine used were 45 μM and 30 μM for MAO-A and MAO-B, respectively, and the rate data are expressed as nmoles 4-hydroxyquinoline formed/min/mg protein.

4.6.3. Reversibility studies

To confirm that the test inhibitors bind reversibly in the active site of MAO-A and MAO-B, two representative inhibitors, compounds **3** and **5**, were selected for reversibility studies. As shown in Figure 4.3, when **5** and **3** were preincubated with recombinant human MAO-A and MAO-B for periods of 0, 15, 30 and 60 min, the rate of kynuramine (30 μM) oxidation did not decrease with increased incubation time. From these analyses it can be concluded that **5** and **3** interact reversibly with the active sites of human MAO-A and MAO-B.

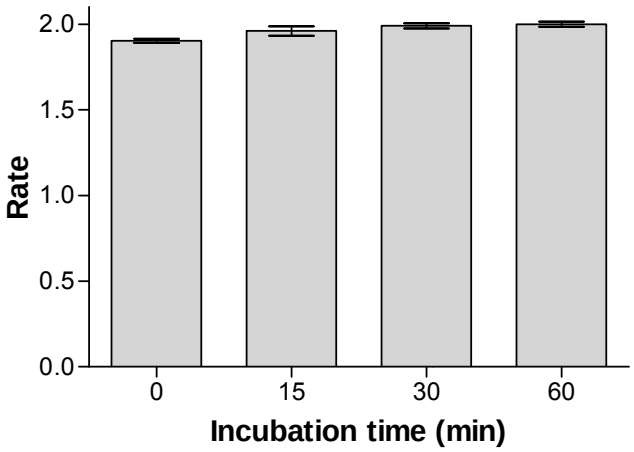

Panel A (MAO-A)

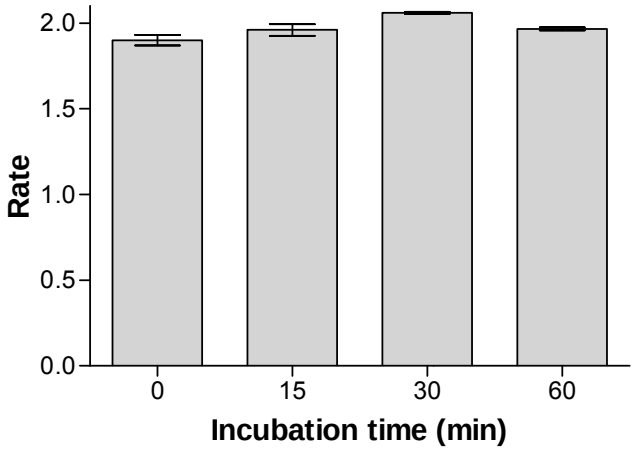

Panel B (MAO-B)

Figure 4.3 Time-dependent inhibition of recombinant human MAO-A (Panel A) and recombinant human MAO-B (Panel B) by **5** and **3**, respectively. The enzymes were preincubated for various periods of time (0–60 min) with **5** (MAO-A) and **3** (MAO-B) at concentrations of 20.8 μM and 6.5 μM, respectively. The concentrations of the enzyme substrate, kynuramine, were 45 and 30 μM for the studies with MAO-A and MAO-B, respectively. The catalytic rates are expressed as nmoles 4-hydroxyquinoline formed/min/mg protein.

4.6.4. Construction of Lineweaver-Burk plots

Sets of Lineweaver-Burk plots were constructed to determine the modes of inhibition for human MAO-A and MAO-B. As illustrated by example in Figure 4.4, the lines of the Lineweaver-Burk plots intersected which indicates that the mode of inhibition is competitive and that the inhibition is therefore reversible. These results are in accordance with expectation since (*E*)-8-styrylcaffeinyl analogues are also reported to inhibit MAO-B competitively (Vlok *et al*., 2006.)

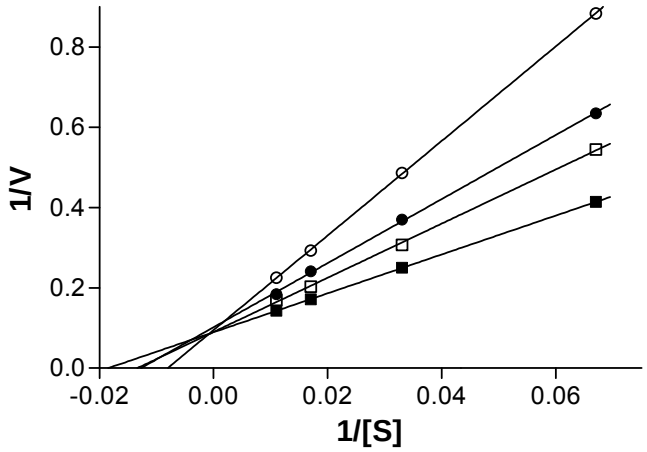

Panel A (MAO-A)

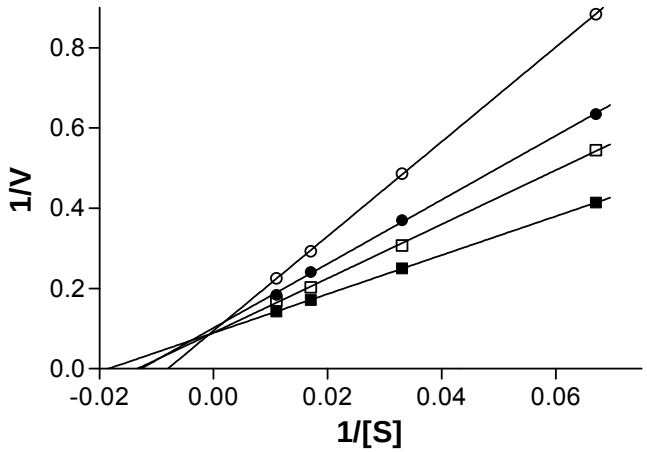

Panel B (MAO-B)

Figure 4.4 Lineweaver-Burk plots of the recombinant human MAO-A (Panel A) and recombinant human MAO-B (Panel B) catalyzed oxidation of kynuramine in the absence (filled squares) and presence of various concentrations of **5** and **3**, respectively. For the studies with MAO-A (Panel A) the concentrations of **5** were: 2.6 μM (open squares), 5.2 μM (filled circles), 10.4 μM (open circles). For the studies with MAO-B (Panel B) the concentrations of **3** were: 0.8 μM (open squares), 1.6 μM (filled circles), 3.2 μM (open circles).The rates (V) are expressed as nmol product formed/min/mg protein.

4.7 Summary

All the compounds synthesized were evaluated as inhibitors of recombinant human MAO-B and MAO-A. A fluorometric assay which relies on the measurement of the amount of 4-hydroxyquinoline formed as a result of MAO-catalysed kynuramine oxidation was used. The results showed that the target compound inhibit human MAO-B. The most potent inhibitor was compound **4** with an IC_{50} of 0.656 μM toward human MAO-B. Additionally, the inhibitors showed inhibition activity towards human MAO-A, with the most potent inhibitor, **5** having an IC_{50} of 10.4 μM. It was determined that selected compounds bind reversibly to both enzymes and that the mode of inhibition is competitive. The finding that the test analogues inhibit both MAO isoforms suggests that these compounds may be useful in the treatment of PD. Comparison of the IC_{50} value of the most potent MAO-B inhibitor with that of the lead compound, (E)-8-styrylcaffeine, shows that **4** is approximately 4.4 fold more potent than (E)-8-styrylcaffeine as an MAO-B inhibitor. It may therefore be concluded that the phenylpentyl side chain is more optimal for enhancing the MAO-B inhibition potency of caffeine than the styryl side chain. Based on the observation that halogen substitution of the styryl ring further enhances the MAO-B inhibition potency of (E)-8-styrylcaffeine, this study proposes that the phenylpentyl side chain be further optimized via halogen substitution on the phenyl ring.

Chapter 5

Conclusion

Parkinson's disease (PD) is a progressive neurodegenerative disorder characterized pathologically by a marked loss of dopaminergic nigrostriatal neurons and clinically by disabling movement disorders. There are four primary symptoms characterizing the disease: tremor, rigidity, bradykinesia and postural instability (Ballard *et al*., 1985). The motor disabilities characterizing PD are primarily due to the loss of dopaminergic neurons in the substantia nigra resulting in a dramatic decrease in the dopamine levels in the brain (Jenner, 1998). Once dopaminergic neuronal cell death reaches the critical level of 85-90%, the neurological symptoms of PD appear (Reiderer., 2004). PD can be treated by inhibiting monoamine oxidase (MAO), specifically MAO-B, since this is an important enzyme in the catabolism of dopamine in the substantia nigra of the brain. Inhibition of MAO-B may provide symptomatic relief for PD patients due to increased levels of dopamine in the brain.

Selegiline is an irreversible MAO-B inhibitor and is currently being used for the treatment of PD. Irreversible inhibitors inactivate enzymes by forming stable covalent complexes. Irreversible inhibition may not be reversed by removal of the inhibitor nor by increasing the substrate concentration. Even dialysis does not dissociate the enzyme inhibitor complex and restore enzyme activity. From a safety point of view it may therefore be more desirable to develop reversible inhibitors of MAO-B. Selegiline is a highly potent and selective irreversible inhibitor of MAO-B and has been shown to inhibit the metabolism of dopamine *in vivo*. Selegiline also has psychotoxic and cardiovascular side effects. This justifies the need to develop new, safe and reversible inhibitors of MAO-B for the treatment of PD.

For this purpose a series of C-8 substituted caffeine analogues were examined in the present study as potential inhibitors of MAO-A and –B. As lead compound, the known MAO-B inhibitor, (E)-8-styrylcaffeine was used. (E)-8-Styrylcaffeine inhibits MAO-B with an IC_{50} value of 2.86 μM (Vlok *et al*., 2006). The main goal of this study was therefore to discover novel side chains that enhances the MAO-B inhibition potency of caffeine to a larger degree than observed with the (E)-styryl side chain. The compounds tabulated below were selected for evaluation in this study and consisted of the following:

- Caffeine analogues with linkers containing 2, 3, 4 and 5 carbon atoms (phenylethyl (**1**), phenylpropyl (**2**), phenylbutyl (**3**) and phenylpentyl (**4**) functional groups)
- Caffeine analogues with a cyclohexane ring, the corresponding cyclohexylethyl (**5**)
- Two compounds with carbonyl functional groups in the side chain linker, the 3-oxo-3-phenylpropyl (**6**), 4-oxo-4-phenylbutyl (**7**) containing homologues.
- One compound containing an unsaturated linker between the caffeine and phenyl rings, compound **8**.

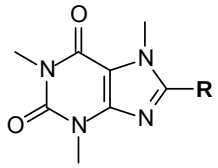

	R
1	$-(CH_2)_2-C_6H_5$
2	$-(CH_2)_3-C_6H_5$
3	$-(CH_2)_4-C_6H_5$
4	$-(CH_2)_5-C_6H_5$
5	$-(CH_2)_2-CO-C_6H_5$
6	$-(CH_2)_3-CO-C_6H_5$
7	$-(CH_2)-CH=CH-C_6H_5$
8	$-(CH_2)_2-C_6H_{11}$

Chemistry: The target compounds (**1-8**) were successfully synthesized by reacting 1,3-dimethyl-5,6-diaminouracil with the appropriate carboxylic acid in the presence of a carbodiimide dehydrating agent. Following ring closure and methylation at C-7 the target inhibitors were obtained. The structures of the compounds were confirmed by MS, ^{1}H-NMR and ^{13}C-NMR, and the purity of the compounds were confirmed by HPLC. Both the ^{1}H NMR and ^{13}C NMR spectra corresponded with the proposed structures and the expected exact masses were also recorded for each compound. HPLC analysis revealed a single peak for each compound analyzed which indicates a high degree of purity for each compound.

MAO inhibition studies: The caffeine analogues under investigation were evaluated as inhibitors of recombinant human MAO-A and –B which are commercially available. A fluorometric assay was employed to measure the inhibition potencies of the test compounds, and the activities were expressed as the IC_{50} values. The MAO activity measurements were based on measuring the amount 4-hydroxyquinoline formed from the MAO-catalysed oxidation of kynuramine. 4-Hydroxyquinoline fluoresces at an excitation wavelength of 310 nm and an emission wavelength of 400 nm (Ref).

The results showed that all of the caffeine analogues were inhibitors of MAO-A and –B. The most potent MAO-A inhibitor was **5** with an IC_{50} value of 10.4 μM. In general the compounds were better MAO-B inhibitors and with the exception of **5** all of the compounds displayed selective inhibition towards MAO-B. The most potent MAO-B inhibitor was compound **4** with an IC_{50} value of 0.656 μM toward human MAO-B. When compared to the IC_{50} value for the inhibition of MAO-B by (E)-8-styrylcaffeine, **4** is approximately 4.4 fold more potent than (E)-8-styrylcaffeine as an MAO-B inhibitor. This study therefore concludes that the phenylpentyl side chain of **4** is more optimal for enhancing the MAO-B inhibition potency of caffeine than the styryl side chain. The major goal of this study, namely the discovery of a novel side chain that enhances the MAO-B inhibition potency of caffeine to a larger degree than observed with the (E)-styryl side chain, has therefore been achieved.

Time-dependency and mode of inhibition: Reversibility studies showed that two representative inhibitors, **5** and **3**, were not time- dependant inactivators but interacted reversibly with MAO-A and MAO-B, respectively. This makes the C-8 substituted caffeine analogues examined here more desirable. Lineweaver-Burke studies were also carried out and the intersecting lines of these plots indicate that the mode of inhibition is competitive. The finding that the test analogues inhibit both MAO isoforms suggests that these compounds may be useful in the treatment of PD.

Future recommendations: This study recommends that the best MAO-B inhibitor identified in this study, 8-(phenylpentyl)caffeine (**4**), be substituted on the phenyl ring with halogens such as bromine, chlorine and fluorine. This suggestion is based on the observation that halogen substitution of the styryl ring further enhances the MAO-B inhibition potency of (E)-8-

styrylcaffeine. These halogen substituted 8-(phenylpentyl)caffeine analogues are therefore expected to also possess improved MAO-B inhibition properties.

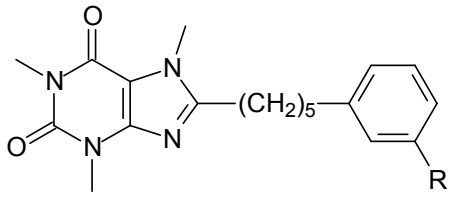

R
Cl
Br
F

Also, since the most potent MAO-B inhibitor identified in this study, **4**, contains the longest side chain on C8 of the caffeine ring, further extending the length of the C8 side chain may further enhance MAO-B inhibition potency. This study therefore proposes that the following caffeine analogues containing six and seven carbon linkers between the caffeine and phenyl rings be synthesized and evaluated as MAO-B inhibitors.

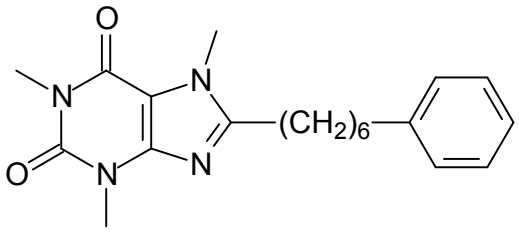

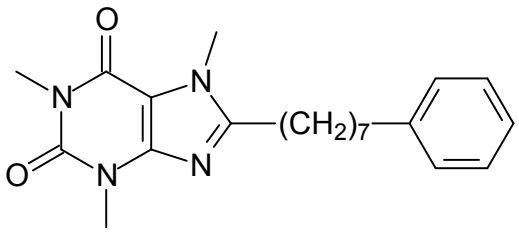

BIBLIOGRAPHY

Betarbet, R., Sherer, T. B., Mackenzie, G., Garcia-osuna, M., Panov, A. V. & Greenamyre, J. T. (2000). Chronic systemic pesticide exposure reproduces features of Parkinson disease. *Nat. Neurosci.* 3: 268-273.

Binda C, Hubaiek, F., Li, M., Edmondson, D. E. & Mattevi, A. (2004). Crystal structure of human monoamine oxidase B, a drug target enzyme monotopically inserted into the mitochondrial outer membrane. *FEBS Lett.* 564:225-228.

Binda, C., Li, M., Hubalek, F., Restelli, N., Edmondson, D. & Mattevi, A. (2003). Insights into the mode of inhibition of human mitochondrial monoamine oxidase B from high-resolution crystal structures. *Proceedings of the national academy of sciences of the United States of America,* 100: 9750-9755.

Binda, C., Mattevi, A. & Edmondson, D. (2002a). Structure-function relationships in flavoenzyme-dependent amine oxidations: a comparison of polyamine oxidase and monoamine oxidase. *Journal of biological chemistry,* 277: 23973-23976.

Binda, C., Newton-Vinson, P., Hubalek, F., Edmondson, D. & Mattevi, A. (2002b). Structure of human monoamine oxidase B, a drug target for the treatment of neurological disorders. *Nature structural biology,* 9: 22-26.

Binda, C., Wang, J., Pisani, L., Caccia, C., Carotti, A. & Salvati, P. (2007). Structures of human monoamine oxidase B complexes with selective noncovalent inhibitors: safinamide and coumarin analogues. *Journal of medicinal chemistry,* 50: 5848-5852.

Blum, D., Torch, S., Lambeng, N., Nissou, M., Benabid, A., Sadoul, R. & Verna, J. (2001). Molecular pathways involved in the neurotoxicity of 6-OHDA, dopamine and MPTP: contribution to the apoptotic theory in Parkinson's disease. *Progress in Neurobiology, 65*, 135-172.

Bove', J., Prou, D., Perier, C. & Przedborski, S. (2005). Toxin-induced models of Parkinson's disease: *J. Am. Soc. Exp. NeuroTherapeutics.* 2:484-494.

Chen, J. F., Xu, K., Petzer, J. P., Staal, R., Xu, Y. H., Beilstein, M., Sonsalla, P. K., Castagnoli, K., Castagnoli, N. Jr. & Schwarzschild, M. A. (2001). Neuroprotection by caffeine and A_2A adenosine receptor inactivation in a model of Parkinson's disease *J. Neurosci.* 21:1-6.

Cheng, Y. & Prusoff, W. (1973). Relationship between the inhibition constant (K_i) and the concentration of inhibitor which causes 50 per cent inhibition (I_{50}) of an enzymatic reaction. *Biochemical Pharmacology, 22*, 3099-3108.

Dauer, W. & Przedborski, S. (2003). Parkinson's disease: Mechanisms and models. *Neurons.* 39:889-909.

Day, B. T., Patel, M., Calavetta, L., Chang, L. Y. & Stamler, J. S. (1999). A mechanism of paraquat toxicity involving nitric oxide synthase. *Proc. Natl. Acad. Sci. USA.* 96:12760-12765.

De Colibus, L., Li, M., Binda, C., Lustig, A., Edmondson, D.E. & Mattevi, A. (2005). Three-dimensional structure of human monoamine oxidase A (MAO-A): Relation to the structures of rat MAO-A and human MAO-B. *The National Academy of Sciences of the USA, 102*, 12684-12689.

Deleu, D., Northway, M.G., Hanssens, Y. (2002). An evidence-based review of dopamine receptor agonists in the treatment of Parkinson's disease. *Neurosciences* 7 (4), pp. 221-231.

Dixon, M. (1953). The determination of enzyme inhibitor constants. *Biochemical journal, 55*: 170-171.

Edmondson, D., Mattevi, A., Binda, C., Li, M. & Hubalek, F. (2004). Structure and mechanism of monoamine oxidase. *Current medicinal chemistry, 11:* 1983-1993.

Elbaz, A. & Tranchant, C. (2007). Epidemiologic studies of environmental exposures in Parkinson's disease. *Journal of the Neurological Sciences, 262*, 37-44.

Factor, S. (2008). Current status of symptomatic medical therapy in Parkinson's disease. *Neurotherapeutics,* 5: 210-225.

Fernandez, H. & Chen, J. (2007). Monoamine oxidase-B inhibition in the treatment of Parkinson's disease. *Pharmacotherapy, 2*: 174S-185S.

Finberg, J.P.M., Tenne, M., Youdim, M.B.H. (1981). Tyramine antagonistic properties of AGN 1135, an irreversible inhibitor of monoamine oxidase type B. *British Journal of Pharmacology* 73 (1), pp. 65-74

Finberg, J.P.M., Tenne, M., Youdim, M.B.H. 1982. Pharmacological effects of selective type A and type B MAO inhibitors. *Advances in the Biosciences* 40 (C), pp. 219-225

Fischer, E. & Reese, L. (1883). Ueber Caffein, Xanthin und Guanin. *Liebigs Annalen der Chemie, 221*, 336-344.

Green, A.R., Mitchell, B.D., Tordoff, A.F.C., Youdim, M.B.H. (1977). Evidence for dopamine deamination by both type A and type B monoamine oxidase in rat brain in vivo and for the degree of inhibition of enzyme necessary for increased functional activity of dopamine and 5 hydroxytryptamine. *British Journal of Pharmacology* 60 (3), pp. 343-349.

Gnerre, C., Catto, M., Leonetti, F., Weber, P., Carrupt, P. & Altomare, C. (2000). Inhibition of monoamine oxidase by functionalized coumarin derivatives: biological activities, QSAR's, and 3D-QSAR's. *Journal of medicinal chemistry, 43*: 4747-4758.

Guttman, M., Kish, S. & Furukawa, Y. (2003). Current concepts in the diagnosis and management of Parkinson's disease. *Canadian Medical Association Journal, 168*, 293-301.

Hallett, P.J., Standaert, D.G. (2004). Rationale for and use of NMDA receptor antagonists in Parkinson's disease. *Pharmacology and Therapeutics* 102 (2), pp. 155-174.

Hansch, C. & Leo, A. (1995). Exploring QSAR. Fundamentals and applications in chemistry and biology. Washington DC: American Chemical Society. 1-124.

Hefti, F., Melamed, E., Sahakian, B.J., Wurtman, R.J. (1980). Circling behavior in rats with partial, unilateral nigro-striatal lesions: Effect of amphetamine, apomorphine, and DOPA. *Pharmacology Biochemistry and Behavior* 12 (3), pp. 185-188.

Ho, T., W., Bristol, L., A., Coccia, C., Li, Y., Milbrandt, J., Johnson, E., Jin, L., Bar-Peled, O., Griffin, J., W. & Rothstein, J., D. (2000). TGFb trophic factors differentially modulate motor axon outgrowth and protection from excitotoxicity. *Experimental Neurology 161: 664–675*

Holt, A., Sharman, D., Baker, G. & Palcic, M. (1997). A continuous spectophotometric assay for monoamine oxidase and related enzymes in tissue homogenates. *Analytical biochemistry, 244*: 384-392.

Hubalek, F., Binda, C., Khalil, A., Li, M., Mattevi, A., Castagnoli, N. & Edmondson, D. E. (2005). Demonstration of isoleucine 199 as a structural determinant for the selective inhibition of human monoamine oxidase B by specific reversable inhibitors. *Journal of biological chemistry, 280*: 15761-5766.

Huston, R. & Allen, W. (1934a). Caffeine derivatives. I. The 8-Ethers of caffeine. *Journal of the American Chemical Society, 56*, 1356-1358.

Huston, R. & Allen, W. (1934b). Caffeine derivatives. II. Molecular rearrangement of the 8-ethers of caffeine. *Journal of the American Chemical Society, 56*, 1358-1359.

Inoue, H., Castagnoli, K., Van der Schyf, C., Mabic, S., Igarashi, K. & Castagnoli, N. J. (1999). Species-dependant differences in monoamine oxidase A and B-catalyzed oxidation of various C4 substituted 1-methyl-4-phenyl-1,2,3,6-tetrahydropyridinyl derivatives. *Journal of pharmacology and experimental therapeutics, 291*: 856-864.

Jalkanen, S. & Salmi, M. (2001). Cell surface monoamine oxidases: enzymes in search of a function. *The EMBO journal, 20*: 3893-3901.

Javitch, J. A., D'Amato, R. J., Strittmetter, S. M. & Syner, S. H. (1985). Parkinsonism-inducing neurotoxin, 1-methyl-4-phenyl-1,2,3,6-tetrahydropyridine: uptake of the metabolite 1-methyl-4-phenylpyridine by dopamine neurons selective toxicity. Proc. *Natl. Acad. Sci.* USA . 82:2173-2177.

Javoy, F., Sotelo, C., Herbet, A., Agid, Y. (1976). Specificity of dopaminergic neuronal degeneration induced by intracerebral injection of 6 hydroxydopamine in the nigrostriatal dopamine system. *Brain Research* 102 (2), pp. 201-215.

Knetgel, R.M.A., Kuntz, I.D. & Oshiro, C.M. (1997). Molecular docking to ensembles of protein structures. *Journal of Molecular Biology, 266*,424-440.

Langston, J. W. (1990). Predicting Parkinson's disease. *Neurology.* 40:70-76.

Lee, Y., Ling, K., Lu, X., Silverman, R.B., Shepard, E.M., Dooley, D.M. & Sayre, L.M. (2002). 3-Pyrrolines are mechanism-based inactivators of the quinone-dependant amine oxidases but only substrates of the flavin-dependent amine oxidases. *Journal of the American Chemical Society, 124*, 12135-12143.

Lees, A. (2005). Alternatives to levodopa in the initial treatment of early Parkinson's disease. *Drugs & aging , 22*: 731-740.

Leroy, E., Boyer, R., Auburger, G., Leube, B., Ulm, G. & Mezey, E. (1998). The ubiquitine pathwayin Parkinson's disease. *Nature, 395*, 451-452.

LeWitt, P. & Taylor, D. (2008). Protection Against Parkinson’s Disease Progression:Clinical Experience. *Neurotherapeutics: the journal of the American society for experimental neurotherapeutics, 5*: 210-225.

Li, M., Binda, C., Mattevi, A. & Edmondson, D.E. (2006). Functional role of the “aromatic cage” in human monoamine oxidase B: Structures and catalytic properties of Tyr435 mutant proteins. *Biochemistry, 45*, 4775-4784.

Livingstone, D. J. & Salt, D. W. (2005). Judging the significance of multiple linear regretion models. *Journal of medicinal chemistry,* 48: 661-663.

Luthman, J., Fredriksson, A., Sundstrom, E., Jonsson, G., Archer, T. (1989). Selective lesion of central dopamine or noradrenaline neuron systems in the neonatal rat: Motor behavior and monoamine alterations at adult stage. *Behavioural Brain Research* 33 (3), pp. 267-277.

Mandel, S., Grunblatt, E., Riederer, P., Amariglio, N., Hirsch, J.J., Rechavi, G., Youdim, M.B.H. (2005). Gene expression profiling of sporadic Parkinson's disease substantia nigra pars compacta reveals impairment of ubiquitin-proteasome subunits, SKP1A, aldehyde dehydrogenase, and chaperone HSC-70**.** *Annals of the New York Academy of Sciences* 1053, pp. 356-375.

Manning-Bog, A. B., Mccormack, A. L., Li, J., Uversky, V. N., Fink., A. L & Di Monte, D. A. (2002). The herbicide paraquat causes up-regulation and aggregation of alpha-synuclein in mice: paraquat and alpha-synuclein. *J. Biol. Chem.* 277:1641-1644.

Manley-King, C.I., Terre'Blanche, G., Castagnoli Jr. N., Bergh, J.J. & Petzer, J.P. (2009). Inhibition of monoamine oxidase B by *N*-methyl-2-phenylmaleimides. *Bioorganic & medicinal chemistry*, 17: 3104-3110.

Meyerson, L., McMurtrey, K. & Davis, V. (1978). A rapid and sensitive potentiometric assay for monoamine oxidase using a ammonia-selective electrode. *Analytical biochemistry, 86*: 287-297.

Matsumoto, T., Suzuki, O., Furuta, T., Asai, M., Kurokawa, Y., Nimura, Y., Katsumata, Y. & Takahashi, I. (1985). A sensitive fluorometric assay for serum monoamine oxidase with kynuramine as substrate. *Clinical Biochemistry, 18*, 126-129.

Miller, J. R. & Edmondson, D. E. (1999). Structure-activity relationships in the oxidation of para-substituted benzylamine analogues by recombinant human liver monoamine oxidase A. *Biochemistry.* 38:13670-13683.

Mizuno, Y., Sone, N., Suzuki, K. & Saitoh, T. (1988). Studies on the toxicity of 1-methyl-4-phenylpyridinium ion (MPP^+) against mitochondria of mouse brain. *J. Neurol. Sci.* 86:97-110.

Nagatsu, T. (2004). Progress in monoamine oxidase (MAO) research in relation to genetic engineering. *Neurotoxicology, 25*: 197-217.

Newton-Vinson, P., Hubalek, F. & Edmondson, D.E. (2000). High-level expression of human liver monoamine oxidase B in Pichia pastoris. *Protein Expression and Purification, 20*, 334-345.

Nicotra, A. & Parvez, S. (1999). Methods for assaying monoamine oxidase A and B activity: recent developments. *Biogenic amines, 15*: 307-320.

Novaroli, L., Reist, M., Favre, E., Carotti, A., Catto, M. & Carrupt, P. (2005). Human recombinant monoamine oxidase B as reliable and efficient enzyme source for inhibitor screening. *Bioorganic & medicinal chemistry*, *13: 6212-6217*

O'Brien, E., Kiely, K. & Tipton, K. (1978). A discontinuous luminometric assay for monoamine oxidase using an ammonia-selective electrode. *Analytical biochemistry, 86*: 287-297.

O'Brien, E.M., Kiely K.A. & Tipton, K.F. (1993). A discontinuous luminometric assay for monoamine oxidase. *Biochem. Pharmacol.* 46:301-1306.

Olanow, C.W. (1993). MAO-B inhibitors in Parkinson's disease. *Advances in neurology* 60, pp. 666-671

Ogunrombi, M.O., Malan, S.F., Terre'Blanche, G., Castagnoli Jr. N., Bergh, J.J. & Petzer, J.P. (2007). Neurotoxicity studies with the monoamine oxidase B substrate 1-methyl-3-phenyl-3-pyrroline. *Life sciences*, 81: 458-467.

Ogunrombi, M.O., Malan, S.F., Terre'Blanche, G., Castagnoli Jr. N., Bergh, J.J. & Petzer, J.P. (2008). Structure–activity relationships in the inhibition of monoamine oxidase B by 1-methyl-3-phenylpyrroles. *Bioorganic & medicinal chemistry*, 16: 2463-2472.

Ooms, F., Frederick, R., Durant, F., Petzer, J.P., Castagnoli, N., Van der Schyf, C.J. & Wouters, J. (2003). Rational approaches towards reversible inhibition of type B monoamine oxidase. Design and evaluation of a novel 5H-Indenol[1,2-c]pyridazin-5-one derivative. *Bioorganic & Medicinal Chemistry Letters, 13*, 69-73.

Parkinson Study Group (1996). Impact of deprenyl and tocopherol treatment on Parkinson's disease in DATATOP subjects not requiring levodopa. *Annals of Neurology.* 39: 29–36.

Petzer, J. P., Steyn, S., Castagnoli, K. P., Chen, J., Schwarzchild, M. A., Van der Schyf, C. J. & Castagnoli, N. (2003). Inhibition of monoamine oxidase B by selective adenosine A_2A receptor antagonists. *Bioorg. Med. Chem.* 11:1299-1310.

Pretorius, J., Malan, S.F., Castagnoli, N., Jr., Bergh, J.J. & Petzer, J.P. (2008). Dual inhibition of monoamine oxidase B and antagonism of the adenosine A_{2A} receptor by (E,E)-8-(4-phenylbutadien-1-yl)caffeine analogues. *Bioorganic & medicinal chemistry*, 16: 8676-8684.

Przedborski, S. (2005). Pathogenesis of nigral cell death in Parkinson's disease. *Parkinsonism and related disorders , 11*: S3-S7.

Ramsay, R. R., Krueger, M. J., Youngster, S. K., Gluck, M. R., Casida, J. E & Singer, T. P. (1991). Interaction of 1-methyl-4-phenylpyridinium ion (MPP^+) and its analogs with the rotenone/piericidin binding site of NADH dehydrogenase. *J. Neurochem.* 56:1184-1190.

Ramsay, R. R., Salach, J. I. & Singer, T. P. (1986). Uptake of the neurotoxin 1-methyl-4-phenylpyridine (MPP^+) and its relation to the inhibition of mitochondrial NADH-linked substrates by MPP^+. *Biochem. Biophys. Res. Commun. 134:743-748.*

Rascol, O., Goetz, C., Koller, W., Poewe, W. & Sampaio, C. (2002). Treatment interventions for Parkinson's disease. *Lancet, 359*, 1589-1598.

Riederer, P., Danielczyk, W. & Grunblatt, E. (2004a). Monoamine oxidase-B inhibition in Alzheimer's disease. *Neurotoxicology, 25*: 271-277.

Riederer, P., Lachenmayer, L. & Laux, G. (2004b). Clinical applications of MAO-inhibitors. *Current medicinal chemistry, 11*: 2033-2043.

Riederer, P., Konradi, C., Hebenstreit, G. (1989). Neurochemical perspectives to the function of monoamine oxidase. *Psychiatrische Praxis* 16 (SUPPL. 1), pp. 7-10.

Rodwell, A. & Kennely, V. W. 2000. Enzymes: Kinetics. In Harper's Biochemistry. 25^{th} Edition. David A. Barnes (Ed), APPLETON & LANGE. Stanford, Connecticut, pp 95-97.

Salach, J. & Weyler, W. (1987). Preperation of the flavin-containing aromatic amine oxidases of human placenta and beef liver. *Methods in enzymology, 142*: 627-637.

Shih, J., Chen, K. & Ridd, M. (1999). Monoamine oxidase: from genes to behaviour. *Annual r*

Silverman, R. (1995). Radical ideas about monoamine oxidase B. *Accounts of Chemical Research, 28*, 335-342.

Silverman, R. B. (1996). In Contemporary Enzyme Kinetics and Mechanism. 2nd edition, Purick D.L (Ed.) Academic Press, San Diego, pp 291-334. *eview of neuroscience , 22*: 197-217.

Singer, T. P., Ramsay, R. R., Mckeown, K., Trevor, A. & Castagnoli, N. Jr. (1988). Mechanisms of the neurotoxicity of 1-methyl-4-phenylpyridinium (MPP^+), the toxic bioactivation product of 1-methyl-4-phenyl-1,2,3,6-tetrahydropyridine (MPTP). *Toxicology.* 49:17-23.

Smeyne, R. & Jackson-Lewis, V. (2004). The MPTP model of Parkinson's disease. *Molecular brain research, 134*: 57-66.

Son, S., Ma, J., Kondou, Y., Yoshimura, M., Yamashita, E. & Tsukihara, T. (2008). Structure of human monoamine oxidase A at 2.2-Å resolution: the control of opening the entry for substrates/inhibitors. *Proceedings of the national academy of sciences of the United States of America,* 105: 5739-5744.

Strydom, B., Malan, S. F., Castagnoli Jr. N., Bergh, J. J. & Petzer, J. P. (2010). Inhibition of monoamine oxidase by 8-benzyloxycaffeine analogues. *Bioorganic & medicinal chemistry*, 18: 1018-1028.

Suzuki, F., Shimada, J., Mizumoto, H., Karasawa, A., Kubo, K., Nonaka, H., Ishii, A. & Kawakita, T. (1992). Adenosine A1 antagonists. 2. Structure-activity relationships on diuretic activities and protective effects against acute renal failure. *Journal of medicinal chemistry*, 35: 3066–3075.

Symes, A.L., Sourkes, T.L., Youdim, M.B., Gregoriadis, G., Birnbaum, H. (1969). Decreased monoamine oxidase activity in liver of iron-deficient rats. *Canadian journal of biochemistry* 47 (11), pp. 999-1002.

Taipade, D. J., Greene, J. G., Higgins, D. S, Jr. & Greenamyre, J. T. (2000). In vivo labeling of mitochondrial complex I (NADH:ubiquinone oxidoreductase) in rat brain using [(3)H]dihydrorotenone. *J Neurochem.* 75:2611-2621.

Ungerstedt, U. (1971). Postsynaptic supersensitivity after 6-hydroxy-dopamine induced degeneration of the nigro-striatal dopamine system. *Acta Physiologica Scandinavica, Supplement* 367, pp. 69-93.

Vlok, N., Malan, S. F., Castagnoli, N. Jr, Bergh, J. J & Petzer, J. P. (2006). Inhibition of monoamine oxidase B by analogues of the adenosine A_{2A} receptor antagonist (E)-8-(3-chlorostrylcaffeine). *Bioorg. Med. Chem.* 74:3512-3521.

Yacoubian, T. A. & Standaert, D. G. (2009). Targets for neuroprotection in Parkinson's disease. *Biochimica et biophysica acta,* 1792: 676-687.

Youdim, M. B. H. (1988). Platelet monoamine oxidase B: Use and misuse. *Cellular & Mol. Life Sci.* 44:137-141.

Youdim, M. B. & Bakhle, Y. S. (2006). Monoamine oxidase: isoforms and inhibitors in Parkinson's disease and depressive illness. *Br. J. Pharmacol.* 147 (Suppl 1):S287-S296.

Youdim, M. B. & Green, A. R. (1975). Biogenic monoamine metabolism and functional activity in iron-deficient rat; behavioural correlates. *Ciba Found Symp.* 51:201-22.

Youdim, M. B. H., Collins, G. G. S., Sandier, M., Bevan Jones, A. B., Pare, C. M. B. & Nicholson, W. J. (1972). Biological Sciences: Human brain monoamine oxidase: Multiple forms and selective inhibitors. *Nature.* 236:225-228.

Youdim, M. B. H., Edmondson, D. & Tipton K. F.(2006).The therapeutic potential of monoamine oxidase inhibitors. *Nat. Rev. Neurosci.* 7:295-309.

Youdim, M.B., Grahame-Smith, D.G., Holzbauer, M. (1975). Effect of age on the development and properties of brain monoamine oxidase. *Biochemical Society Transactions* 3 (5), pp. 702-704

Zecca, L., Stroppolo, A., Gatti, A., Tampellini, D., Toscani, M., Gallorini, M., Giaveri, G., Zucca, F.A. (2004). The role of iron and molecules in the neuronal vulnerability of locus coeruleus and substantia nigra during aging. *Proceedings of the National Academy of Sciences of the United States of America* 101 (26), pp. 9843-9848.

Zhou, J., Zhong, B. & Silverman, R. (1996). Direct continuous fluorometric assay for monoamine oxidase. *Analytical biochemistry, 234*: 9-12.

Annexure

Supplementary Material

HPLC analysis of purity

Method: To determine the purity of the previously unreported compounds (**PG1**–**PG8**), HPLC analyses were carried out. HPLC analyses were performed with an Agilent 1100 HPLC system equipped with a quaternary pump and an Agilent 1100 series diode array detector. A Venusil XBP C18 column (4.60 × 150 mm, 5 µm) was used and the mobile phase consisted initially of 30% acetonitrile and 70% MilliQ water at a flow rate of 1 mL/min. At the start of each HPLC run a solvent gradient program was initiated by linearly increasing the composition of the acetonitrile in the mobile phase to 85% acetonitrile over a period of 5 min. Each HPLC run lasted 15 min and a time period of 5 min was allowed for equilibration between runs. A volume of 20 µL of solutions of the test compounds in acetonitrile (1 mM) was injected into the HPLC system and the eluent was monitored at wavelengths of 210, 254 and 300 nm.

HPLC traces of the following new/unknown compounds

- 8-(2-Phenylethyl)caffeine (**1**)
- 8-(3-Phenylpropyl)caffeine (**2**)
- 8-(4-Phenylbutyl)caffeine (**3**)
- 8-(5-Phenylpentyl)caffeine (**4**)
- 8-(3-Oxo-3-phenylpropyl)caffeine (**5**)
- 8-(4-Oxo-4-phenylbutyl)caffeine (**6**)
- 8-[(2E)-3-Phenylprop-2-en-1-yl]caffeine (**7**)
- 8-(2-Cyclohexylethyl)caffeine (**8**)

8-(2-Phenylethyl)caffeine (**1**)

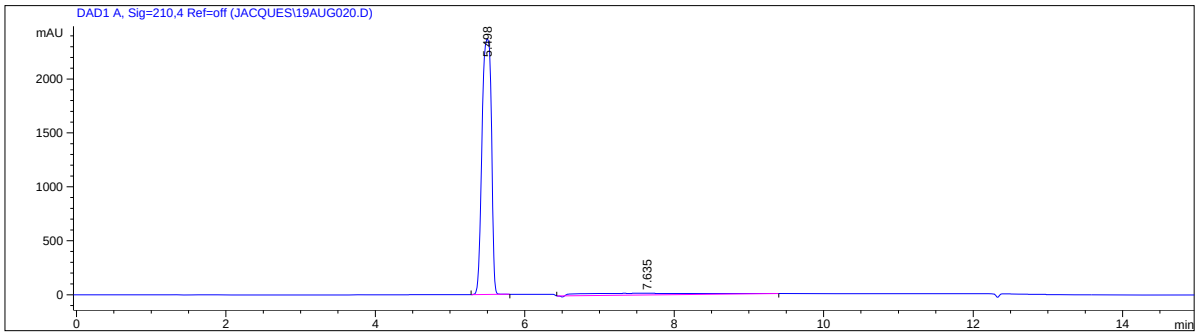

8-(3-Phenylpropyl)caffeine (**2**)

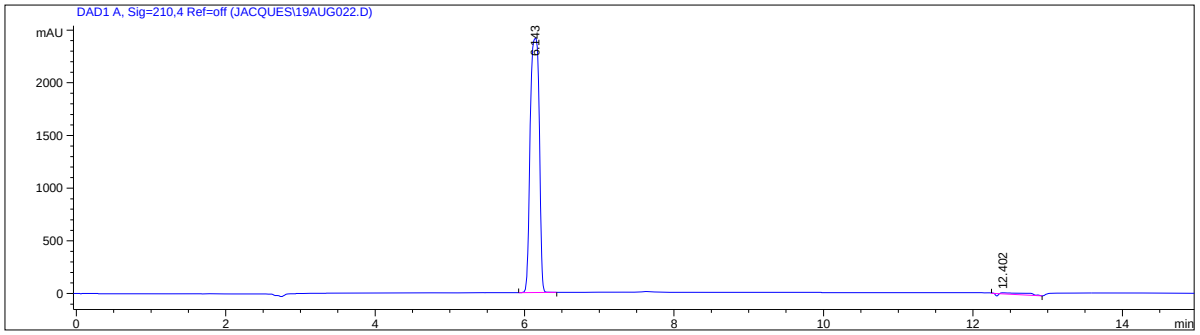

8-(4-Phenylbutyl)caffeine (**3**)

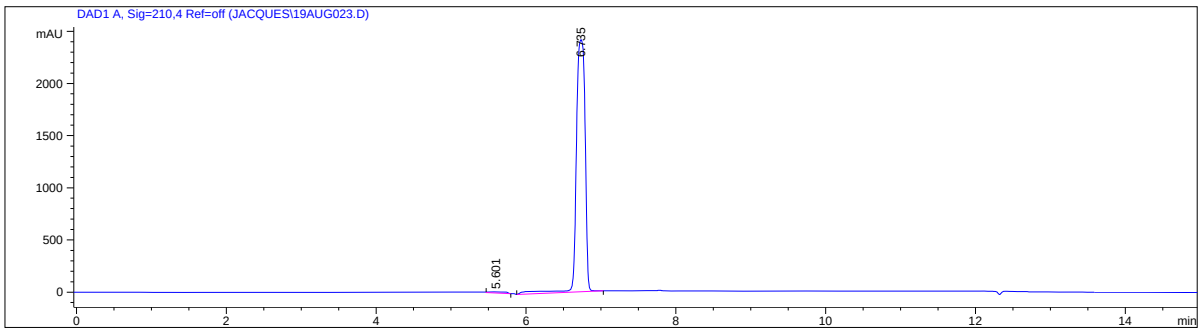

8-(5-Phenylpentyl)caffeine (**4**)

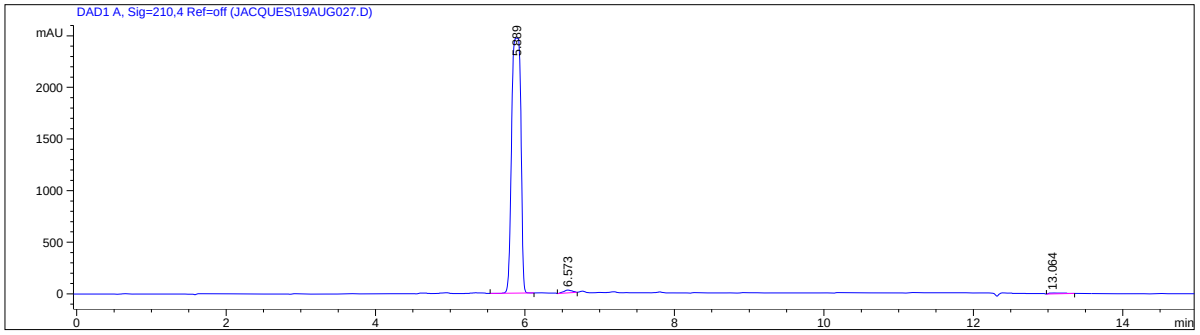

8-(3-Oxo-3-phenylpropyl)caffeine (**5**)

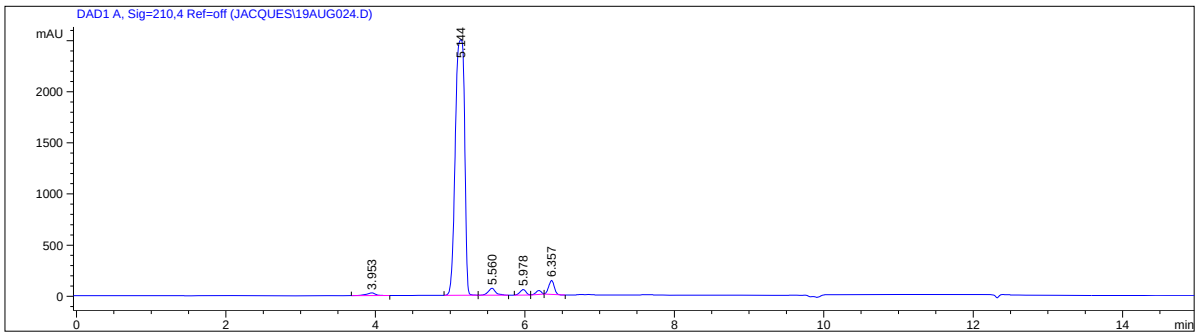

8-(4-Oxo-4-phenylbutyl)caffeine (**6**)

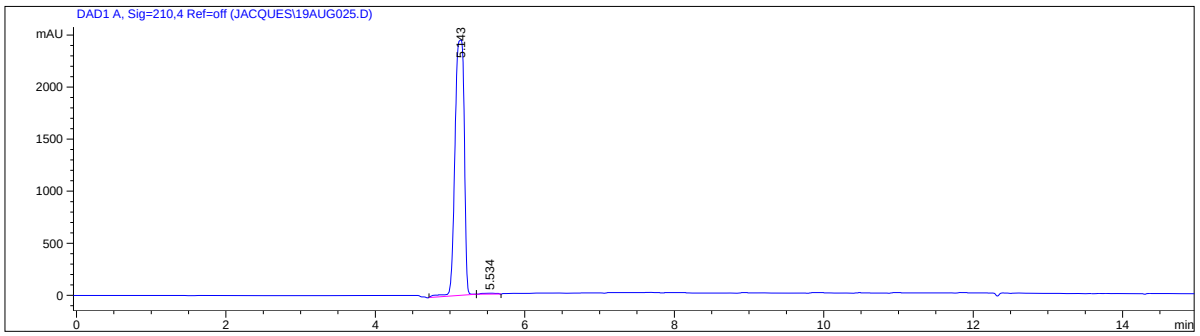

8-[(2E)-3-Phenylprop-2-en-1-yl]caffeine (**7**)

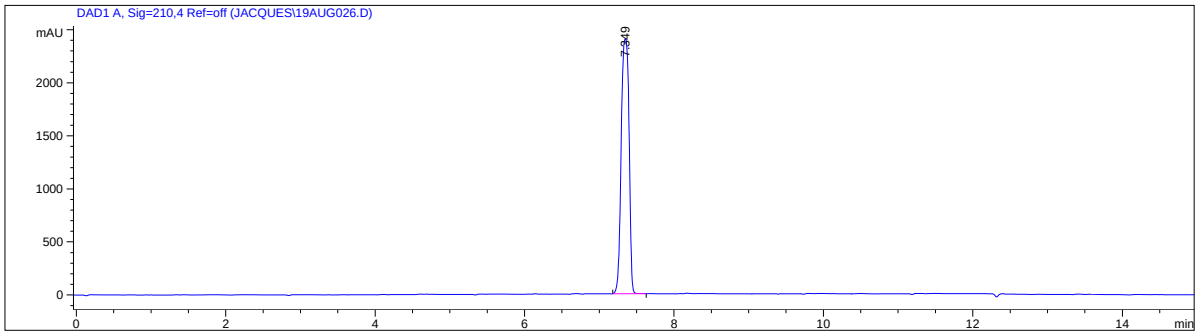

8-(2-Cyclohexylethyl)caffeine (**8**)

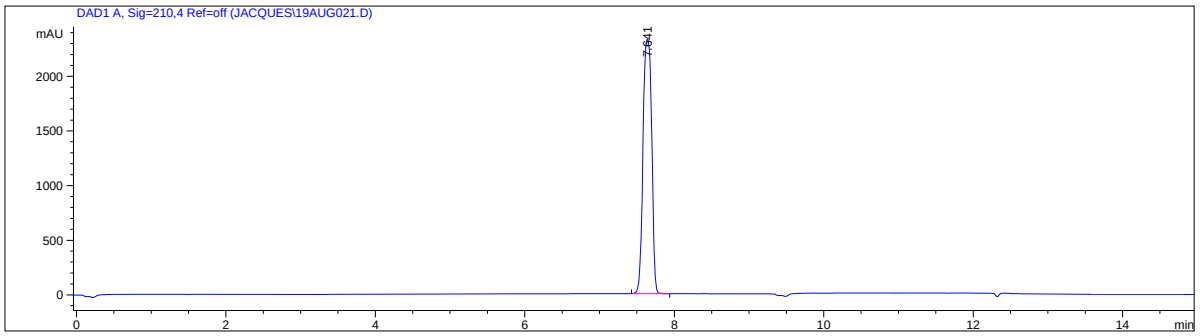

NMR spectra

^{1}H NMR and ^{13}C NMR spectra of the following new/unknown compounds

- 8-(2-Phenylethyl)caffeine (**1**)
- 8-(3-Phenylpropyl)caffeine (**2**)
- 8-(4-Phenylbutyl)caffeine (**3**)
- 8-(5-Phenylpentyl)caffeine (**4**)
- 8-(3-Oxo-3-phenylpropyl)caffeine (**5**)
- 8-(4-Oxo-4-phenylbutyl)caffeine (**6**)
- 8-[(2E)-3-Phenylprop-2-en-1-yl]caffeine (**7**)
- 8-(2-Cyclohexylethyl)caffeine (**8**)

Proton (^{1}H) and carbon (^{13}C) NMR spectra were recorded on a Bruker Avance III 600 spectrometer at frequencies of 600 MHz and 150 MHz, respectively. All NMR measurements were conducted in $CDCl_3$.

^{1}H-NMR and ^{13}C-NMR

8-(2-Phenylethyl)caffeine **(1)**

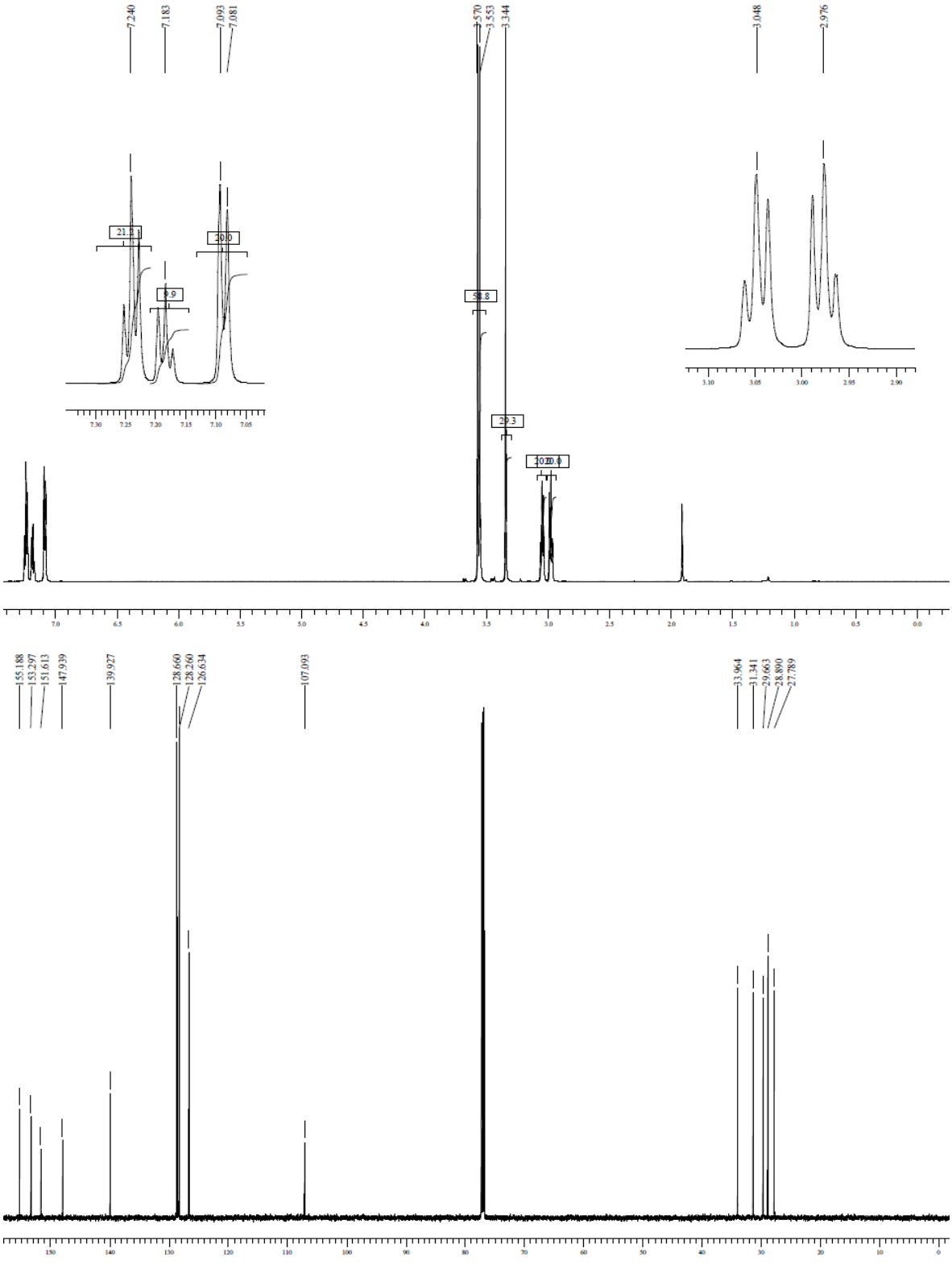

8-(3-Phenylpropyl)caffeine **(2)**

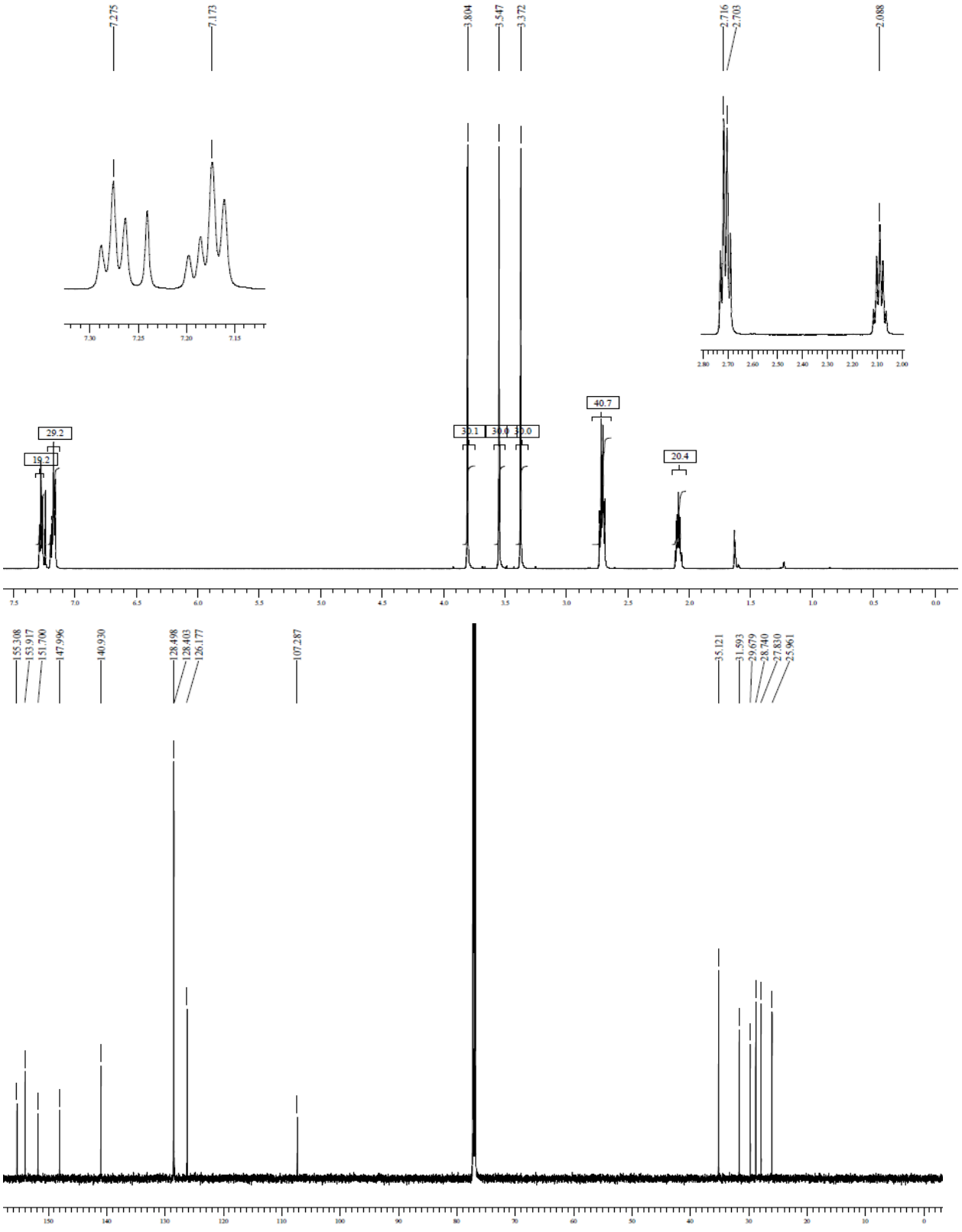

8-(4-Phenylbutyl)caffeine **(3)**

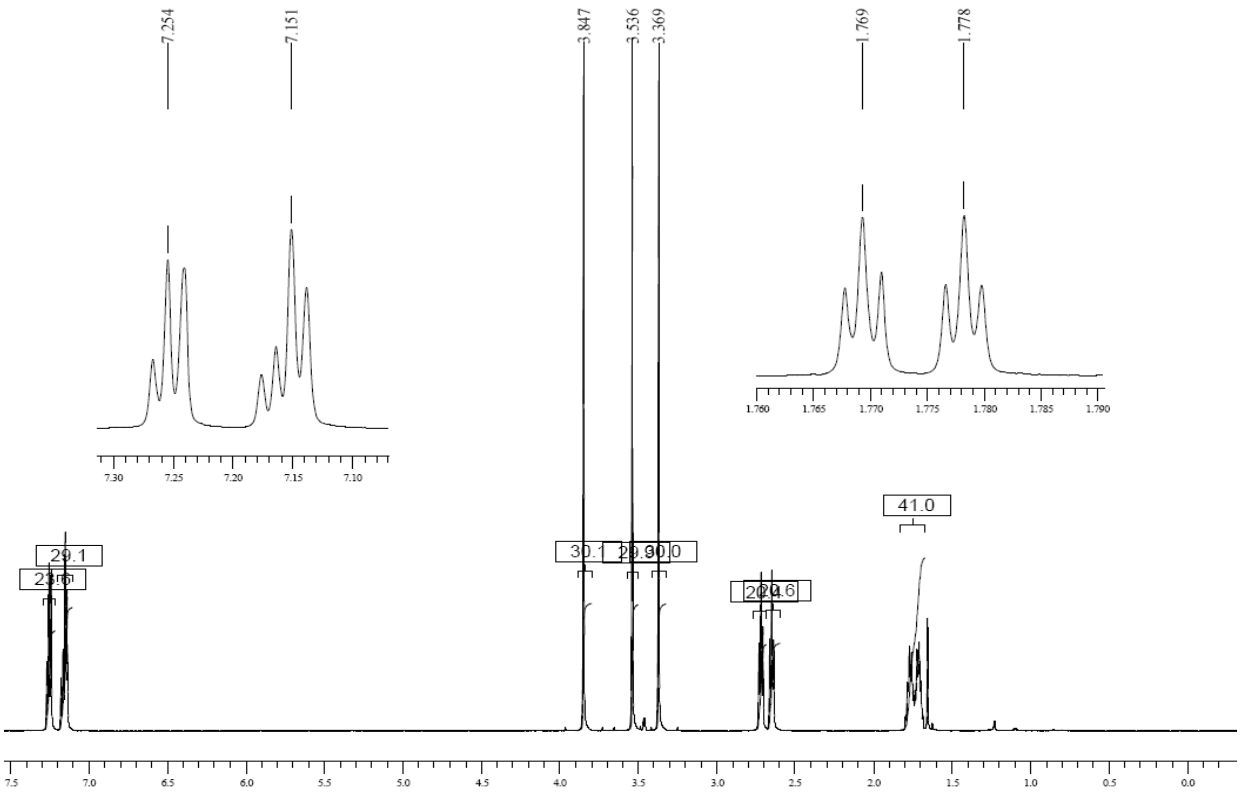

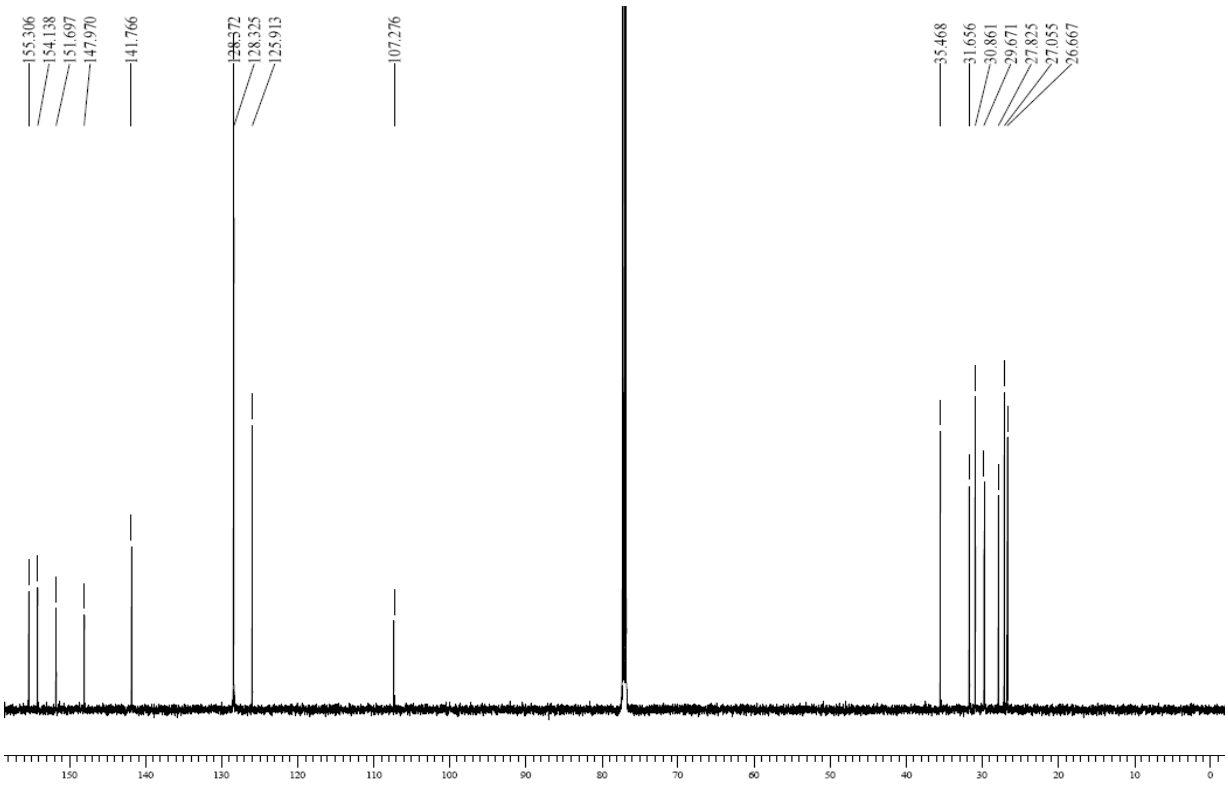

8-(5-Phenylpentyl)caffeine **(4)**

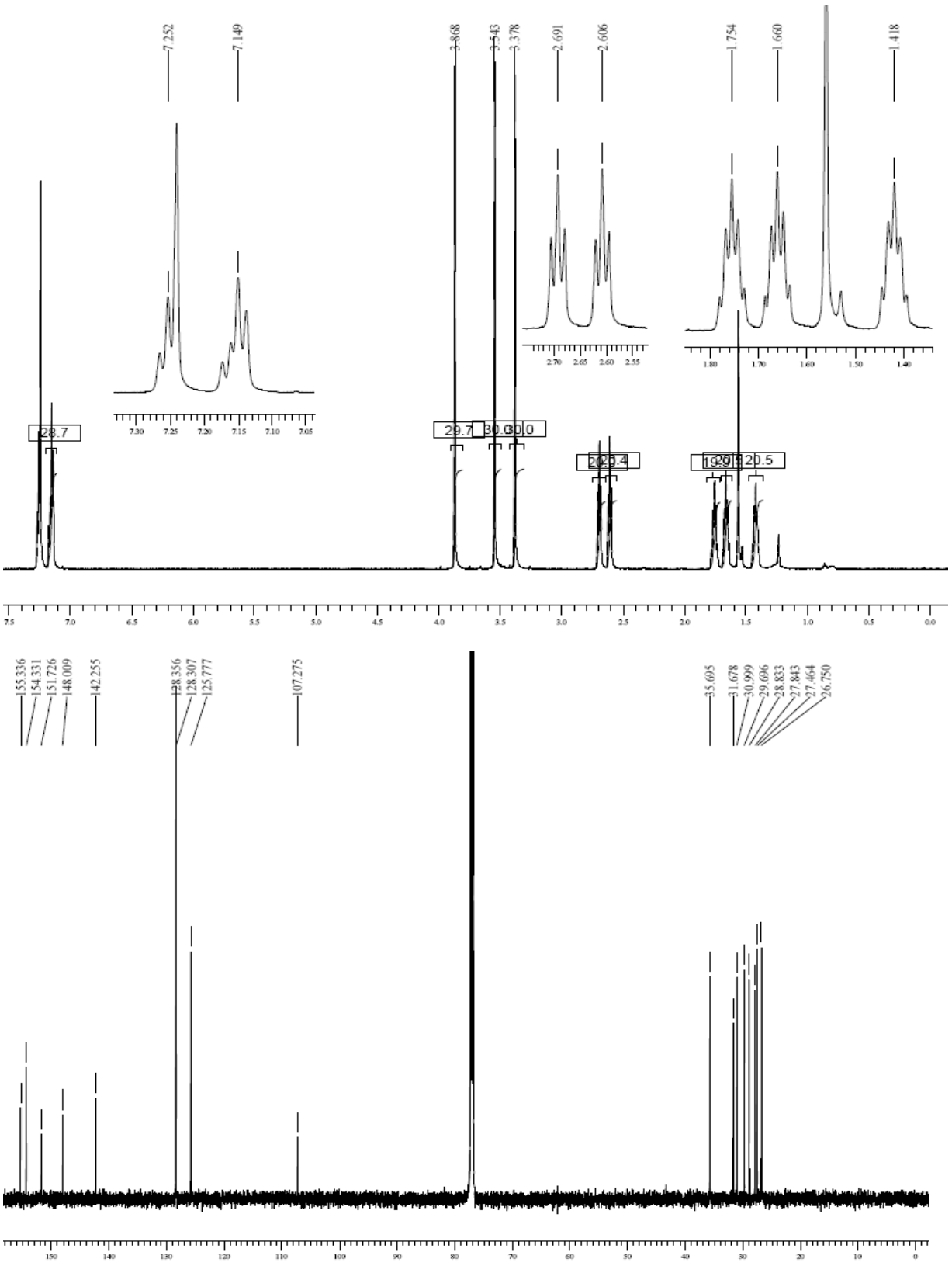

8-(3-Oxo-3-phenylpropyl)caffeine **(5)**

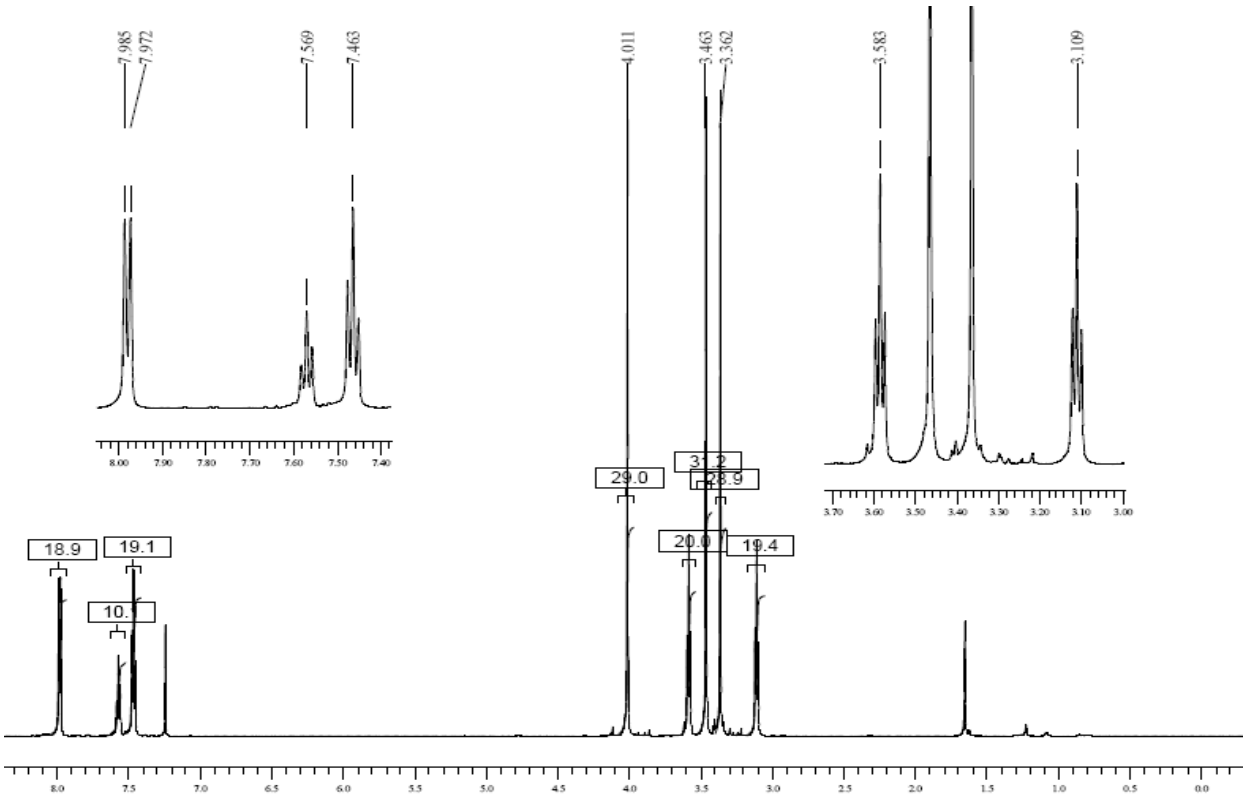

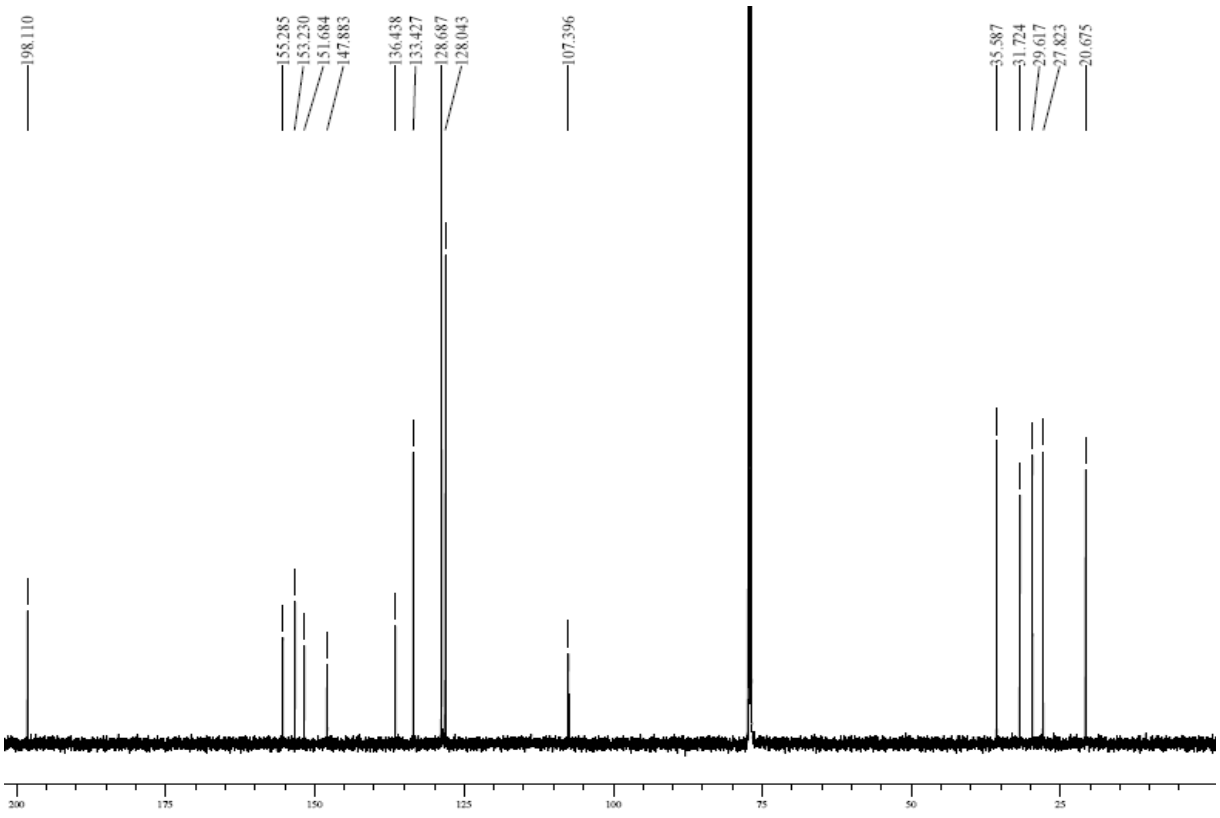

8-(4-Oxo-4-phenylbutyl)caffeine **(6)**

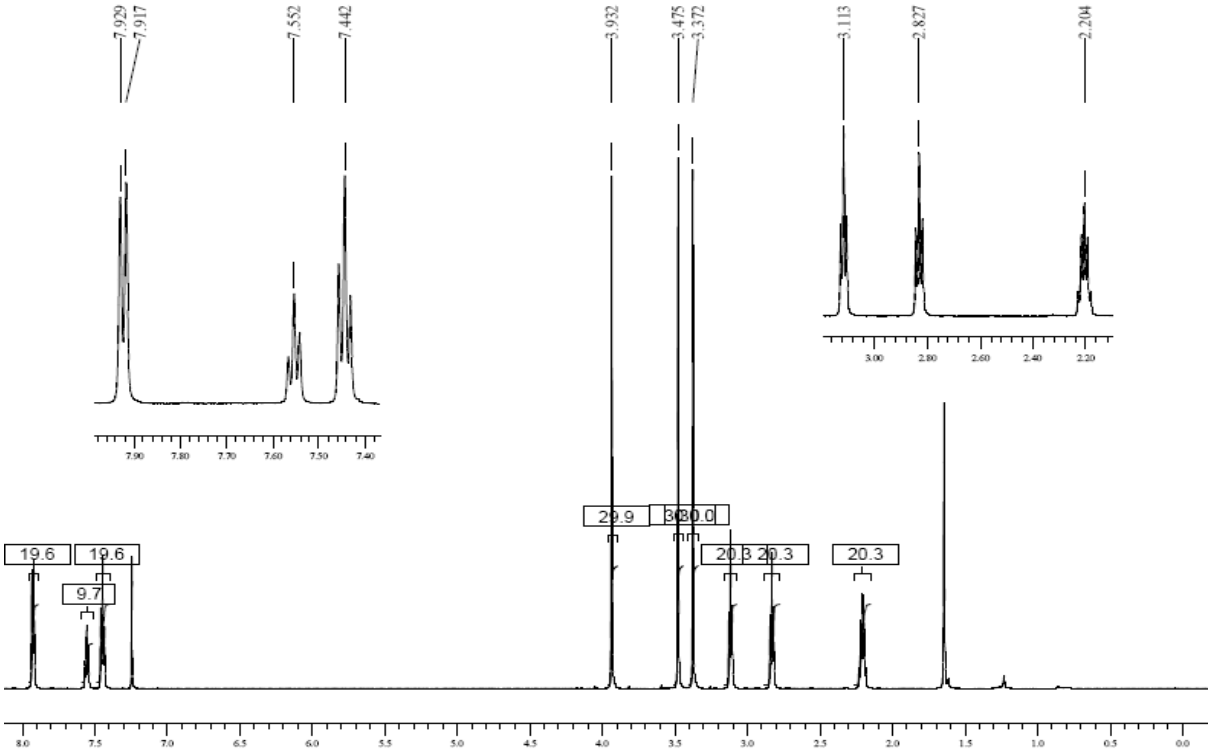

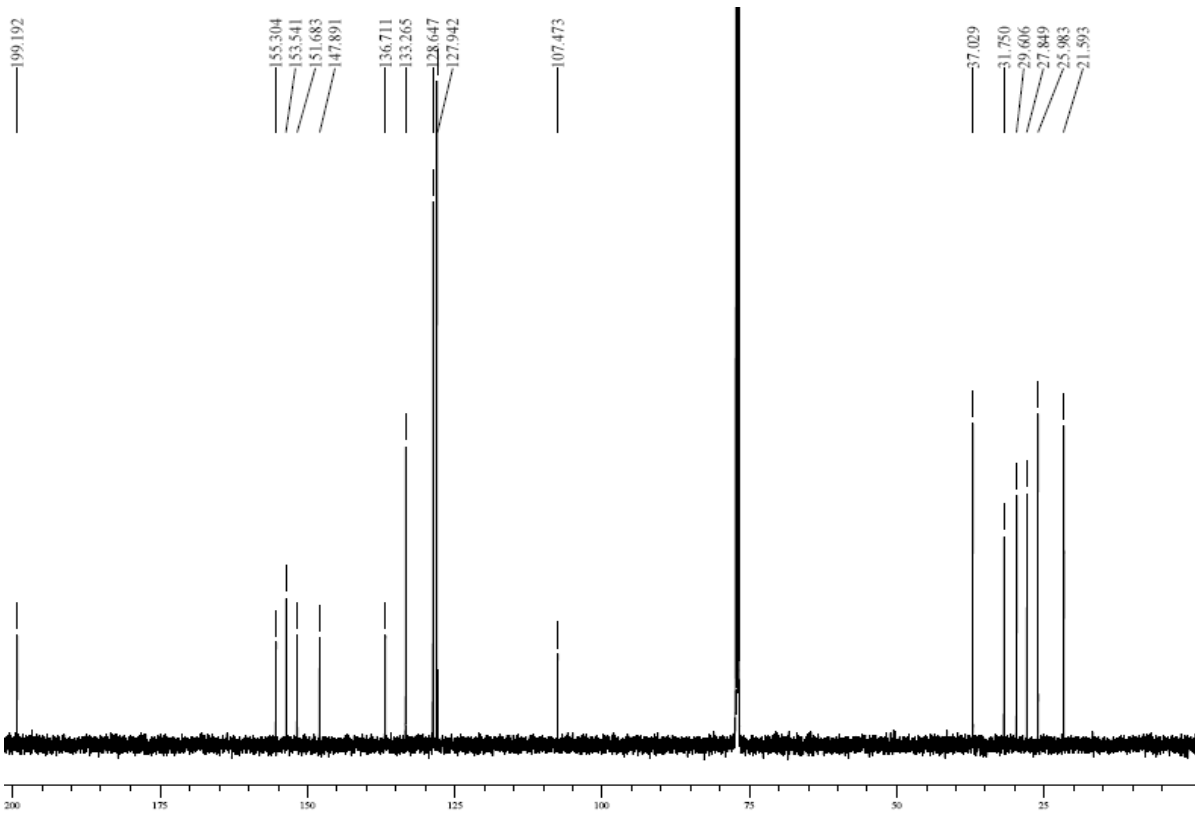

8-[(2E)-3-Phenylprop-2-en-1-yl]caffeine **(7)**

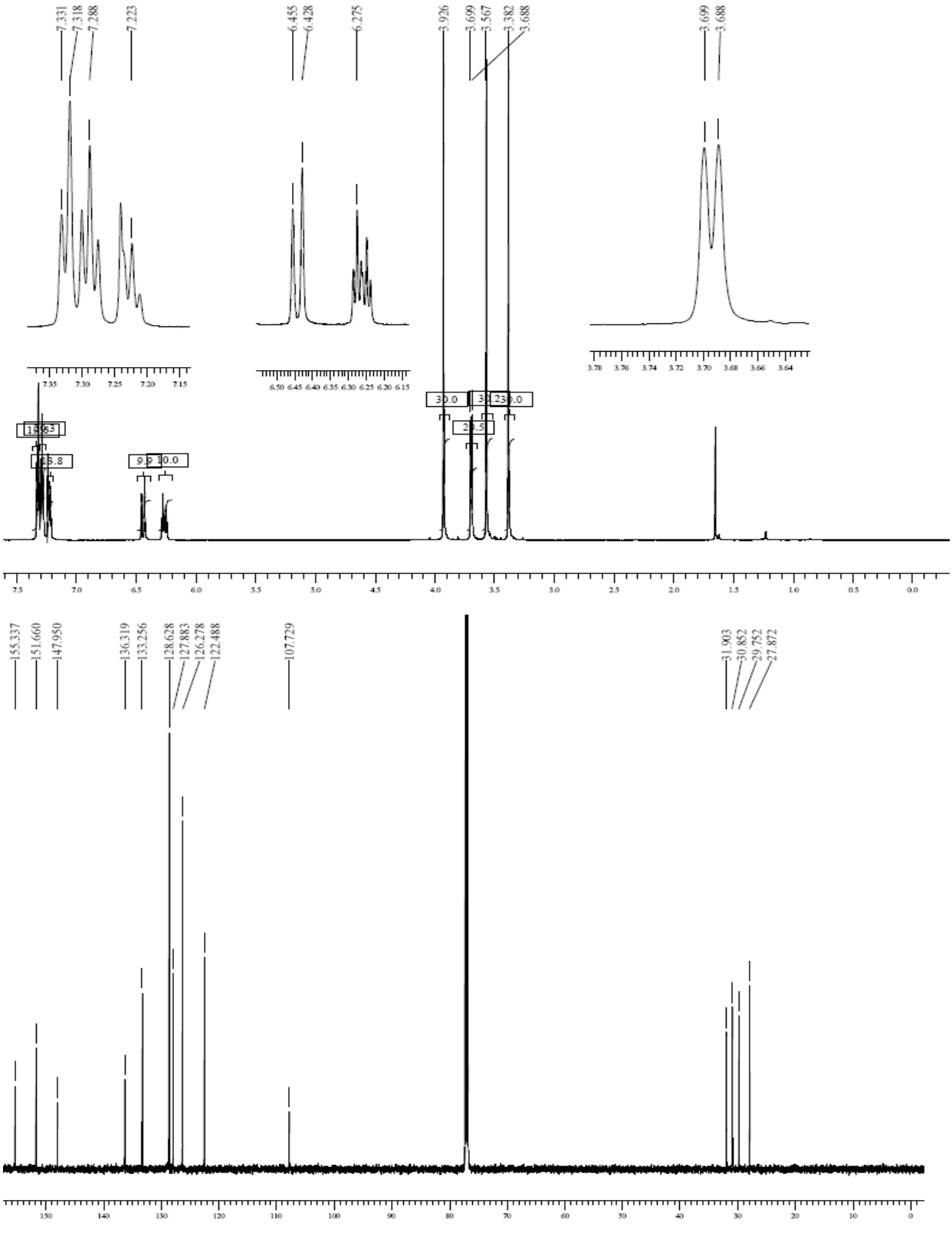

8-(2-Cyclohexylethyl)caffeine **(8)**

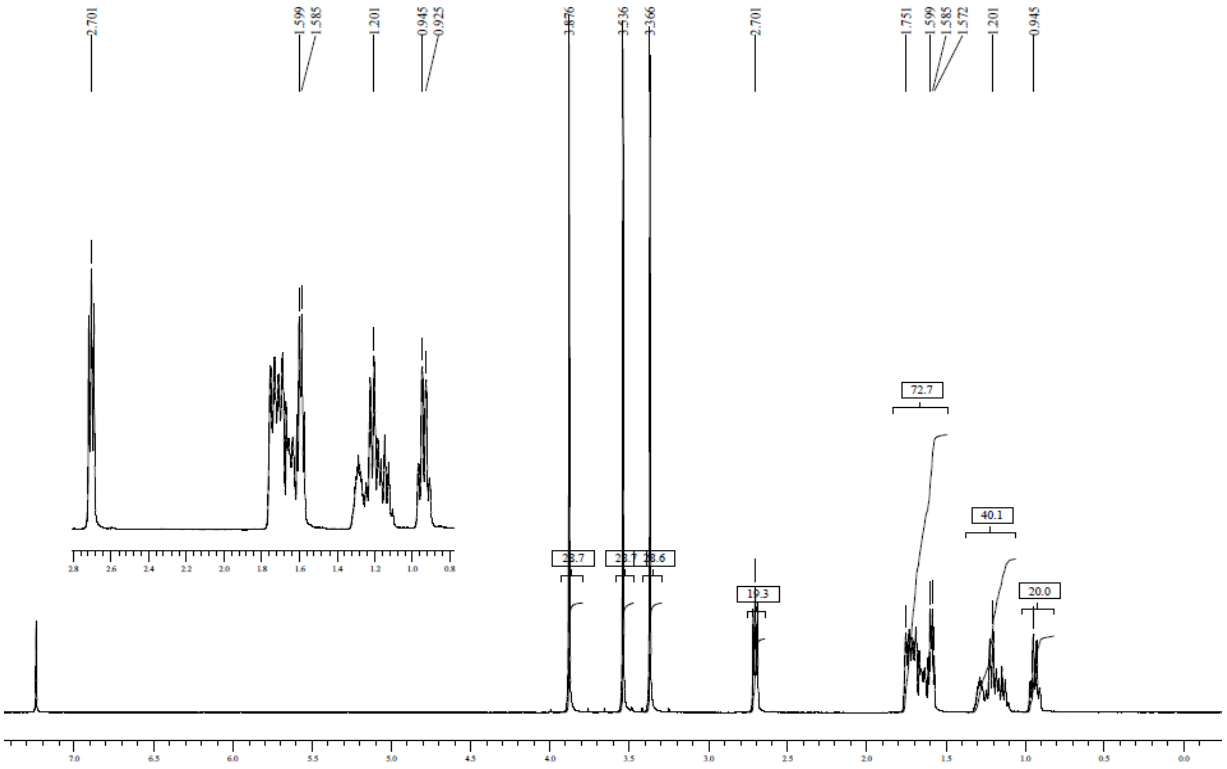

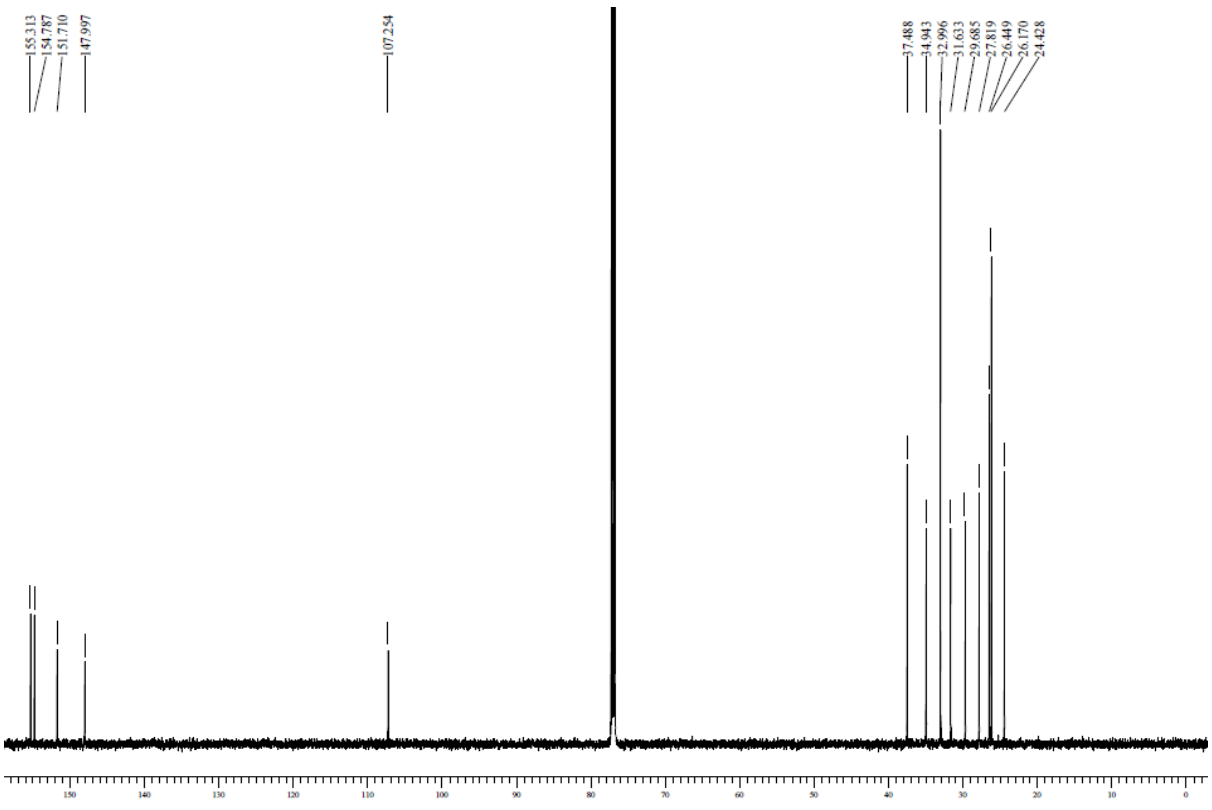

Mass spectrometry

High resolution mass spectra of the following new/unknown compounds

- 8-(2-Phenylethyl)caffeine (**1**)
- 8-(3-Phenylpropyl)caffeine (**2**)
- 8-(4-Phenylbutyl)caffeine (**3**)
- 8-(5-Phenylpentyl)caffeine (**4**)
- 8-(3-Oxo-3-phenylpropyl)caffeine (**5**)
- 8-(4-Oxo-4-phenylbutyl)caffeine (**6**)
- 8-[(2E)-3-Phenylprop-2-en-1-yl]caffeine (**7**)
- 8-(2-Cyclohexylethyl)caffeine (**8**)

Direct insertion electron impact ionization (EIMS) and high resolution mass spectra (HRMS) were obtained on a DFS high resolution magnetic sector mass spectrometer (Thermo Electron Corporation) in electrospray ionization (ESI) mode.

8-(2-Phenylethyl)caffeine **(1)**

PG1_HR-c1 #12 RT: 4.58 AV: 1 NL: 2.09E6
T: + c ESI Full ms [229.50-330.50]

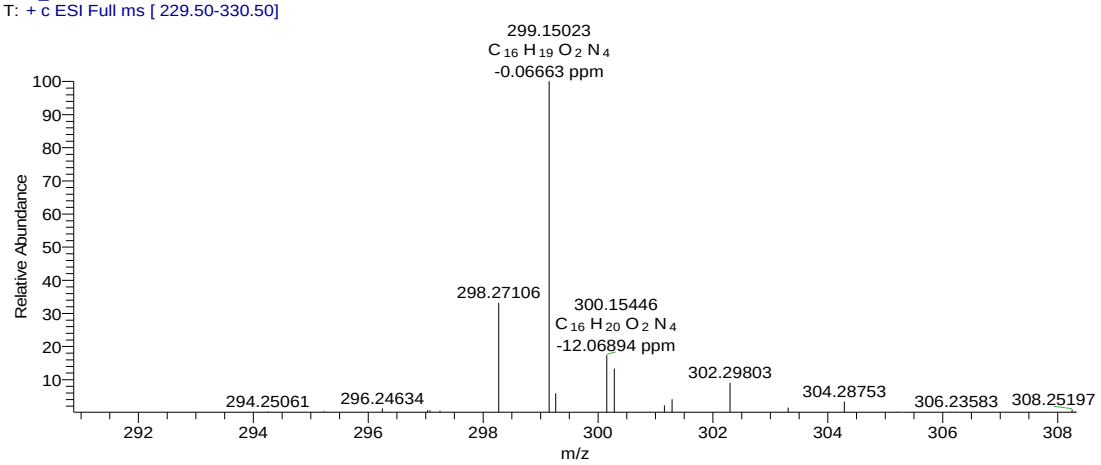

8-(3-Phenylpropyl)caffeine (**2**)

PG3_HRESI_1-c2 #8 RT: 0.26 AV: 1 NL: 2.36E6
T: + c ESI Full ms [229.50-365.50]

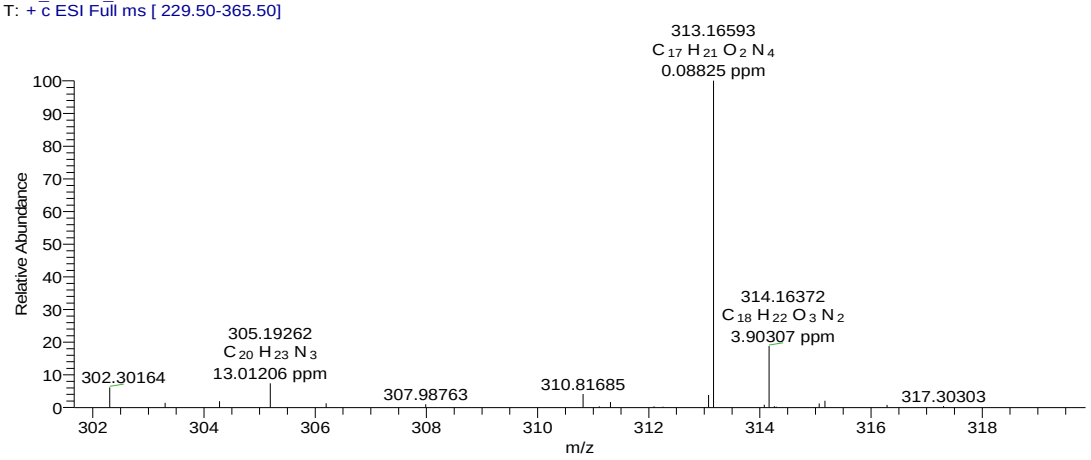

8-(4-Phenylbutyl)caffeine (**3**)

PG4_HRESI-c1 #9-10 RT: 0.23-0.26 AV: 2 SB: 7 0.06-0.23 NL: 6.05E5
T: + c ESI Full ms [259.50-365.50]

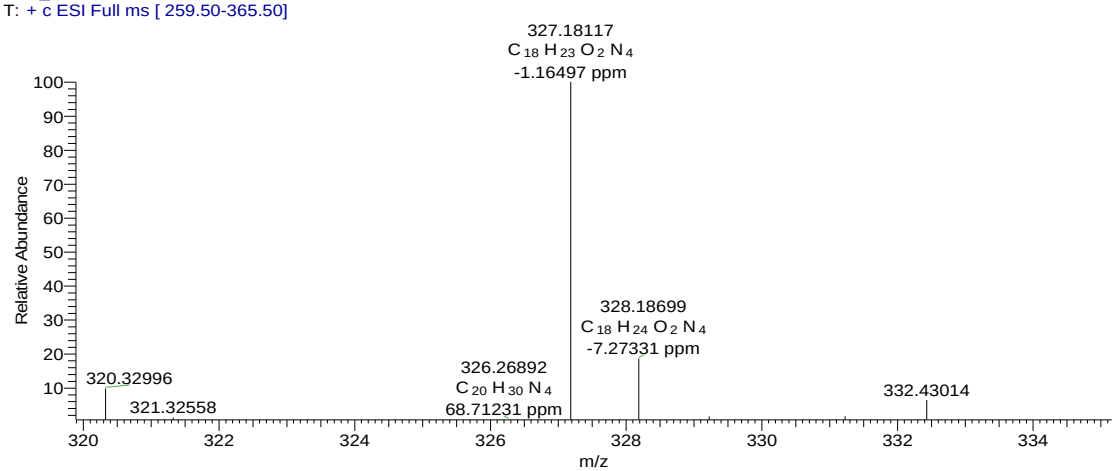

8-(5-Phenylpentyl)caffeine (**4**)

PG7_HRESI-c1 #41 RT: 1.12 AV: 1 NL: 4.36E5
T: + c ESI Full ms [229.50-322.50]

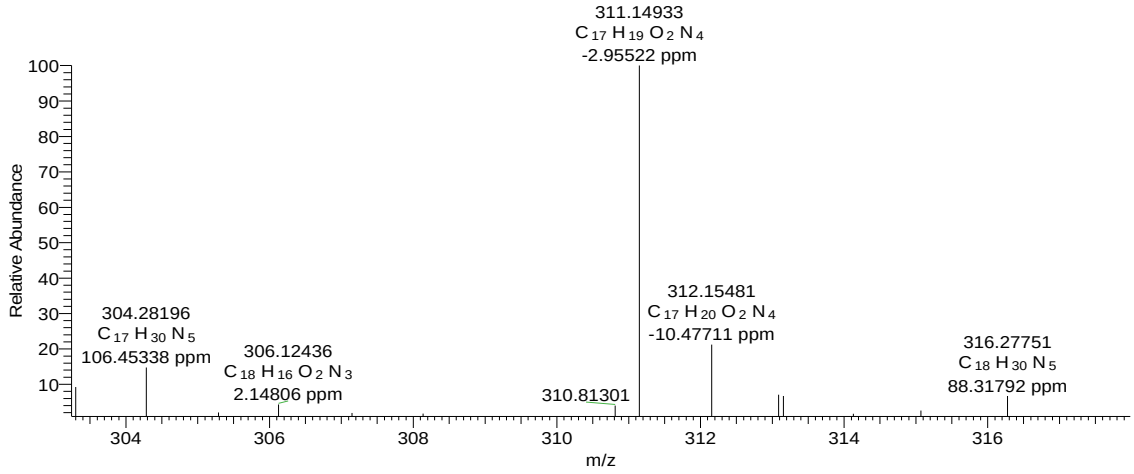

8-(3-Oxo-3-phenylpropyl)caffeine (**5**)

PG5_HRESI-c1 #9 RT: 0.73 AV: 1 SB: 4 0.56-0.65 NL: 2.72E6
T: + c ESI Full ms [259.50-365.50]

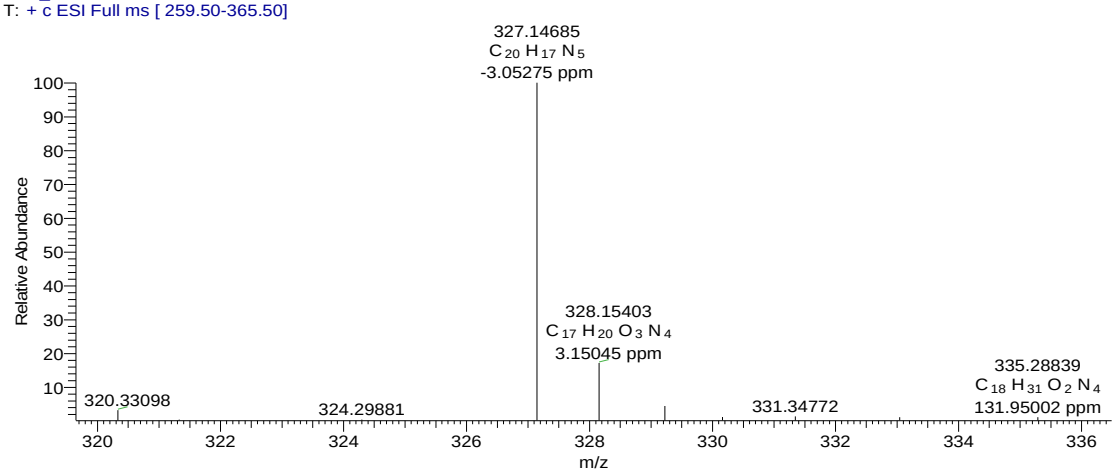

8-(4-Oxo-4-phenylbutyl)caffeine (**6**)

PG6_HRESI-c1 #21 RT: 1.50 AV: 1 NL: 4.58E6
T: + c ESI Full ms [314.50-410.50]

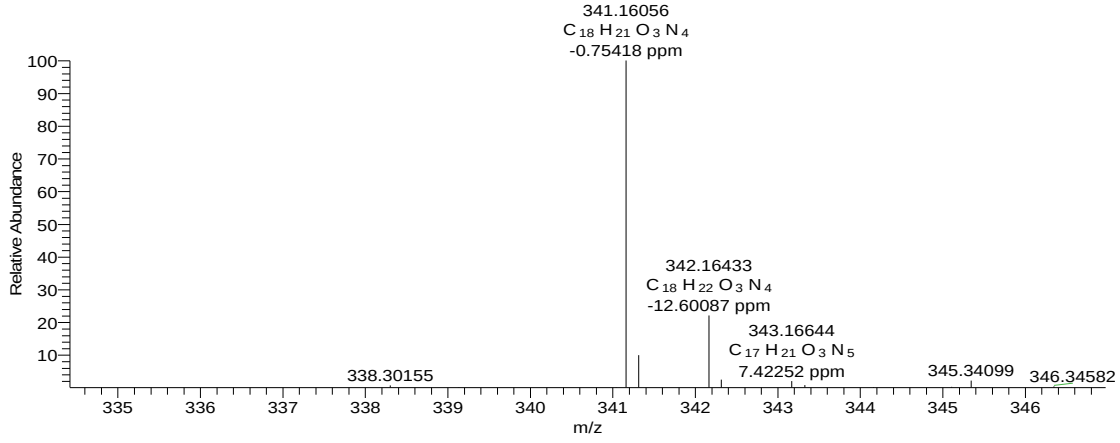

8-[(2E)-3-Phenylprop-2-en-1-yl]caffeine (**7**)

PG8_HRESI-c1 #29 RT: 0.79 AV: 1 NL: 5.66E5
T: + c ESI Full ms [259.50-365.50]

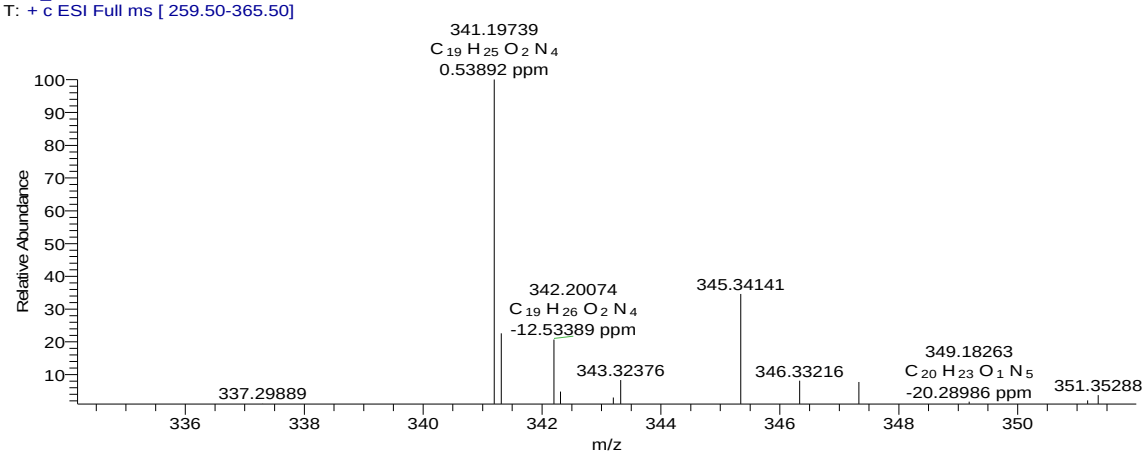

8-(2-Cyclohexylethyl)caffeine (**8**)

PG2_HRESI-c1 #12 RT: 0.33 AV: 1 NL: 1.90E6
T: + c ESI Full ms [229.50-330.50]